STIM1 regulates spatiotemporal calcium signals and the cytoskeleton in motile growth cones

Macarena Pavez
BMedRes (Hons)

Submitted in fulfilment of the requirement for the
Degree of Doctor of Philosophy (Medical Research)

University of Tasmania

DECLARATION OF ORIGINALITY

This thesis contains no material which has been accepted for a degree or diploma by the Institute or any other University or institution and, to the best of my knowledge, no material previously published or written by another person, except where due acknowledgement is made in the text of this thesis, nor does the thesis contain any material that infringes copyright.

Macarena Pavez

December 2017

AUTHORITY OF ACCESS

This thesis may be made available for loan and limited copying and communication in accordance with the Copyright Act 1968.

Macarena Pavez

December 2017

STATEMENT OF ETHICAL CONDUCT

The research associated with this thesis abides by the international and Australian codes on human and animal experimentation, the guidelines by the Australian Government's Office of the Gene Technology Regulator and the rulings of the Safety, Ethics and Institutional Biosafety Committees of the University.

Macarena Pavez

December 2017

Acknowledgements:

I'd like to start by thanking my incredible SUPERvisors (pun intended), Professor Lisa Foa and Dr Rob Gasperini. Lisa and Rob, you have both been absolute role models for me this whole time. You both inspire me to be the best scientist I can be, I couldn't have asked for more supportive mentors. You have supported and encouraged me throughout my candidature (and even before), to pursue my goals until the race is over. Thank you for seeing greatness in me, even when I didn't see it myself, and for getting me to work on those things that were (and still are) challenging for me, including public speaking. I cannot describe in words how much I have learned from both of you over these years, but I can only hope that one day I'll be able to pass on all that knowledge and passion for science to the coming generations.

I also want to thank Dr Adrian Thompson for being by my side (literally) this whole time. Thanks for keeping me up to date on the literature, and for providing me with sweet treats when necessary. I am truly grateful to have shared this journey with you, you have taught me so much. Thanks for your support and encouragement, and many STIM1 conversations. I'll miss those.

To members of the Foa/Young/Small/Lin labs, past and present. Thank you all for your encouragement, constructive feedback, advice, technical support and friendly chats these last years. You have all become part of my second family, and I am incredibly humbled by all your support and faith in me. I especially want

to thank Yilan Zhen and Solene Ferreira for our many adventures shared, thanks for keeping me sane and cheerful this whole time.

Thanks also to those friends who've been with me since undergrad, including Megan O'Rourke, Rachel Atkinson and Amanda Patchett. We have been through a lot together, and I'm incredibly thankful to have made it to the end with you all, thanks for everything. Also, big shout out to all fellow PhD students who have cared, inspired, and shared a cup of tea with me, I owe a great deal to all of you and I hope I can be there for you as you have been for me.

Finally, I would like to thank my family, for without them I would not be here today. To my parents and sisters, I dedicate this thesis to you and I thank you now and always for supporting me through this time, it has been tough but possible because of your constant encouragement.

Table of Contents

Chapter 1: Introduction and literature review 1

1.1 Axon pathfinding drives connectivity during development 2

1.1.1 Directed axon motility in response to a range of cues: Growth cones lead the way 3

1.2 The growth cone cytoskeleton 5

1.2.1 Actin cytoskeleton 5

1.2.2 Microtubule cytoskeleton 9

1.3 Calcium and cyclic nucleotides are key second messengers that mediate growth cone dynamics 14

1.3.1 Cyclic nucleotides 15

1.3.2 Calcium 18

1.4 Extracellular and intracellular sources of calcium at the growth cone 20

1.4.1 Extracellular calcium: transient receptor potential channels and voltage-gated calcium channels 20

1.4.2 Intracellular calcium: endoplasmic reticulum 21

1.4.3 Store Operated Calcium entry 22

1.5 Stromal Interacting Molecule 1 (STIM1) is a key regulator of store operated calcium entry 23

1.6 Endoplasmic reticulum in growth cones: a source of localized calcium? 28

1.7 Hypothesis 33

1.7.1 Aims 34

Chapter 2: Methods and Key Resources 35

2.1 Experimental model details 36

2.2 Materials/Reagents 36

2.3 Sensory neurons cell culture and pharmacology 36

2.3.1 Cell culture 36

2.3.2 Protein knockdown 36

2.3.3 Pharmacology 37

2.4 *In vitro* growth cone turning assay 37

2.5 Immunocytochemistry 38

2.5.1 Immunocytochemistry in turning growth cones 38

2.5.2 Immunocytochemistry for protein colocalisation analysis 39

2.6 Transfection methods used for protein overexpression 39

2.6.1 BacMam transfection 39

2.6.2 Magnetofection 40
2.6.3 Lentivirus production and transduction 40
2.6.4 Electroporation by nucleofection method 41
2.7 Live cell imaging: Analysis of OptoSTIM1-induced growth cone motility 41
2.8 Live cell imaging: Analysis of EB3 dash dynamics 42
2.9 Live cell imaging: Analysis of Ca^{2+}_{ER} dynamics at filopodia 43
2.10 Statistical analyses 44
Chapter 3: STIM1 interacts with the growth cone cytoskeleton 45
3.1 Introduction 46
3.2 Results 50
3.2.1 STIM1 regulates the expression of actin and focal adhesion kinase in motile growth cones 50
3.2.2 STIM1 regulates expression of the actin-associated protein drebrin in growth cones 55
3.2.3 STIM1 localises with EB-1/3 at the periphery of randomly extending growth cones in a Ca^{2+}_{ER}-dependent manner 58
3.3 Discussion 63
Chapter 4: STIM1 is required for the spatial distribution and polymerization of microtubules in steering growth cones 69
4.1 Introduction 70
4.2 Results 73
4.2.1 STIM1 activation is sufficient to steer growth cones 73
4.2.2 STIM1 is necessary for microtubule polymerization and growth cone turning 76
4.2.3 STIM1 is required for EB3 movement and recruitment in sensory neuron growth cones 79
4.2.4 The spatial organization of microtubules and microtubule-associated proteins necessary for appropriate growth cone turning requires STIM1 expression 89
4.3 Discussion 97
Chapter 5: STIM1 regulates ER remodelling and microtubule protrusion into filopodia 104
5.1 Introduction 105
5.2 Results 108
5.2.1 STIM1 expression is required for microtubule protrusion and ER remodeling into growth cone filopodia 108
5.2.2 STIM1 regulates endoplasmic reticulum-derived Ca^{2+} signals in growth cone filopodia 114
5.3 Discussion 123

Chapter 6: Conclusions and future directions 130
Appendix 1. KEY RESOURCES 145
References: 149

List of abbreviations:

$[Ca^{2+}]_i$	concentration of intracellular calcium
+TIP	microtubule plus-end binding protein
APC	adenomatous polyposis coli
BDNF	brain-derived neurotrophic factor
Ca^{2+}	calcium
Ca^{2+}_{ER}	endoplasmic reticulum calcium
cAMP	cyclic adenosine monophosphate
CaN	calcineurin
CaMKII	calcium/calmodulin-dependent kinase II
Cdc42	cell division control 42 homolog
cGMP	cyclic guanosine monophosphate
CICR	calcium-induced calcium release
CRAC	calcium release activated calcium
DRG	dorsal root ganglion
EB1-3	end binding protein 1 and 3
ER	endoplasmic reticulum
F-actin	filamentous actin
I_{CRAC}	calcium release activated calcium current
IICR	IP_3-induced calcium release
IP_3	inositol-1,4,5-triphosphate
IP_3R	inositol-1,4,5-triphosphate receptor
NGF	nerve growth factor
PI3K	phosphatidylinositol-4,5-bisphosphate 3-kinase
PKA	protein kinase A
PKG	protein kinase G
PM	plasma membrane

Rho GTPase	Rho guanosine-5’-triphosphatases
Rac1	Ras-related C3 botulinum toxin substrate 1
RhoA	Ras homolog gene family, member A
RyR	ryanodine receptor
Sema-3a	semaphorin-3a
SNM	sensory neuron media
SOCE	store-operated calcium entry
STIM1	stromal interaction molecule 1
TAC	tip attachment complex
TRPC	transient receptor potential canonical
VAMP2	vesicle-associated membrane protein 2
VGCC	voltage-gated calcium channel

Abstract

The precise connectivity that underlies neural circuitry in the central nervous system is regulated by axon guidance. This process is regulated by a highly specialized sensory structure at the tip of extending axons called the growth cone, which responds to extrinsic guidance cues in the embryonic environment. Disorders of growth cone motility and axon guidance are thought to underlie a range of neurological disorders such as autism and schizophrenia due to defects in neuronal targeting and connectivity. The spatial and temporal regulation of calcium signalling at the neuronal growth cone is essential for axon guidance and motility, however the exact mechanisms that regulate these localised calcium signals are not fully elucidated. Growth cone filopodia are the "first responders" during axon guidance, transducing guidance cues through receptor-mediated calcium transients. However, what regulates and sustains the spatiotemporal calcium signals at filopodia and precisely how these signals are instructional for growth cone motility remains unclear.

As a major store of intracellular calcium, the endoplasmic reticulum (ER) would be predicted to have a vital role in growth cone calcium regulation, although ER function in the growth cone and in particular, the filopodia is largely unexplored. An important calcium-regulatory mechanism that occurs in growth cones is store operated calcium entry (SOCE) which is activated when Stromal Interacting Protein 1 (STIM1), an ER-embedded calcium-sensing protein, and Orai1 on the plasma membrane form a highly selective calcium channel allowing calcium to enter the cell. STIM1 expression is necessary for transduction of filopodial calcium transients in *Xenopus* growth cones. In DRG neurons, STIM1 is required for attractive growth cone turning towards BDNF, where STIM1 functions to sustain calcium by refilling depleted ER stores through SOCE. STIM1 also regulates motility in response to a calcium-independent cue Sema-3a, suggesting that STIM1 functions in multiple pathways. In non-neuronal cells, STIM1 has also been

reported to act as a microtubule plus-end tracking protein, where it facilitates microtubule-dependent ER remodelling through direct interaction with end-binding protein-1 and 3 (EB-1/3), in a tip-attachment complex. Given these findings, the central hypothesis of this thesis is that STIM1 mediates instructive ER-microtubule dynamics which are necessary to spatially and temporally localise calcium signals required to sustain motile or turning behaviours in pathfinding growth cones.

This study tested whether STIM1 functions in a tip-attachment complex to mediate ER-remodelling into filopodia of motile growth cones from rodent DRG sensory neurons. STIM1 localised with the microtubule cytoskeleton through an association with EB1/3, that was required for remodelling ER to peripheral areas of steering growth cones. Filopodial protrusion and stabilisation by microtubules is a well-known correlate of directed growth cone motility, but how microtubules are recruited to facilitate SOCE at filopodia has not been determined until now. The data presented in this study supports the hypothesis that microtubule-ER remodelling in sensory neuron filopodia is regulated by STIM1. Reduced STIM1 expression significantly perturbed microtubule assembly and organization in growth cones turning to BDNF and Sema-3a. STIM1 was necessary for appropriate distribution and dynamics of microtubule-associated proteins EB-1/3, as well as expression levels of filamentous-actin, actin-associated proteins and adhesion-regulating elements. Additionally, using an ER-targeted low affinity calcium indicator, calcium dynamics and spatiotemporal localization of ER in filopodia were shown to be perturbed in growth cones with reduced STIM1 expression. Taken together, the data presented here demonstrate that STIM1-EB3 interaction represent a direct physical link between ER-derived calcium signals and the cytoskeleton. These data support a mechanism where ER remodelling, particularly in filopodia, supports and sustains crucial spatiotemporal regulation of calcium which is instructive for pathfinding axons during wiring of developing neural circuitry.

Chapter 1:

Introduction and literature review

1.1 Axon pathfinding drives connectivity during development

The nervous system is comprised of a functional network of billions of precisely, interconnected neurons and supporting glia that work in synchronisation to regulate all aspects of body activity and behaviour. Accurate wiring of the nervous system is essential for communication between the neurons and their targets. This intricate connectivity is finely regulated during development and adulthood (Jüttner and Rathjen, 2005; Colon-Ramos, 2009). Alterations in synapse formation and connectivity are commonly observed in neurodevelopmental disorders such as autism (Geschwind and Levitt, 2007), epilepsy, injury (Yaron and Zheng, 2007) and degenerative diseases such as amyotrophic lateral sclerosis (Vickers et al., 2009). Precisely how neuronal connectivity is established and what the exact mechanisms that regulate this complex process are questions of ongoing research.

During development, neurons extend processes or axons towards their appropriate targets in a process known as axon pathfinding. A specialised sensory structure at the tip of extending axons, the growth cone, senses and responds to various diffusible and contact-mediated cues using chemotaxis (Sperry, 1963; Tessier-Lavigne and Goodman, 1996a; Mortimer et al., 2008). The growth cone is activated when membrane receptors closest to the guidance source trigger asymmetric signaling events within the growth cone, which are transmitted by second messengers to the cytoskeleton to regulate motility (Tessier-Lavigne and Goodman, 1996a; Song and Poo, 1999; Chilton, 2006; Mortimer et al., 2009). In this manner, guidance cues elicit the reorganisation of cytoskeletal structures at the growth cone through second messengers such as calcium and trigger the directed extension of axons to their targets and subsequent formation of synapses during synaptogenesis. This chapter will review what is currently known about directed axon motility focusing on the role of the important second messenger calcium and how it controls the organization of the growth cone cytoskeleton.

1.1.1 Directed axon motility in response to a range of cues: Growth cones lead the way

During axon pathfinding, molecular cues instruct growth cone motility and ultimately direct appropriate synapse formation. Chemotropic guidance cues may attract or repel growth cones (Tessier-Lavigne and Goodman, 1996a; Chilton, 2006). Guidance cues may be tethered to the extracellular matrix (ECM) or encountered as a diffusible concentration gradient released from final or intermediate targets (Tessier-Lavigne and Goodman, 1996a; Rosoff et al., 2004; Chilton, 2006). Various chemotropic cues that regulate growth cone pathfinding have been identified and defined, including nerve growth factor (Gundersen and Barrett, 1979; Levi-Montalcini, 1987; Paves and Saarma, 1997), netrins (Kennedy et al., 1994; Hong et al., 2000), collapsin-1/semaphorin-3a (Luo et al., 1993), neurotransmitters (Zheng et al., 1994) and brain derived neurotrophic factor (BDNF) (Paves and Saarma, 1997). Contact-mediated mechanisms directing axon guidance over shorter distances have also been described such as adhesion molecules and extracellular matrix proteins (Suter et al., 1998; Suter and Forscher, 2000; Henle et al., 2013). Defects in axon guidance can result from mutations or deletions of these guidance cues and potentially cause neuropathological disorders. For example, mice lacking netrin-1, a chemotropic agent for developing axons, display aberrant formation of hippocampal networks (Barallobre et al., 2000).

Growth cones were first identified and described by Santiago Ramón y Cajal (de Castro et al., 2007). He accurately described the structure of the growth cone using histological techniques. The growth cone was described by Ramón y Cajal as a chemically-sensitive structure that exhibits rapid amoeboid movements upon the presentation of chemotropic cues, a behaviour used to reach a desired target during development (de Castro et al., 2007). The growth cone is made up of three domains: the peripheral domain consisting

of filopodia and lamellipodia, the central domain where supporting organelles such as the endoplasmic reticulum are concentrated and the intermediate transition zone (Suter and Forscher, 2000; Vitriol and Zheng, 2012). Filopodia and lamellipodia are membranous extensions that protrude from the peripheral domain of the growth cone and which function as sensory structures mediating motility and pathfinding (Argiro et al., 1984). The rate of growth cone advance is directly correlated with filopodial and lamellipodial dynamics (Argiro et al., 1984). Filopodia are essential for axon guidance as they are the most distal part of the growth cone that comes into contact with a guidance cue and as such, filopodia are abundant in receptors that transduce guidance cues to intracellular signalling molecules (Gomez and Letourneau, 1994; Gomez et al., 2001). Given the crucial role of filopodia in transducing signals during axon guidance, this thesis will investigate filopodial calcium signalling.

During pathfinding, growth cones integrate extracellular and intracellular signals into a range of motile behaviours such as turning (attraction or repulsion), retraction, stalling, fasciculating and branching, as well as outgrowth (Suter and Forscher, 2000). During outgrowth, growth cones undergo protrusion, engorgement and consolidation (Goldberg and Burmeister, 1986; Godement et al., 1994; Halloran and Kalil, 1994; Dent and Gertler, 2003). During lamellipodial protrusion, the initial formation and elongation of filopodia and lamellipodia take place at the leading edge. Lamellipodia then become engorged with vesicles and organelles, while filopodia move to the lateral portions of the growth cone (Dent and Gertler, 2003). At consolidation, filopodia retract to the base, promoting the formation of an axon shaft and the addition of a new distal axon segment (Dent and Gertler, 2003).

Rearrangement and stabilisation of the growth cone cytoskeleton as axons extend and steer, are regulated by polymerisation and depolymerisation of the actin and microtubule cytoskeleton (Figure 1.1). The growth cone is a major site of microtubule assembly

(Bamburg et al., 1986) which, combined with assembly-disassembly of actin microfilaments at the periphery of the growth cone, regulate processes like calcium-dependent axonal growth (Lankford and Letourneau, 1989). As the growth cone advances, a balance between actin polymerisation and depolymerisation maintains axon protrusion and retraction respectively (Marsh and Letourneau, 1984; Bentley and Toroian-Raymond, 1986; Forscher and Smith, 1988; Chien et al., 1993). Microtubule and actin stabilisation at the side of the growth cone facing an attractive guidance cue results in growth cone motility towards that cue, while cytoskeletal destabilisation in response to an inhibitory/repulsive guidance cue results in growth away from that cue (Lin et al., 1994; Buck and Zheng, 2002; Hur et al., 2012). Cell stabilisation towards a signalling source and the asymmetric rearrangement of cytoskeletal components and signalling complexes are crucial for cell extension and oriented migration (Etienne-Manneville, 2004). Second messengers including calcium regulate the stabilisation and destabilisation of the actin and microtubule cytoskeleton to direct growth cone motility (Lankford and Letourneau, 1989; Buck and Zheng, 2002). Given this, the growth cone cytoskeleton and the molecules that regulate cytoskeletal stability and organisation will be reviewed in greater detail.

1.2 The growth cone cytoskeleton

1.2.1 Actin cytoskeleton

Actin is the major component of lamellipodia and, indeed, one of the most abundant proteins in eukaryotic cells. Actin filaments are composed of actin monomers organised in double helical polymers (Dominguez and Holmes, 2011). This structure establishes molecular polarity and results in strong orientation of the filament ends, with barbed or

Figure 1.1- Cytoskeletal rearrangements underlying growth cone turning

An attractive cue triggers the bundling of F-actin into filamentous structures within filopodia and meshwork array within lamellipodia. The stable ends of microtubules bundle in the axon shaft. At the growth cone periphery, actin and microtubule polymerization (P) on the side facing the highest concentration of attractant induces filopodial and lamellipodial activity. Actin-bundling proteins stabilise filamentous (F)-actin bundles where substrate adhesion is being favoured. Membrane collapse on the far side (facing lowest concentration of attractant) results from decreased cytoskeletal polymerisation and/or increased depolymerisation (D). This process of membrane collapse can also be triggered by repulsive cues.

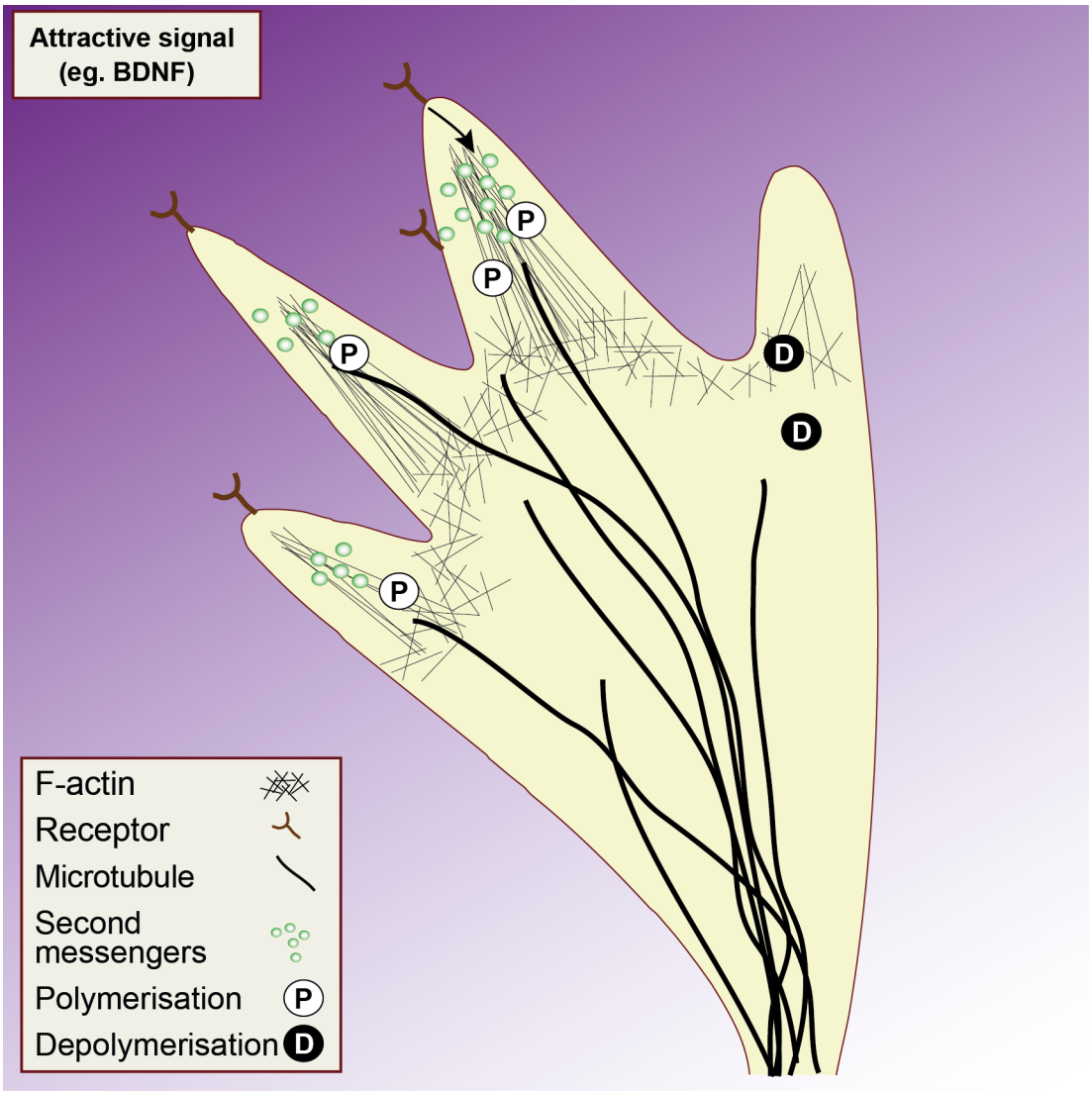
Attractive signal
(eg. BDNF)
P
P
P
P
D
D
F-actin
Receptor
Microtubule
Second messengers
Polymerisation
P
Depolymerisation
D

rapidly-growing ends extending outwards and pointed or slower-growing ends facing inwards (Pantaloni et al., 2001; Pollard and Borisy, 2003). Addition of actin subunits to the barbed-end enables the rapid growth of actin filaments during polymerisation. The spatial regulation of actin polymerisation is crucial for cell motility and is responsible for the generation of membranous protrusions like lamellipodia (Pak et al., 2008). Actin filaments polymerise at barbed-ends of actin filaments at the leading edge, and depolymerise at pointed-ends in a process described as “treadmilling” (Wang, 1985).

Treadmilling regulates protrusion in fast-moving cells, and retrograde flow in slow-moving cells. The control of depolymerisation-polymerisation at the respective ends of the actin filaments determines protrusive force and the rate of treadmilling is regulated by the activity of actin-binding proteins (Le Clainche and Carlier, 2008). These include cofilin (actin depolymerising factor, ADF), profilin and barbed-end capping proteins (Schafer and Cooper, 1995; Carlier et al., 1997; Didry et al., 1998; Pantaloni et al., 2001; Le Clainche and Carlier, 2008). Cofilin binds to actin filaments, inducing pointed-end depolymerisation and increasing the production of actin monomers (Carlier et al., 1997). Increasing the rate of depolymerisation at the pointed ends promotes barbed end growth. The activity of cofilin is regulated by profilin which assists in the recycling of actin monomers and directs movement towards barbed ends, increasing the rate of treadmilling (Didry et al., 1998). In addition, capping proteins bind or cap the barbed ends of actin with high affinity, causing an increase in monomeric actin levels. An increase in concentration of monomeric actin leads to “funnelling” of monomers to faster-growing non-capped filaments, further enhancing the rate of treadmilling (Schafer and Cooper, 1995; Pantaloni et al., 2001; Le Clainche and Carlier, 2008). Actin assembly, remodelling and turnover are interdependent and recurring processes that are essential for cellular motility.

Actin assembly and turnover directs and sustains growth cone motility during axon protrusion. Growth cones treated with the actin-stabilising drug jasplakinolide, which inhibits F-actin turnover, collapse and are unable to protrude (Gallo et al., 2002). During random growth, a balance between actin polymerisation and depolymerisation maintains both protrusion and retraction of the growth cone (Pak et al., 2008). During growth cone turning or steering, actin anti-capping proteins promote actin polymerisation on the motile/turning side by supporting actin-monomer associations and barbed-end elongation (Lebrand et al., 2004; Mattila and Lappalainen, 2008). Actin is stabilised against retraction by actin-bundling proteins and substrate-adhesion components (Suter and Forscher, 2000). Growth cone steering in response to bone morphogenic proteins (BMPs) for example, can be modulated by the bidirectional phosphorylation of cofilin by LIM kinase (LIMK) or Slingshot (SSH) resulting in growth cone attraction or repulsion, respectively (Wen et al., 2007). Enabled/vasodilator-stimulated phosphoprotein (Ena/VASP) proteins antagonise the action of capping proteins and promote extension at the barbed-end of actin filaments, which is necessary for the formation of filopodia in response to Netrin-1 and protein kinase A (PKA) activation (Lebrand et al., 2004). Many other actin-binding proteins regulate polymerisation in response to guidance cues including profilin, Abelson tyrosine kinase (Abl) and capulet (Slit/Robo pathway), and actin-binding LIM (Netrin/DCC pathway) which are beyond the scope of this review (Dent and Gertler, 2003). Cytoskeletal binding proteins and molecular motors regulate actin assembly and disassembly, which is necessary for movement and function of growth cones.

1.2.2 Microtubule cytoskeleton

The microtubule cytoskeleton is vital for many cellular processes including the maintenance of cell structure, involvement in cell division as a major component of the mitotic spindle and serving as a scaffold for intracellular transport (Stephens and Edds,

1976). Microtubules are polarised filaments composed of alternating tubulin subunits, or dimers, arranged into linear arrays. Tubulin subunits, α- and β-tubulin, assemble to form α/β tubulin dimers (Breuss et al., 2017). The α/β tubulin dimers are organised head-to-tail, producing polarised filaments with two inherently distinct ends: the plus-end and minus-end. Tubulin preferentially assembles at the plus-end and disassembles, or becomes capped, at the minus-end (Geraldo and Gordon-Weeks, 2009). Microtubules exhibit a property known as dynamic instability where polymers cycle between periods of shrinkage or catastrophe and growth or rescue (Mitchison and Kirschner, 1984). Dynamic instability of microtubules is more efficient than the common intrinsic mechanism for assembly-disassembly of polymers (reversible polymerisation), as it significantly reduces the time required for probing intracellular spaces to find a target (Holy and Leibler, 1994) likely to be important for dynamic axon growth. These intrinsic properties, along with the activity of associated proteins, influence microtubule distribution and stability. Microtubule dynamics are crucial for axon outgrowth, branching and growth cone turning, where microtubules take on an instructive role (Buck and Zheng, 2002; Dent and Gertler, 2003).

Microtubule distribution and organisation is differentially regulated within distinct compartments in neurons. In axons, microtubules are uniformly distributed with plus-ends oriented distal to the cell body. In dendrites, microtubules display non-uniform polarity with only about half of the microtubule plus ends oriented distally (Baas et al., 1988). In the growth cone, microtubules are either splayed apart with their plus-ends facing towards the periphery or distal end of the growth cone, or looped and curved within the central domain (Dent et al., 1999). It was initially thought that microtubule extension was inhibited within actin-rich areas of the growth cone, perhaps by steric hindrance of microtubule polymerisation. This was supported by studies showing that drug-induced depolymerisation of actin enhanced microtubule extension towards the leading edge of neutrophils and neuronal growth cones (Forscher and Smith, 1988; Etienne-Manneville,

2004). However, it is clear that microtubules are present in actin-rich domains of the growth cone as they extend and retract from the peripheral domain, and extend well into filopodia (Letourneau, 1983; Gordon-Weeks, 1991; Dent and Kalil, 2001). This raises an interesting point regarding the functional interaction between microtubules and the actin cytoskeleton. While both microtubule and actin have distinct roles, it is clear that neither cytoskeletal component acts alone, and that interactions between the two cytoskeletal elements are vital for growth cone motility. The work described in this thesis will examine this idea.

Dynamic interactions between microtubules and actin regulate a plethora of cellular events. One of the earliest examples of such interactions arose from a report that microtubules provide the basis of stabilisation of actin-dependent structures at the leading edge of fibroblasts (Vasiliev et al., 1970). It has since been suggested that interactions between microtubules and actin may be either regulatory or structural (Rodriguez et al., 2003). Regulatory interactions are described as those in which actin and microtubules control each other indirectly through signalling cascades. Signalling by the Rho family of small guanosine-5'-triphosphatases (GTPases) provides good examples of such interactions.

Rho GTPases belong to the superfamily of Ras-related small GTPases. Rho GTPases cycle between an inactive state (GDP-bound) and an active state (GTP-bound) resembling other molecular switches (Ridley, 2001; Jaffe and Hall, 2005). Rho guanine nucleotide exchange factors (GEF) and GTPase-activating proteins (GAP) activate or inactivate the Rho GTPase molecular switch, respectively (Dickson, 2001; Gonzalez-Billault et al., 2012). Three members of the Rho GTPase family are Rho, Rac and Cdc42. Rho and Rac regulate actin polymerisation required for the formation of stress fibers and lamellipodia, respectively, and Cdc42 functions in filopodia formation (Ridley and Hall, 1992; Ridley et al., 1992; Kozma et al., 1995; Nobes and Hall, 1995). At the growth cone,

activation of Rac and Cdc42 is thought to promote axon extension and stabilisation, whilst RhoA activity increases the likelihood of growth cone retraction (Luo et al., 1997). This suggests that during growth cone turning, asymmetries of Rho GTPases are created within the growth cone through the activity of Rac and Cdc42 on the turning side (in response to an attractive cue) and Rho on the retracting side (in response to a repulsive cue) (Hall, 1998; Dickson, 2001). While Rho GTPases act as instructive molecules during growth cone guidance, it is possible that they merely participate in a permissive manner assisting the dynamic cytoskeletal structures without conveying directional cues (Dickson, 2001).

The activity of Rho GTPases is also regulated in a reciprocal manner by microtubules and actin. Microtubule and actin disassembly activates RhoA, and microtubule assembly is known to promote the activation of Rac1 (Ren et al., 1999; Waterman-Storer et al., 1999). Microtubule depolymerisation is thought to activate RhoA through GEF-H1; a Rho GEF that localises to microtubules and regulates actin organisation in cell lines (Krendel et al., 2002). In contrast, microtubule polymerisation regulates the activity of Rac and Cdc42, both involved in actin polymerisation and microtubule dynamics (Jaffe and Hall, 2005). Activation of Rac1 is known to regulate lamellipodial actin polymerisation and dynamic microtubule instability through p21-activated kinases (Pak). Inhibition of Pak inhibits Rac1-induced microtubule dynamics *in vivo,* including microtubule growth and retrograde flow (Wittmann et al., 2003; Kalil and Dent, 2005). Rho GTPases bridge microtubule and actin interactions in a regulatory manner, which is less direct than structural interactions. Structural interactions between microtubules and actin are static or dynamic and are mediated by the formation of cytoskeleton-associated protein complexes (Geraldo and Gordon-Weeks, 2009).

Microtubule-associated proteins (MAPs) regulate spatiotemporal microtubule dynamics by modulating the stabilisation and destabilisation of microtubule filaments. MAPs,

including plus-end tracking proteins (+TIPs), target soluble non-polymerised tubulin (Akhmanova and Steinmetz, 2008). +TIPs are a heterogeneous family of proteins ranging from motor proteins to transmembrane proteins, which localise at the growing plus-ends of microtubules. +TIPs have been proposed to regulate microtubule-actin interactions within the growth cone (Geraldo and Gordon-Weeks, 2009). Two members of the end-binding (EB) family of proteins, EB1 and EB3, function as +TIPs. Both EB1 and EB3 are expressed in growth cones (Stepanova et al., 2003) where they regulate microtubule growth by inhibiting microtubule catastrophes (Komarova et al., 2009). When visualised, EB1 and EB3 proteins appear as comet-like dashes on the plus-ends of extending microtubules, with their 'tails' pointing towards the minus ends. EB-GFP dashes are thought to disappear, and presumably rapidly disassemble, when microtubules are no longer extending or become depolymerised (Geraldo et al., 2008; Geraldo and Gordon-Weeks, 2009). In growth cones, EB3 coordinates actin-microtubule interactions through a direct interaction with the F-actin-associated protein drebrin (Geraldo et al., 2008). This interaction occurs when drebrin is present in the proximal region of the growth cone filopodia, as EB3 caps the microtubules invading filopodia (Geraldo et al., 2008). EB1 also regulates microtubule-actin interactions through crosstalk with the Rho GTPase system by mediating the complex formed between the +TIP, Navigator 1 (NAV1) and the Rho GEF, TRIO. NAV1-TRIO complexes localise and selectively activate Rac1 for the regulation of neurite growth (van Haren et al., 2009; 2014).

In non-neuronal cells, EB1 proteins regulate directional migration by forming +TIP complexes with the actin-associated protein, adenomatous polyposis coli (APC) (Su et al., 1995). APC is a multi-functional microtubule plus-end-binding protein that can interact with a range of proteins (Hanson and Miller, 2005). The local distribution of APC is necessary for appropriate growth cone steering, indicating its essential role in the dynamic regulation of microtubule organisation (Koester et al., 2007). The ability to

interact with a range of proteins enables APC to participate in intracellular signalling, cell migration (Hanson and Miller, 2005), and the regulation of microtubule-actin interactions through crosstalk with the Rho GTPases. For example, in non-neuronal cells APC is recruited to the plus-ends of growing microtubules during cell migration to form complexes with a Rac-specific GEF for the regulation of membrane flattening, ruffling, and lamellipodia formation (Näthke et al., 1996; Kawasaki et al., 2000; 2003). Similarly, the Rac1/Cdc42-effector IQ motif-containing GTPase-activating protein 1 (IQGAP1), interacts directly with APC to form a tripartite complex with activated Rac1/Cdc42. IQGAP1 and APC are interdependently recruited to the leading edge of migrating cells and are necessary for actin meshwork formation, polarised migration, and localisation of the microtubule plus-end stabilising protein CLIP-170 (Fukata et al., 2002; Watanabe et al., 2004; Noritake et al., 2005). Stabilisation of microtubules and cell migration are also promoted by the EB1-APC-mDia1 (a Rho effector) complex formation in fibroblasts (Wen et al., 2004a). The processes that regulate cell motility are heavily reliant on the activity of regulatory and structural microtubule-actin effectors. Key second messengers, particularly calcium, regulates the organisation and localised stabilisation of the cytoskeleton as well as focal adhesions and membrane recycling which are crucial for directing growth cone steering. As such, the function of these second messengers will be reviewed in detail.

1.3 Calcium and cyclic nucleotides are key second messengers that mediate growth cone dynamics

Within the growth cone, calcium (Ca^{2+}) and cyclic nucleotides are two key second messenger systems that regulate bidirectional switching, intracellular signal amplification and precise axon pathfinding (Tojima et al., 2011). For example, in the developing vertebrate nervous system, the bifunctional guidance cue netrin-1 is permissive for extension of some axons into the floor plate and simultaneously steers others away (Colamarino and Tessier-Lavigne, 1995). This reflects receptor-mediated signal

transduction through select second messengers. The modulatory effects exerted by second messengers enable the regulation of cellular processes in a manner that is cell-type specific and dependent on the spatiotemporal activity of effectors.

1.3.1 Cyclic nucleotides

Cyclic adenosine monophosphate (cAMP) and cyclic guanosine monophosphate (cGMP) are second messengers known to be crucial for the regulation of axon pathfinding (Lohof et al., 1992; Kim and Wu, 1996; Ming et al., 1997). High levels of cAMP or the downstream effector protein kinase A (PKA) are associated with attractive growth cone turning, while high levels of cGMP or protein kinase G (PKG) regulate growth cone repulsion (Lohof et al., 1992; Ming et al., 1997; Song et al., 1997; 1998; Song and Poo, 1999). The levels of cyclic nucleotides are regulated by reciprocal inhibition, a process mediated by specific phosphodiesterases (PDE) which degrade cyclic nucleotides to monophosphate nucleotides (Shelly et al., 2010). Importantly, the ratio of cAMP-to-cGMP determines growth cone turning behaviours to various guidance cues, with high ratios of cAMP-to-cGMP favouring growth cone attraction and low ratios favouring repulsion or growth-inhibition (Song et al., 1997; 1998; Nishiyama et al., 2003). This suggests that growth cones are able to switch their turning response to chemotropic cues by establishing polarity through the ratio of cyclic nucleotides (Figure 1.2).

The cyclic nucleotide-induced switch in growth cone turning is activated by a number of guidance cues. For example, in *Xenopus* spinal neuron growth cones netrin-1, usually an attractive cue, can induce repulsion by activating PKG and suppressing L-type voltage gated Ca^{2+} channels (VGCC) (Song and Poo, 1999; Nishiyama et al., 2003). Similarly, growth cone attraction in response to the Ca^{2+}-dependent guidance cues brain derived neurotrophic factor (BDNF) and acetylcholine (ACh), can be turned to

Figure 1.2- Regulation of growth cone turning through second messenger signalling (cyclic nucleotide-dependent switch and CaMKII/CaN bimodal switch)

High ratios of $[cAMP]_i$:$[cGMP]_i$ favour attractive growth cone turning responses, while low ratios of $[cAMP]_i$:$[cGMP]_i$ favour repulsive turning. Cyclic nucleotides exert reciprocal inhibition over each other, and regulate the rate of Ca^{2+} flux from the endoplasmic reticulum (ER) by facilitating or inhibiting mobilisation through IP_3R/RyR. A smaller rise of $[Ca^{2+}]_i$ is sufficient to activate calcineurin (CaN). CaN mediates cytoskeletal depolymerisation (D) which results in membrane collapse or repulsive turning away from a guidance cue, such as sema-3a. A larger rise of $[Ca^{2+}]_i$ is necessary to activate Ca^{2+}-calmodulin dependent protein kinase II (CaMKII). CaMKII mediates cytoskeletal polymerisation (P) resulting in an attractive turning response towards a guidance cue, such as BDNF. CaN is also involved in reciprocal inhibition of the attractive-CaMKII pathway by activating protein phosphatase 1 (PP1), which is able to inhibit CaMKII activity. Similarly, the dephosphorylation pathway can be inhibited by the production of protein kinase A (PKA), which inhibits PP1 activity.

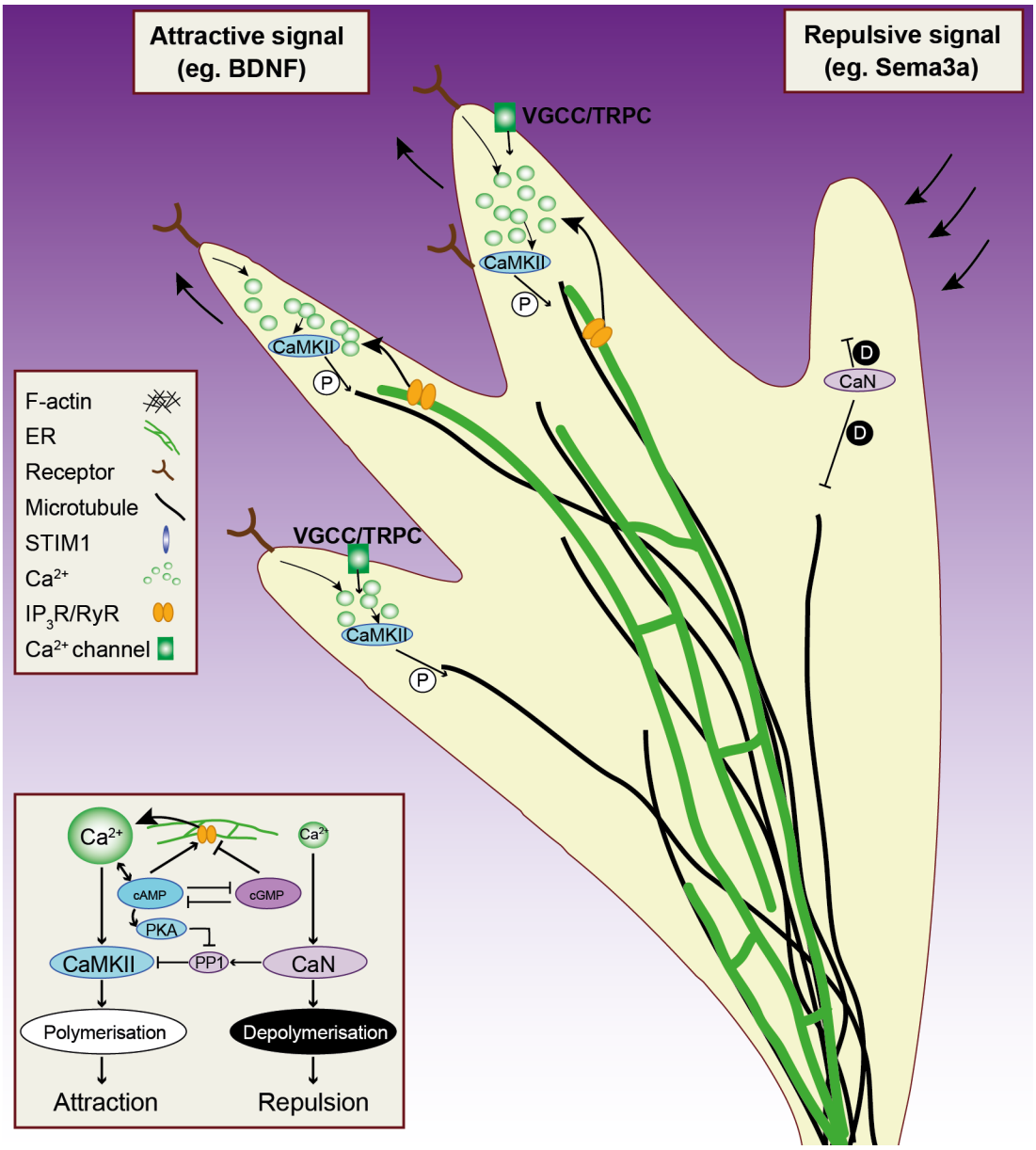
Attractive signal
(eg. BDNF)
Repulsive signal
(eg. Sema3a)
VGCC/TRPC
CaMKII
P
D
CaN
F-actin
ER
Receptor
Microtubule
STIM1
Ca2+
IP3R/RyR
Ca2+ channel
Ca2+
cAMP
cGMP
PKA
CaMKII
PP1
CaN
Polymerisation
Depolymerisation
Attraction
Repulsion

repulsion when inhibiting either cAMP or PKA (Song et al., 1997). The Ca^{2+}-independent cue semaphorin-3a (sema-3a) triggers soluble guanylyl cyclase (sGC) to activate cGMP and allow a small influx of Ca^{2+} via cyclic nucleotide gated channels (CNGCs) (Togashi et al., 2008). Nishiyama and colleagues (Nishiyama et al., 2008) reported that repulsive cues sema-3a and Slit2 cause membrane hyperpolarisation at the growth cone, while attractive cues including BDNF and DCC-mediated netrin-1 shift potentials towards depolarization. When cGMP production is greater than cGMP hydrolysis, PKG activates sodium channels and induces PKG-mediated depolarization, switching sema-3a induced repulsion to attraction (Nishiyama et al., 2008). Evidence suggests that electrical activity is important for steering, for example pre-exposure to electrical stimulation enhances growth cone attraction to netrin-1 and switches repulsion in response to myelin-associated glycoprotein (MAG) to attraction, in a mechanism mediated by both extracellular Ca^{2+} and increased cAMP activity (Ming et al., 2001). Reciprocal crosstalk between cyclic nucleotides and Ca^{2+} signalling is necessary for growth cone steering, it is not either/or that is more important. An example of this includes cyclic nucleotide-dependent mobilisation of Ca^{2+} from intracellular stores (Lohof et al., 1992). Hence, growth cone motility can be seen as the result of intricate crosstalk signalling mediated by second messenger activity, but how are these second messengers regulated spatially?

1.3.2 Calcium

Calcium (Ca^{2+}) is a ubiquitous second messenger required for axon outgrowth and growth cone motility (Kater et al., 1988; Gomez et al., 1995; Hong et al., 2000). Various outcomes of growth cone motility including pausing and differential turning (attraction or repulsion) in response to the same guidance cue, depend on intracellular Ca^{2+} ($[Ca^{2+}]_i$) within a permissive range (Kater and Mills, 1991). Seminal work by Zheng demonstrated that a spatially-restricted change of $[Ca^{2+}]_i$ is sufficient to direct growth cone extension

and steering, by focally increasing $[Ca^{2+}]_i$ on one side of the growth cone to initiate attraction, and focally decreasing resting $[Ca^{2+}]_i$ to induce repulsion from the side of stimulation (Zheng, 2000). The multifunctionality of Ca^{2+} in cell migration, relies on the tightly regulated spatiotemporal organisation of Ca^{2+} signals, and the generation of patterned signal activation within specific cellular microdomains (Wei et al., 2009). Due to limited diffusion of local Ca^{2+}, a rise of $[Ca^{2+}]_i$ is spatially restricted to the open channel(s) (Gabso et al., 1997; Augustine et al., 2003). The remainder of this review will focus on what is known of how spatial Ca^{2+} signals within growth cones are regulated, including the amplitude and the source from which Ca^{2+} originates and is sustained.

The amplitude and spatial localisation of Ca^{2+} is a vital determinant and regulator of growth cone behaviour and steering (Wen et al., 2004b) as Ca^{2+} can regulate both repulsive and attractive signals, in other words Ca^{2+} can elicit bidirectional turning responses (Tojima et al., 2011). Growth cone turning is regulated by the downstream Ca^{2+} effectors Ca^{2+}-calmodulin dependent protein kinase II (CaMKII) and Ca^{2+}-calmodulin dependent protein phosphatase, calcineurin (CaN) (Wen et al., 2004b). Due to their different affinities for Ca^{2+}, a small intracellular Ca^{2+} signal activates CaN or protein phosphatase 1 (PP1) causing growth cone repulsion, while a large local Ca^{2+} rise activates CaMKII causing an attractive turning response (Wen et al., 2004b) (Figure 1.2). A CaMKII/CaN-PP1 bimodal switch integrates local Ca^{2+} signals in order to control the direction of Ca^{2+}-dependent growth cone extension (Wen et al., 2004b). CaMKII and CaN phosphorylate and dephosphorylate cytoskeleton-associated proteins respectively, to modulate the assembly and stability of microtubules (Goto et al., 1985; Yamamoto et al., 1985).

Another determinant of Ca^{2+}-mediated growth cone steering and the regulation of cytoskeletal organisation is the source of Ca^{2+}. In growth cones Ca^{2+} mobilises from either extracellular or intracellular source. The source of Ca^{2+} determines the amplitude

change in $[Ca^{2+}]_i$ which is important for the regulation of growth cone behaviour (Ooashi et al., 2005; Arie et al., 2009). Extracellular and intracellular sources of Ca^{2+} at the growth cone are discussed in more detail below.

1.4 Extracellular and intracellular sources of calcium at the growth cone

1.4.1 Extracellular calcium: transient receptor potential channels and voltage-gated calcium channels

Extracellular Ca^{2+} is necessary for growth cone turning in response to Ca^{2+}-dependent guidance cues such as the neurotransmitter acetylcholine (ACh), BDNF, MAG and netrin-1 (Zheng et al., 1994; Ming et al., 1997; Song et al., 1997; 1998). Ca^{2+} is mobilised from the extracellular environment through plasma membrane Ca^{2+} channels, including transient receptor potential canonical (TRPC) channels and voltage-gated Ca^{2+} channels (VGCC) (Berridge et al., 2003). TRPC channels, typically thought of as sensory channels, are transiently activated by receptor tyrosine kinases and G-protein-coupled receptors in response to various stimuli including temperature, pain, osmolarity and mechanical stress (Clapham, 2003). During axon pathfinding, TRPC channels (including TRPC1 and TRPC3) regulate growth cone turning responses to guidance cues such as netrin-1, BDNF and MAG (Shim et al., 2005; Li et al., 2005b; Gasperini et al., 2009). TRPC5 has been implicated in the regulation of filopodial length and neurite extension, suggesting a role of TRPC channels in neurite outgrowth as well as growth cone pathfinding (Greka et al., 2003). TRPC channels are likely to regulate distinct pathways in growth cones by generating different spatiotemporal Ca^{2+} signals regulated by the activation of phospholipase C (PLC) and phosphatidylinositol 4,5-biphosphate (PIP_2) (Ramsey et al., 2006; Mori et al., 2015).

VGCC are plasma membrane ion channels that are activated upon membrane depolarisation to mobilise Ca^{2+} into cells. VGCC generate fast Ca^{2+} fluxes that control a

range of physiological processes including neurotransmission, muscle contraction and cell differentiation (Catterall, 2000; Bootman et al., 2001; Catterall, 2011). With respect to growth cone pathfinding, L-type VGCC regulate netrin-1 induced growth cone turning (Hong et al., 2000; Nishiyama et al., 2003). However, this necessity is likely to be context dependent or cell specific as L-type VGCC are also non-essential for netrin-1 and BDNF induced growth cone turning in rat sensory neurons (Gasperini et al., 2017).

1.4.2 Intracellular calcium: endoplasmic reticulum

In addition to influx from extracellular sources, Ca^{2+} can also be mobilised from internal stores, such as the endoplasmic reticulum (ER). Ca^{2+} release from the ER regulates signal amplification by sustaining an initial rise in $[Ca^{2+}]_i$ through a process that can be induced by Ca^{2+}, known as Ca^{2+}-induced Ca^{2+} release (CICR) through activation of ryanodine receptors, or inositol-1,4,5-triphosphate (IP_3), termed IP_3-induced Ca^{2+} release (IICR) (Tojima et al., 2011). At the growth cone, Ca^{2+} mobilisation through ryanodine and IP_3 receptors (RyR and IP_3R) is necessary for extension and Ca^{2+}-dependent growth cone attraction (Takei et al., 1998; Hong et al., 2000; Jin et al., 2005a; Ooashi et al., 2005; Li et al., 2005b; Tojima et al., 2007; Akiyama et al., 2009; Akiyama and Kamiguchi, 2010; Wada et al., 2016). Release of Ca^{2+} from the ER increases the magnitude of $[Ca^{2+}]_i$, and sustains these signals (Hong et al., 2000).

Ca^{2+} can also be mobilised from the ER upon cyclic nucleotide signalling, a process known to be necessary for axon pathfinding (Lohof et al., 1992). cAMP facilitates attractive turning by activating ligand-dependent RyR and IP_3R, whilst cGMP facilitates repulsive turning by inactivating RyR and inhibiting Ca^{2+} mobilisation from the ER (Nishiyama et al., 2003; Ooashi et al., 2005; Tojima et al., 2009). IP_3R and RyR on the ER can be phosphorylated by the cyclic nucleotide-dependent protein kinases, PKA and PKG. Phosphorylation of IP_3R and RyR channels increase Ca^{2+} release from ER stores,

while receptor dephosphorylation decreases Ca^{2+} release (Foskett et al., 2007; Zalk et al., 2007). In this manner, second messenger crosstalk regulates mobilisation of Ca^{2+} from the ER stores to sustain Ca^{2+} signalling within growth cones. The ER however is a finite store of Ca^{2+} and becomes depleted following sustained release of Ca^{2+}. Depleted ER stores activate a process known as store operated Ca^{2+} entry to replenish Ca^{2+} levels.

1.4.3 Store Operated Calcium entry

One source of Ca^{2+} and an important regulator of Ca^{2+} levels and replenishment of intracellular Ca^{2+} stores is store operated Ca^{2+} entry (SOCE). Sarcoplasmic/endoplasmic reticulum Ca^{2+} ATPase (SERCA) pumps refill the ER by transporting Ca^{2+} from the cytoplasm to the ER lumen (Higgins et al., 2006). A mechanism that allows Ca^{2+} to re-enter the cytoplasm in response to ER depletion is required to refill the ER stores and maintain Ca^{2+} signals. This mechanism is known as capacitative Ca^{2+} entry or SOCE (Putney, 1986; Lewis, 2007). SOCE mobilises Ca^{2+} from the extracellular space and refills the depleted ER stores to prolong Ca^{2+} signalling (Tsien et al., 1988; Hoth and Penner, 1992; Harraz and Altier, 2014) and sustain growth cone turning responses (Mitchell et al., 2012).

The influx of Ca^{2+} triggered by SOCE, is referred to as Ca^{2+} release-activated Ca^{2+} (CRAC) current or I_{CRAC} and functions independently of membrane voltage changes (Hoth and Penner, 1992). It was initially thought that CRAC currents predominate in non-excitable cells and VGCC predominate in excitable cells including neurons, however the machinery for both sources of Ca^{2+} influx are present in neuronal cells (Park et al., 2010; Wang et al., 2010). I_{CRAC}, is gated through a number of ion channels including TRPC and Orai, and is triggered after store depletion. I_{CRAC} is mediated by the Ca^{2+} sensing ER proteins stromal interacting molecule 1 and 2 (STIM1 and STIM2) (Huang et al., 2006; Yuan et al., 2007). In non-neuronal cells, STIM1 is known to activate SOCE through its

interaction with plasma membrane proteins Orai1, 2 and 3, resulting in the formation of a CRAC current (Liou et al., 2005; Roos et al., 2005; Zhang et al., 2005; Prakriya et al., 2006; Soboloff et al., 2006). The roles of STIM1 and STIM2 have been well studied in non-excitable tissues, however less is known about STIM function and how SOCE regulates Ca^{2+} dynamics in the developing nervous system. STIM1 and/or Orai have more recently been implicated in neuronal Ca^{2+} homeostasis and axon pathfinding (Gasperini et al., 2009; Steinbeck et al., 2011; Mitchell et al., 2012; Shim et al., 2013). STIM1 regulates growth cone navigation in sensory neurons by mediating SOCE in response to BDNF induced chemoattraction. STIM1 also functions in sema-3a induced chemorepulsion by an unknown mechanism likely to be SOCE-independent (Mitchell et al., 2012). Within the growth cone STIM1 is actively recruited asymmetrically during growth cone turning, dynamically participating in the regulation of growth cone motility (Mitchell et al., 2012). Mechanisms that regulate STIM1 motility and subsequent Ca^{2+} influx have yet to be determined.

1.5 Stromal Interacting Molecule 1 (STIM1) is a key regulator of store operated calcium entry

STIM1, the main regulator of SOCE following store depletion (Liou et al., 2005; Roos et al., 2005; Zhang et al., 2005), is structurally complex and multifunctional. The three most studied STIM proteins are STIM1, STIM2 and D-STIM; however, due to its role in neuronal Ca^{2+} homeostasis and growth cone dynamics, the focus of this thesis is on STIM1. STIM1 is a 90 kDa single-pass transmembrane phosphoprotein that is ubiquitously expressed in most tissues (Dziadek and Johnstone, 2007). STIM proteins possess a number of motifs which allow this family of proteins to interact with a range of molecules. The N-terminus of STIM1 is located within the ER lumen and contains a single helix-loop-helix motif, also known as the EF-hand Ca^{2+}-binding domain which binds Ca^{2+} within the ER. The N-terminus also contains a conserved single sterile-α motif (SAM)

domain involved in protein-protein interactions (Schultz et al., 1997; Williams et al., 2001; 2002; Dziadek and Johnstone, 2007). The C-terminus contains two alpha helices that are predicted to form coiled-coils, and which reside within an ezrin/radixin/moesin (ERM) domain (Dziadek and Johnstone, 2007). The C-terminus of STIM1 also contains a highly conserved small polypeptide motif, (TRIP), which participates in hydrophobic interactions with microtubule-associated proteins and makes STIM1 a SxIP-consensus protein (Honnappa et al., 2009; Kumar and Wittmann, 2012). The function of SxIP motif in STIM1 will be discussed in more detail in the coming section.

The process of SOCE occurs following STIM1 oligomerisation and CRAC activation. Upon store depletion, the luminal tertiary fold of STIM1 becomes unstable and exposes the hydrophobic unpaired EF-hand and the SAM domain. This conformational change allows STIM1 to oligomerise and activate SOC channels (Dziadek and Johnstone, 2007; Luik et al., 2008). STIM1 oligomers translocate and form puncta in close proximity to the plasma membrane (ER-PM junctions) (Carrasco and Meyer, 2011). Here, STIM1 triggers the formation of CRAC channels (Liou et al., 2005; Zhang et al., 2005; Baba et al., 2006; Wu et al., 2006; Luik et al., 2008). STIM1 oligomers interact with plasma membrane proteins Orai1, the pore-forming subunits of CRAC channels (Feske et al., 2006; Prakriya et al., 2006). Orai1 proteins cluster into tetramers and form CRAC channels (Soboloff et al., 2006; Lewis, 2007; Stathopulos et al., 2008) (Figure 1.3). While most of the SOCE literature focuses on the interaction of STIM1 and Orai1, SOCE has been reported to occur through STIM1-activation of other ion

Figure 1.3- STIM1 senses luminal ER Ca^{2+} levels to activate Orai1 for SOCE

(i) Under Ca^{2+} replete conditions monomers of the endoplasmic reticulum-(ER) protein stromal interacting molecule 1 (STIM1), which bind Ca^{2+} by the unpaired EF hand domain, are uniformly distributed along the ER membrane. (ii) As ER Ca^{2+} is released from the stores through IP_3R/RyR, (iii) Ca^{2+} depletion causes STIM1 monomers to oligomerise and translocate into larger complexes at ER-PM junctions (arrowhead). STIM1 interacts with Orai, causing Orai dimerisation and the formation of a Ca^{2+} release-activated Ca^{2+} (CRAC) channel that facilitates store operated Ca^{2+} entry (SOCE) into the cytoplasm. (iv) Ca^{2+} entering the cytosol through SOC channels is rapidly sequestered to the ER via the sarco/endoplasmic reticulum Ca^{2+}-ATPase (SERCA) pump, facilitating store repletion.

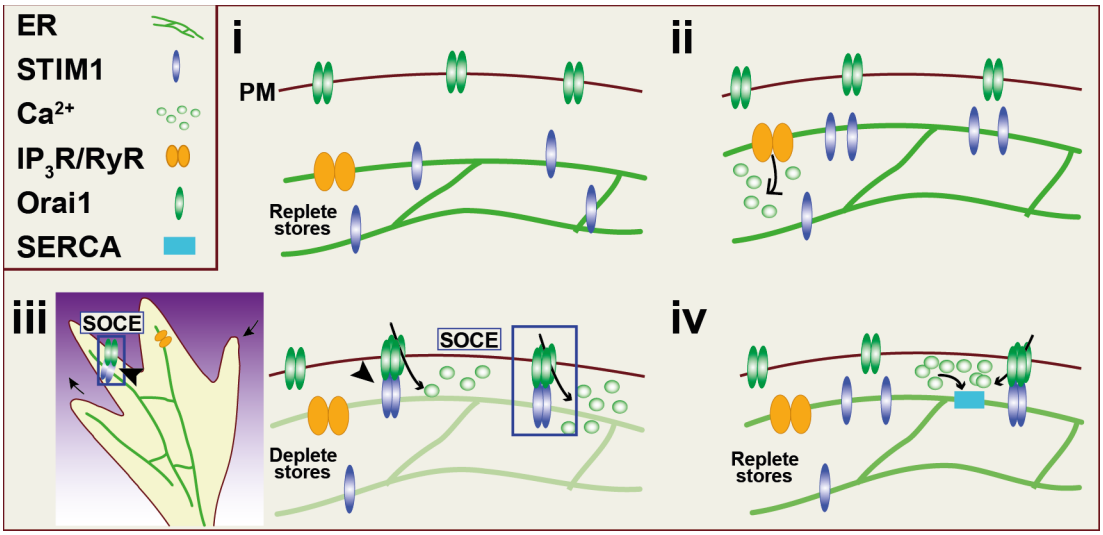
ER
STIM1
Ca2+
IP3R/RyR
Orai1
SERCA
i
PM
Replete stores
ii
iii
SOCE
Deplete stores
SOCE
iv
Replete stores

channels including TRPC channels (Yuan et al., 2007) and CRACM2 and 3 (Orai2 and 3) (Lis et al., 2007).

The molecular mechanisms by which STIM1 mediates SOCE are well understood, however it remains unclear whether STIM1 also regulates ER rearrangement to facilitate SOCE and if so, by what mechanism. Localisation and motility of intracellular signalling proteins and organelles is in most cases regulated by the cytoskeleton. ER structure and function is known to be influenced by the microtubule cytoskeleton (Terasaki et al., 1986). A number of studies have reported that drug-induced depolymerisation of actin and microtubules into monomers does not negatively impact or inhibit SOCE in various cell lines (Ribeiro et al., 1997; Patterson et al., 1999; Baba et al., 2006). In contrast, there is evidence that the organisation of STIM1 and microtubules is strikingly similar (Baba et al., 2006; Mercer et al., 2006) and that microtubule depolymerisation using nocodazole disrupts SOCE, I_{CRAC} and the organisation of EYFP-STIM1 in HEK 293 cells (Smyth et al., 2007). These findings indicate that, through the organisation of STIM1, microtubules might facilitate SOCE by optimising communication between STIM1 and PM-channel Orai (Smyth et al., 2007). STIM1-directed reorganisation of microtubules has also been demonstrated to function in mast cell activation (Hájková et al., 2011a), further supporting a mechanism of tight crosstalk between Ca^{2+} signalling and cytoskeleton structures. As discussed earlier in this review, Ca^{2+} signalling in growth cones regulates the assembly and disassembly of the cytoskeleton by activating kinase and phosphatase activity respectively however, whether a direct physical link between the main source of Ca^{2+} and the cytoskeleton exists is unclear.

1.6 Endoplasmic reticulum in growth cones: a source of localized calcium?

The ER is a major store of intracellular Ca^{2+} and release of Ca^{2+} from the ER is important for axon outgrowth in various models, including *Xenopus* motor neurons (Gomez and Spitzer, 2000; Gu and Spitzer, 1995) and chicken dorsal root ganglion neurons (Wada et al., 2016). However, it is unknown whether ER can regulate the spatiotemporal localisation of Ca^{2+} signals in motile growth cones, which would require the remodelling of ER. The mechanisms that would control this process have not been previously explored. What little is known about ER organisation in growth cones is from early work that examined the spatial and temporal dynamics of ER-like membranes at the neuronal growth cone using a fluorescent lipophilic dye which targets and marks membrane-bound organelles (Dailey and Bridgman, 1989). ER-membrane distribution was examined during growth cone advance and was seen to actively remodel (extend, retract and change direction) at the advancing peripheral edge. By co-labelling with a microtubule marker, a striking colocalisation (79%) between microtubules and ER-like membranous-organelles was observed at the growth cone periphery (Dailey and Bridgman, 1989). The authors concluded that ER-like membranes were possibly regulating local Ca^{2+} signals to affect microtubule stability and overall coordination of growth cone activity (Dailey and Bridgman, 1989). At the time, this conclusion was in agreement with findings from Kater and colleagues who had proposed that localised Ca^{2+} signals of different magnitudes are required to regulate motile growth cone behaviours (Kater et al., 1988). Taking these findings into consideration, Dailey and Bridgman inferred that a Ca^{2+}-sequestering organelle such as the ER, was likely to distribute with microtubules to regulate the localisation of Ca^{2+} in growth cones (Dailey and Bridgman, 1991). Furthermore, the authors proposed that ER-like membranes formed transport tracks with microtubules to facilitate movement of other organelles after observing that vesicle-like structures

followed tubular membranous-organelles into the growth cone periphery (Dailey and Bridgman, 1989).

Since these studies, membrane trafficking has been extensively studied in steering growth cones and Kamiguchi and colleagues have recently reported that ER-derived Ca^{2+} signals facilitate the microtubule-dependent trafficking of vesicle-associated membrane protein 2 (VAMP2)-positive vesicles (Wada et al., 2016). VAMP2-vesicle trafficking was asymmetrically distributed to the side of the growth cone with highest Ca^{2+} concentration. The Ca^{2+}-dependent motor protein, myosin Va (MyoVa), was shown to tether VAMP2-positive vesicles to the ER via IP_3R/RyR binding sites and localise the vesicles to the side of elevated Ca^{2+} in growth cones responding to attractive cues (Wada et al., 2016). Exocytosis-induced growth cone attraction resulted from dissociation of MyoVa from ER binding site and release of VAMP2-positive vesicles following activation of CICR (Wada et al., 2016). This work demonstrates a mechanism in which Ca^{2+}-induced membrane targeting regulates growth cone motility and indicates that direct interactions between ER and microtubules facilitate signal localisation, membrane recycling and spatial localisation of store Ca^{2+}. Exactly how ER is spatially localised or remodelled in growth cones is unknown.

Microtubule-dependent ER remodelling can occur in three ways in non-neuronal cells (Waterman-Storer and Salmon, 1998): ER-membrane sliding (Allan and Vale, 1991; Schroer and Sheetz, 1991; Allan and Vale, 1994; Friedman et al., 2010), microtubule-based movement (Vale and Hotani, 1988), and movement via a microtubule tip attachment complex (TAC) (Waterman-Storer et al., 1995). ER remodelling is often regulated by ER-sliding mechanism through motor proteins kinesin1 and dynein (Wozniak et al., 2009; Friedman et al., 2010), rather than a TAC. However a TAC, which comprises the binding of ER-protein STIM1 to the microtubule-binding-protein EB1 (and EB3) (Grigoriev et al., 2008) via the SxIP motif (Honnappa et al., 2009), enables ER

tubules to grow and shrink in parallel with the polymerising microtubule plus-ends. Recently, STIM1-mediated SOCE was shown to regulate axon guidance of sensory neurons (Mitchell et al., 2012) and the oscillatory filopodial Ca^{2+} dynamics of *Xenopus* spinal cord commissural interneurons (Shim et al., 2013). Co-distribution of ER and microtubules through TAC might be a specific mechanism by which STIM1 regulates ER remodelling at the growth cone periphery for the sustainment of filopodial Ca^{2+} transients, which are necessary for the regulation of pathfinding behaviours.

Following the report that STIM1 functions as a microtubule plus-end-tracking protein to regulate ER remodelling by bridging ER and microtubules in non-neuronal cells (Grigoriev et al., 2008), a relay-type of association between STIM1 and +TIPs EB1 and APC was investigated (Asanov et al., 2013). An association between STIM1 and APC is necessary for the anchoring of STIM1 puncta at ER-PM junctions in non-neuronal cells, which form following store depletion and likely represent sites of CRAC. The authors demonstrated that STIM1 interacts with EB1 when the ER stores are replete, and this interaction is fundamental for tracking of ER along the microtubules (Grigoriev et al., 2008; Asanov et al., 2013). Upon store depletion, STIM1 dissociates from EB1 and interacts with APC in a relay-type mechanism that facilitates the anchoring of STIM1 at ER-PM junctions (Asanov et al., 2013). Such a mechanism of STIM1-mediated ER-microtubule interaction which is dependent on Ca^{2+}_{ER} content, provides a direct link between ER-derived Ca^{2+} signals (CICR and IICR), ER-induced Ca^{2+} signals (SOCE) and the cytoskeleton (microtubules via EB1, and actin via APC). Whether STIM1 facilitates sustained and localised Ca^{2+} within growth cones through direct bridging of ER and the microtubule cytoskeleton, is one of the questions this thesis will aim to answer as it would signify a mechanism for directly regulating spatiotemporal Ca^{2+} signals in motile growth cone.

Early work by Dailey and Bridgman using freeze-etch EM on growth cones from superior cervical ganglia explants (Dailey and Bridgman, 1991), showed that while ER-like membranes occasionally protruded into the periphery of the growth cone unaccompanied by microtubules, smooth ER-like membranes were often observed extending to microtubule tips. Interestingly, associations between microtubules and ER membranes were most obvious at the electron-dense microtubule tip (Dailey and Bridgman, 1991). The presence of cross-bridging elements between microtubules and ER-like membranes were reported and were, at the time, hypothesised to correspond to microtubule-based motors, such as kinesin (Vale et al., 1985; Vale and Hotani, 1988; Dailey and Bridgman, 1991). The significance of a direct association between microtubules and ER, given the ability of ER to sequester and release Ca^{2+} (Somlyo, 1984), lie in the fact that Ca^{2+} is a known local regulator of microtubule stability and polymerisation (Schliwa et al., 1981). Such an interaction would provide less stable microtubules protruding into the growth cone periphery with spatially restricted local Ca^{2+} signals required to sustain extension and growth. Direct ER-microtubule interactions have been previously explored in non-neuronal cells in the context of tethering of STIM1 to +TIP proteins EB1/3 (Grigoriev et al., 2008) and association of ER with the microtubule-based motor protein kinesin-1 (Wozniak et al., 2009; Friedman et al., 2010; Friedman and Voeltz, 2011). IP_3R, embedded within the ER, has also been reported to bind the microtubule +TIP EB3 in endothelial cells. Binding of IP_3R to EB3 occurs through the TxIP motif in IP_3R, and binds with less affinity that when binding to STIM1 (Geyer et al., 2015). Consistent with previously reported roles of microtubules in organising IP_3R-evoked Ca^{2+} signalling, Rac1 has been shown to induce microtubule-dependent ER protrusion into the growth cone periphery whilst simultaneously promoting IP_3-mediated Ca^{2+} release via ROS production (Zhang and Forscher, 2009). Understanding whether Ca^{2+} is sustained and localised within growth cones through direct association between ER and microtubules is a major focus of this thesis as it would provide a direct method for regulating spatiotemporal Ca^{2+} signals in motile and pathfinding growth cone.

1.7 Hypothesis

It has been proposed that EB-STIM1 interactions enable ER tracking along microtubules for the facilitation of SOCE upon ER depletion and the localization of Ca^{2+} (Smyth et al., 2007). Aside from evidence suggesting STIM1 and microtubule organization is strikingly similar (Baba et al., 2006; Mercer et al., 2006), evidence indicates that microtubule depolymerization disrupts SOCE and I_{CRAC} (Smyth et al., 2007) and that STIM1-directed rearrangement of microtubules occurs in mast cell activation (Hájková et al., 2011a). Altogether, these studies suggest that ER and microtubules are interdependent structures likely to function in close apposition and influence the function of the other, and STIM1 is likely to facilitate such interactions as a microtubule-binding protein and mediator of SOCE. Furthermore, STIM1 is expressed at the growth cone of rodent sensory neurons where STIM1 mediates SOCE-dependent growth cone steering to BDNF through CaMKII/CaN switch, as well as SOCE-independent turning to sema-3a by unclear mechanisms (Mitchell et al., 2012). This suggests that STIM1 is multifunctional in growth cones, however it is unknown whether STIM1 functions as a microtubule-binding protein in growth cones to directly link ER-derived Ca^{2+} to the microtubule cytoskeleton for the regulation of growth cone motility. Such mechanism in growth cones would provide a direct target for spatiotemporally localizing Ca^{2+} signals necessary to mediate axon steering. Therefore, the central hypothesis of this work is that **STIM1 regulates ER-microtubule dynamics which are necessary to spatially and temporally localize the Ca^{2+} signals required to sustain growth cone motility and pathfinding**.

1.7.1 Aims

To address the central hypothesis, a series of aims that utilize live cell imaging, immunocytochemistry, and optogenetics, have been devised to examine the role of STIM1 in cytoskeletal remodelling at the motile growth cone:

Aim 1: Investigate whether STIM1 associates with the cytoskeleton in motile growth cones

-Examine whether actin/microtubule-regulatory factors, and adhesion components are disrupted in growth cones with reduced STIM1 expression.

Aim 2: Determine whether STIM1 regulates functions of the microtubule cytoskeleton during growth cone steering

-Examine whether STIM1 acts as a microtubule-binding protein in growth cones, as reported to occur in non-neuronal cells

-Determine whether STIM1 expression is required for polymerization and spatial rearrangement of microtubules

Aim 3: Examine whether STIM1 is required for instructive ER-microtubule remodelling at growth cone filopodia

-Determine if there are functional microtubule-ER interactions at the growth cone filopodia, and whether these interactions are mediated or regulated by STIM1 expression

-Examine whether STIM1 expression is required to maintain and regulate Ca^{2+}_{ER} at growth cone filopodia

Chapter 2:

Methods and Key Resources

2.1 Experimental model details

All animal procedures were conducted under the approval of the University of Tasmania Animal Ethics Committee (Ethics number A14975), consistent with the Australian NHMRC Code of Practice for the Care and Use of Animals for Scientific Purposes. Female Sprague Dawley rats (Animal Facility, University of Tasmania) were used.

2.2 Materials/Reagents

For detailed list of materials/reagents used, see key resources (Appendix 1).

2.3 Sensory neurons cell culture and pharmacology

2.3.1 Cell culture

Primary sensory neuron cultures were prepared as described previously (Gasperini et al., 2009; Mitchell et al., 2012). Pregnant Sprague Dawley rats were euthanized by CO_2 inhalation. Embryonic day (E)16-18 embryos were immediately dissected. Thoracic dorsal root ganglia (DRG) from E16–18 embryos were mechanically dissociated and cultured in sensory neuron media (SNM; Dulbecco's Modified Eagle's Medium/Hams F-12 medium 1:1, Penicillin-Streptomycin [100µg/ml], N2 neural medium supplement [1% v/v], foetal calf serum [%5 v/v], nerve growth factor [50ng/ml]) for 4–6hr prior to imaging.

2.3.2 Protein knockdown

Protein expression was reduced using morpholinos, as described previously. DRG were mechanically dissociated in the presence of morpholinos (5µM) and plated at low density onto glass coverslips treated with poly-ornithine (1mg/ml) and laminin (50ng/ml). Protein knockdown was confirmed by immunofluorescence as previously described (Mitchell et

al., 2012). Similarly, Orai1 siRNA (10nM) was used to reduce the expression of Orai1 protein.

2.3.3 Pharmacology

The microtubule-stabilising drug epothilone D (EpoD) was bath-applied in SNM at 0.1nM (higher concentrations halt axon extension) for 4hrs prior to imaging. An inhibitor of sarco/endoplasmic reticulum Ca^{2+}-ATPase (SERCA), thapsigargin (TG), was bath-applied in SNM at 50nM for 5min to deplete ER Ca^{2+} stores. Control cells were incubated with vehicle (SNM).

2.4 *In vitro* growth cone turning assay

Growth cone turning assays were performed as previously described (Lohof et al., 1992; Gasperini et al., 2009; Mitchell et al., 2012). Brain derived neurotrophic factor (BDNF, 10µg/ml) and semaphorin-3a (sema-3a, 20µg/ml) were loaded into fire-polished micropipettes (tip diameter of 1.0-1.2µm) and positioned at a 45^{o} angle and 75-100µm from isolated growth cones, to obtain a molecular gradient with an estimated concentration of 10^{-3} at the growth cone (Lohof et al., 1992). The molecular gradient was created by pulsatile ejection (Picospritzer, Parker, USA), using a pressure of 5psi at a rate of 1Hz (Gasperini et al., 2009; Mitchell et al., 2012). Phase images were obtained using Matlab analysis software (Mathworks Inc., USA) every 7sec for 30min (acquisition times varied depending on the experiment, parameters specified in individual sections). Analysis of time-lapse images was performed using ImageJ (NIH, USA). Turning angles were measured for growth cones which extended at least 10µm over 30min of imaging and that did not interact with neighbouring cells or debris. The angle of turning was defined as the change in axon trajectory, relative to the pipette, of the distal 10µm axon. Attraction was defined as a positive turning angle towards the micropipette, while repulsion was defined as a negative turning angle away from the micropipette. Statistical

analysis for turning data, Mann-Whitney *t*-test, was performed using GraphPad Prism (GraphPad Software, USA).

2.5 Immunocytochemistry

Protein expression in control and STIM1 morphant cells were determined by immunocytochemistry. Briefly, cells were fixed in 4% paraformaldehyde (in PBS) at room temperature for 5min, and 100% methanol at -20°C for 15min, followed by blocking (5% foetal calf serum in PBS). Primary antibodies for STIM1, β3-tubulin, EB1/3, APC and drebrin (see Appendix 1) were detected using Alexa Fluor 405/488/568/647 secondary antibodies. Images were acquired using an UltraView spinning disk confocal microscope (PerkinElmer, USA), equipped with a 100x 1.5-numerical aperture objective, and acquisition software (Volocity Image Analysis Software, Perkin Elmer).

2.5.1 Immunocytochemistry in turning growth cones

Control and STIM1 morphant cells were grown on gridded coverslips (enabling localization of individual growth cones post-turn and post-processing). Cells were fixed after 15min exposure to guidance cues (vehicle/SNM, BDNF or Sema3a) and processed for immunocytochemistry as previously described (Mitchell et al., 2012). STIM1, EB-1/3, APC, drebrin and F-actin expression, as well as polymerized microtubules were determined using ImageJ software analyses. Protein expression levels or the number of polymerized microtubules on the near and far sides of the growth cone with respect to the micropipette (ie. near side of growth cone is closest to micropipette) were determined and presented as a near/far ratio.

Protein expression was assessed by two analysis methods: integrated pixel intensity and puncta analyses. Integrated pixel intensity (ImageJ) from each half of the growth cone was used to derive a pixel intensity near/far ratio (Leung et al., 2006). Each growth cone

half was determined by parting along the middle of the growth cone relative to the distal axon, and pixel intensity from each half was normalized to area. For puncta analysis, 8-bit images were background subtracted and thresholded (RenyiEntropy filter, ImageJ). Particle numbers from each half were used to derive a puncta near/far ratio. Both methods gave consistent measures for all proteins assessed.

2.5.2 Immunocytochemistry for protein colocalisation analysis

Cultures were grown for 4hr then incubated with vehicle or thapsigargin (50nM) for 5min prior to fixation (Mitchell et al., 2012). Cells were fixed at room temperature for 5min, and permeabilised using 100% methanol at -20°C for 15min. Primary antibodies for STIM1 and EB-1/3 were detected using Alexa Fluor 488/594 secondary antibodies. Overlap coefficients were calculated between colocalisation channels corresponding to STIM1 and EB1/3 in vehicle-treatment and thapsigargin-treated cells. Analysis was conducted using Manders' overlap coefficient plugin (Manders et al., 1993).

2.6 Transfection methods used for protein overexpression

DRG sensory neurons are difficult to transfect, hence four approaches were used to express fluorescently labelled proteins in sensory neurons: transfection using baculovirus-packaged fusion markers, magnetic particles, lentivirus packaging, and electroporation.

2.6.1 BacMam transfection

BacMam technology, which uses baculovirus-packaged fusion constructs, was used for co-labelling of microtubules and ER. Cells were incubated at 37°C and 5% CO_2 overnight with CellLight Tubulin-GFP and CellLight ER-RFP (see Appendix 1) according to manufacturer's instructions (Thermo Fisher Scientific, USA).

2.6.2 Magnetofection

Magnetic particles were used to transfect EB1-RFP and EB3-YFP in sensory neurons. Cells were transfected following manufacturer's instructions (NeuroMag; Oz Biosciences, France). Briefly, NeuroMag-DNA complexes were formed with 0.75μl NeuroMag to 1μg DNA (EB3-YFP) in serum-free solution for 20min. Plated cells (transfected with control or STIM1-specific morpholino, as described in section *2.3.2*) were incubated with NeuroMag-DNA complexes over a magnetic plate for 20min, then incubated at 37°C and 5% CO_2 overnight for imaging.

2.6.3 Lentivirus production and transduction

For transfection of EB3-YFP in growth cones used for turning experiments, a lentiviral approach was also used. The gene sequence encoding EB3-YFP was sub-cloned into a second-generation lentiviral construct with a neuron-specific human synapsin (hSyn) promoter, using ligation of PCR-amplified insert (EB3-YFP) and lentiviral vector. Lentiviral particles were then made as previously described (Lin et al., 2013). Briefly, HEK293A cells were grown to 90% confluency, and transfer vectors pLenti_hsyn_EB3-YFP, psPAX2 and pMD2.G (see Appendix 1) were transfected using Effectene (QIAGene, Germany). Virus particles were harvested from HEK293A cells in low-serum-containing medium and concentrated using an Amicon Ultra centrifugal filter (Millipore, USA). Whole DRG were gently dissociated with lentiviral particles in SNM (particle number not calculated, 20μl of concentrated solution per 12-well coverslip), and cells were incubated for 24hr (in suspension). Media was exchanged and cells were again incubated for 24hr, at 4°C. Cells were gently triturated with morpholinos, plated and incubated at 37°C and 5% CO_2 for 4–6hr prior to imaging.

2.6.4 Electroporation by nucleofection method

Electroporation was used for co-transfection of EB3-tdTomato and ER-GCaMP6, or EB3-YFP and KDEL-mCherry (see Appendix 1). Dissociated sensory neurons were electroporated using a nucleofector protocol, following manufacturer's instructions (Lonza, Switzerland). Briefly, whole DRG were treated with 0.125% trypsin and gently dissociated. Cells were resuspended in P3 buffer (transfection buffer) and 2 x 10^6 cells were electroporated with 2µg DNA. Cells were incubated in plastic T25 culture flask (Corning, USA) for 2hr to remove or reduce the number of fibroblasts and other non-neuronal cells. Neurons were resuspended in media containing morpholinos and plated on laminin-coated coverslips. Cells were incubated overnight then imaged.

2.7 Live cell imaging: Analysis of OptoSTIM1-induced growth cone motility

Optogenetic stimulation of STIM1 was performed using a light-inducible STIM1 known as OptoSTIM1 (Kyung et al., 2015). HEK293A cells were transfected with OptoSTIM1 using Effectene (QIAGene). Cells were loaded with Fura-2 AM (0.5 µM) in FluoroBrite DMEM (Thermo Fisher Scientific) for 10min at room temperature, then washed and incubated in calcium-replete media (5-10mM $CaCl_2$) at 37°C for a minimum of 10min. Images were acquired using an EMCCD digital camera (Evolve, Photometrics) and motorized inverted microscope (Eclipse TiE; Nikon Instruments Inc) with x40 Flour-S oil-immersion objective. Spatially-restricted regions of HEK cells, or whole field of view, were stimulated for 2sec every 5min with LED light (485nm) using a digital mirror device (Mightex, USA) attached to the light path of the motorized inverted microscope. Fura-2 was alternatively excited (340nm and 380nm), and images were acquired at 510nm wavelength using NIS Elements software (Nikon) every 2sec for 10-15min. The ratio of 340/380 fluorescence (a.u.) was calculated following background subtraction, in cells with medium-to-low levels of OptoSTIM1 over-expression before and after LED stimulation using NIS-Elements AR 4.00.12 software (Nikon, Japan).

Sensory neurons were transfected with OptoSTIM1, a light-insensitive OptoSTIM1 variant OptoSTIM1(Cry2(D387A)), or LOVS1K (see Appendix 1) by electroporation using the Nucleofector Kit (Lonza). Cells were imaged using x100/0.95 oil-immersion objective. Spatially-restricted regions of growth cones (ROIs on one side of growth cone, stimulation-sides were randomly selected) were stimulated by LED light (485nm) using a digital mirror device. Optogenetic stimulation was 2sec every 5min. Phase images were acquired every 2sec for 12min. The angle of turning was defined as the change in axon trajectory measured between the initial trajectory and the final trajectory of the distal 10μm of axon after the 12min imaging period. Repulsion was defined as a negative angle of axon extension on the opposite side of the stimulation side, that is axon growth away from stimulation side. Attraction was defined as a positive angle of turning towards the side of stimulation, and no change in the angle of turning was classified as random growth. Analysis of time-lapse images was performed using ImageJ (NIH, USA).

2.8 Live cell imaging: Analysis of EB3 dash dynamics

Microtubule dynamics were measured using fluorescently-labelled EB3. EB3-YFP was observed as comet-like dashes. Sensory neurons transfected with EB3-YFP were imaged in imaging buffer (FluoroBrite DMEM, 15mM HEPES, 1% Penicillin-Streptomycin, 100x N2 neural medium supplement, 5% foetal calf serum, nerve growth factor [50ng/ml]), using an EMCCD digital camera (Evolve, Photometrics) and motorized inverted microscope (Eclipse TiE; Nikon Instruments Inc) with x40 air objective. Acquisition time for dash movement was 0.14-0.17 Hz for 10-12min in randomly extending growth cones and in response to asymmetric guidance cues. Images were acquired using NIS-Elements AR 4.00.12 software (Nikon, Japan). EB3-YFP trajectories were analysed in filopodia of control and STIM1 morphant growth cones, and in growth cones responding to vehicle/SNM, BDNF and Sema3a. Only dashes that could be tracked for a minimum of three consecutive frames were included in analysis, as

previously described (Stepanova et al., 2003). Parameters measured, including distance travelled and velocity of EB3-YFP dashes, were calculated using Manual tracking on ImageJ software analyses.

2.9 Live cell imaging: Analysis of Ca^{2+}_{ER} dynamics at filopodia

Sensory neurons transfected with EB3-YFP and KDEL-mCherry (as readout of polymerizing microtubules and ER-marker respectively), or EB3-tdTomato and ER-GCaMP6 (as readout of polymerizing microtubules and Ca^{2+}_{ER} sensor respectively), were imaged using a x100/0.95 oil-immersion objective. Images were acquired at 0.5 Hz for 5min, with EB3-tdTomato fluorescence and phase images acquired simultaneously. Analysis of microtubule-ER remodelling and microtubule-Ca^{2+}_{ER} dynamics in filopodia included percentage measurement of filopodia expressing KDEL-mCherry or ER-GCaMP6 signal in control and STIM1 morphant growth cones and distance of EB3-KDEL or EB3-ER-GCaMP6 protrusion into filopodia.

Integrated filopodial Ca^{2+}_{ER} ($\Delta F/F_0$) was calculated by averaging $\Delta F/F_0$ values over 20sec at three positions within the filopodia (tip-most, middle and base) where EB3 dashes were present. Average filopodial ER-GCaMP signal ($\Delta F/F_0$) was calculated from the average ER-GCaMP6-150 relative fluoresce at the time coinciding with peak EB3 intensity signal response (ie. point in time where EB3 dash was present at filopodial base, middle, or tip-most section). Measurements of filopodial Ca^{2+}_{ER} in control and STIM1 morphant growth cones were analysed using NIS-Elements AR 4.00.12 analyses software.

2.10 Statistical analyses

All data were organized using Microsoft Excel and analysed using and GraphPad Prism 6 (GraphPad Software Inc., USA). Statistical analyses include Student's *t*-test, Mann–Whitney U-test (growth cone turning data), one-way ANOVA (using Tukey's multiple comparison test) and Two-way ANOVA (Ca^{2+}_{ER} dynamics). p-values are defined as *p < 0.05, **p < 0.01, ***p < 0.0005 and ****p < 0.0001, unless otherwise stated.

Chapter 3:

STIM1 interacts with the growth cone cytoskeleton

Chapter 3: STIM1 interacts with the growth cone cytoskeleton

3.1 Introduction

STIM1 is multifunctional as evidenced by its regulation of Ca^{2+} influx through Orai1 (Lis et al., 2007; Yuan et al., 2007), association with cytoskeletal proteins such as EB-1/3 and APC (Grigoriev et al., 2008; Asanov et al., 2013) and focal adhesion turnover (Yang et al., 2009; Chen et al., 2011; 2013). The question of how STIM1-mediated Ca^{2+} signaling regulates cytoskeletal-dependent events such as motility, migration and cell adhesion has been examined in a range of cell types and models. In migratory cancer cells, STIM1 activates SOCE to regulate actin organization, focal-adhesion turnover and contractility (Yang et al., 2009; Chen et al., 2011; 2013). Additionally, in non-neuronal cells STIM1 binds to homologs of the end-binding (EB) family, EB1 and EB3 (EB-1/3) to form tip attachment complexes at microtubule plus-ends, thereby enabling ER coupling to microtubule plus-ends (Grigoriev et al., 2008; Honnappa et al., 2009). In growth cones, this coupling would be predicted to actively remodel ER adjacent to microtubule polymerization. In this chapter, we sought to examine whether STIM1 interacts with the growth cone cytoskeleton, as such interactions could explain how STIM1 regulates SOCE-dependent and –independent growth cone steering (Mitchell et al., 2012).

Actin and microtubules act co-operatively to regulate growth cone motility (Rodriguez et al., 2003). A number of studies have demonstrated that inhibition of either actin or microtubule polymerization disrupts growth cone pathfinding (Marsh and Letourneau, 1984; Bentley and Toroian-Raymond, 1986; Tanaka et al., 1995). For example, destabilization of actin bundles on one side of the growth cone using collapsing factor ML-7 inhibited local microtubule protrusion to the growth cone periphery and resulted in axon extension away from the treated (collapsing) side (Zhou et al., 2002). Also, microtubule extension at the growth cone periphery is required to sustain lamellipodial protrusions and growth cone turning (Buck and Zheng, 2002). Local microtubule

stabilization using taxol altered growth cone steering by inducing actin-based protrusions through Rho-GTPase activity (Buck and Zheng, 2002). This dynamic interplay between microtubules and actin is regulated by second messengers such as Ca^{2+}, cyclic nucleotides and the Rho GTPases.

The Rho GTPases regulate cytoskeletal phosphorylation and are activated by various proteins including the Ca^{2+}-dependent kinases CaMKII and protein kinase C (PKC) (Jin et al., 2005b). Cdc42/Rac activation promotes axon growth, while RhoA activation inhibits axon growth and favours retraction (Hall, 1998). In growth cones, local rises of Ca^{2+} activate Cdc42/Rac and inactivate RhoA to promote directed axon extension in response to guidance cues (Jin et al., 2005b). Rho GTPases might also facilitate the localization of Ca^{2+} signals in the growth cone. Rac1 promotes microtubule/ER protrusion to the growth cone periphery and facilitates IP_3-dependent Ca^{2+}_{ER} release in response to the signaling cue serotonin (Zhang and Forscher, 2009). Collectively, these studies demonstrate a complex interplay of Ca^{2+}-dependent signaling events which converge on the cytoskeleton to regulate growth cone motility. This dynamic interplay between microtubules and actin is also regulated more directly through the formation of cytoskeleton-associated protein complexes.

Drebrin and adenomatous polyposis coli (APC) are two microtubule-actin associated proteins which form complexes that mediate structural cytoskeletal interactions within growth cones (Geraldo and Gordon-Weeks, 2009). Drebrin is an actin-filament associated protein that binds EB3 at polymerising microtubule tips in proximal areas of filopodia (Geraldo et al., 2008). By binding EB3, drebrin participates in filopodial formation by sustaining microtubule invasion into filopodia at lamellipodial borders (Geraldo et al., 2008). In growth cones, actin-microtubule interactions are also regulated by APC. The local activation of APC stabilizes actin and microtubules in growth cones responding to NGF (Zhou et al., 2004). As a microtubule-tracking protein APC can also

regulate spatiotemporal microtubule dynamics by alternatively stabilising and destabilising microtubule filaments (Akhmanova and Steinmetz, 2008). Like drebrin, APC also binds EB proteins. APC binds EB proteins through a microtubule-tip localization motif, which is also present in STIM1 (SxIP, or TxIP in STIM1). STIM1 associates and dissociates from EB-1/3 in a manner that is dependent on luminal ER Ca^{2+} (Ca^{2+}_{ER}) content (Grigoriev et al., 2008; Honnappa et al., 2009). Asanov and colleagues demonstrated that in HEK293T cells, STIM1 dissociates from EB1 upon store depletion and subsequently binds APC to activate the CRAC and induce SOCE at ER-PM junctions (Asanov et al., 2013).

STIM1 binding to EB-1/3 represents a powerful mechanism for localising ER to microtubules. This interaction regulates ER-remodelling (Grigoriev et al., 2008; Honnappa et al., 2009) and optimizes STIM1 localisation for SOCE in non-neuronal cells (Smyth et al., 2007). Such a mechanism in growth cones could spatially restrict ER-induced Ca^{2+} signals to the cytoskeleton. In support of this idea, STIM1 has been shown to distribute asymmetrically to the motile or protruding side of steering growth cones in response to BDNF and sema-3a (Mitchell et al., 2012). Given the multifunctional nature of STIM1, its active localization could facilitate spatially-restricted SOCE to regulate cytoskeletal-dependent growth cone motility. This chapter will examine the role of STIM1 as a component of tip attachment complexes in growth cones. These experiments will help to understand whether the reported interaction between STIM1 and EB-1/3 is a mechanism employed in growth cones for ER remodelling and facilitation of SOCE.

Finally, STIM1-mediated SOCE signaling has also been linked to the regulation of focal adhesion turnover necessary for cell migration (Yang et al., 2009; Chen et al., 2011; 2013). Focal adhesions are complexes that couple extracellular substrates to the cytoskeleton. The transduction of force required to guide *Aplysia* growth cones in response to extracellular substrates and cues is linked to directed microtubule growth

and contractility of the actomyosin system through cell adhesion elements (Suter et al., 1998). Ca^{2+} regulates focal adhesion turnover through proteins such as calpain, a regulator of actomyosin which drives mechanical forces during cell motility (Huttenlocher et al., 1997). Focal adhesion turnover is impaired in breast tumour cells with reduced STIM1 expression or following treatment with a SOC channel inhibitor, and this effect was rescued by activating the small GTPases Ras and Rac1 (Yang et al., 2009). STIM1 activates calpain and the tyrosine kinase Pyk2, both known to regulate focal adhesion dynamics and migration/motility of cervical cancer cells (Chen et al., 2011). Chen and colleagues reported that STIM1 deficiency and drug induced SOCE inhibition disrupts actomyosin formation and inhibits cervical cancer cell migration, while STIM1 overexpression significantly increases the rate of cell migration (Chen et al., 2013). STIM1 deficiency inhibits the recruitment and association of focal adhesion kinase (FAK) and talin, which associate to regulate adhesion, force transduction and motility (Chen et al., 2013). FAKs are required for the formation of adhesion sites in growth cones to promote integrin dependent growth cone turning and outgrowth by stabilizing lamellipodia (Robles and Gomez, 2006; Myers and Gomez, 2011). For example, inhibition of FAK disrupts growth cone adhesion, force generation and mechano-transduction required for netrin1-induced growth cone attraction (Moore et al., 2012).

In this chapter, we determined whether STIM1 interacts with the growth cone cytoskeleton as has been described in non-neuronal cells. We assessed whether STIM1 regulates the levels or localization of actin, actin and microtubule binding proteins and FAK as these are key regulators of growth cone motility and pathfinding. Here, we also investigated whether STIM1 forms tip attachment complexes with EB-1/3 and whether this association is dependent on the content of Ca^{2+}_{ER}. STIM1 interactions with the growth cone cytoskeleton, would provide a mechanism to explain how STIM1 regulates SOCE-independent growth cone steering in response to sema-3a (Mitchell et al., 2012).

3.2 Results

3.2.1 STIM1 regulates the expression of actin and focal adhesion kinase in motile growth cones

STIM1-dependent SOCE signaling is required for actomyosin organisation, contractility and focal adhesion turnover in migratory cells (Yang et al., 2009; Chen et al., 2011; 2013). A specific morpholino oligonucleotide was used to reduce STIM1 expression in DRG sensory neurons, to determine whether STIM1 regulates the actin cytoskeleton and focal adhesion system in motile growth cones *in vitro*. Sensory neurons treated with mispaired (control) morpholino or a specific STIM1 morpholino (STIM1 morphant) were immunolabelled and protein expression levels were assessed in randomly extending growth cones that were not responding to any externally applied guidance cue. The level of filamentous (F)-actin was significantly decreased in growth cones with reduced STIM1 expression (n=39) compared to control growth cones (n=45; Fig. 3.1.a-b, quantified in Fig. 3.1.c). It is likely that impaired SOCE signaling in growth cones with reduced STIM1 expression indirectly causes the actin cytoskeleton to be less stable resulting in decreased F-actin expression.

To investigate the effects of STIM1 on aspects of growth cone adhesion we examined the expression of focal adhesion kinase (FAK) in growth cones with reduced STIM1 expression. Immunoreactivity of FAK was significantly decreased in growth cones with reduced STIM1 expression (n=20; Fig. 3.2.b,d,f) compared to growth cones treated with control morpholino (n=38; Fig. 3.2.a,c,e, quantified in Fig. 3.2.g). While axon extension is not affected in growth cones with reduced STIM1 expression in the short-term (Mitchell et al., 2012), previous reports together with the findings presented would support a function of STIM1 in regulating force-transduction in growth cones which could perturb extension over time.

Figure 3.1. STIM1 regulates the level of filamentous (F)-actin in growth cones

(a) Control and (b) STIM1 morphant growth cones labelled for actin (phalloidin, green) and STIM1 (red).

(c) F-actin (as represented by phalloidin integrated pixel intensity) in whole growth cone of control (grey bar) and STIM1 morphant (clear bar) sensory neurons. The total number of growth cones assessed per group (corresponding to a minimum of 3 separate experiments) are displayed within bars on graph. Error bars represent SEM.

*** $p<0.0005$; (Students *t*-test). Scale bar 5μm.

Fig 3.1

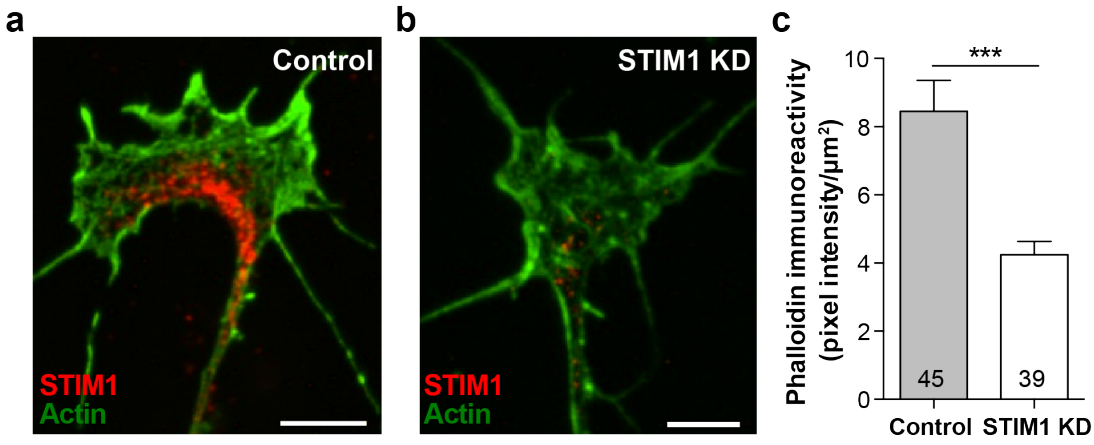
a
Control
STIM1
Actin
b
STIM1 KD
STIM1
Actin
c
Phalloidin immunoreactivity
(pixel intensity/µm²)
10
8
6
4
2
0
***
45
39
Control
STIM1 KD

Figure 3.2. STIM1 expression regulates focal adhesion kinase in motile growth cones

(a-f) Growth cones immunostained for (a-b) focal adhesion kinase (FAK, yellow), (c-d) STIM1 (magenta) and (e-f) F-actin using phalloidin (cyan, merge), in (a, c, e) control and (b, d, f) STIM1 morphants (growth cones are outlined by dash lines in a-d).

(g) Total FAK immunoreactivity (as represented by integrated pixel density) in whole growth cone of control (grey bar) and STIM1 morphant (clear bar) neurons. Error bars represent SEM.

* $p<0.05$; (Students *t*-test). Scale bar 5μm.

Fig 3.2

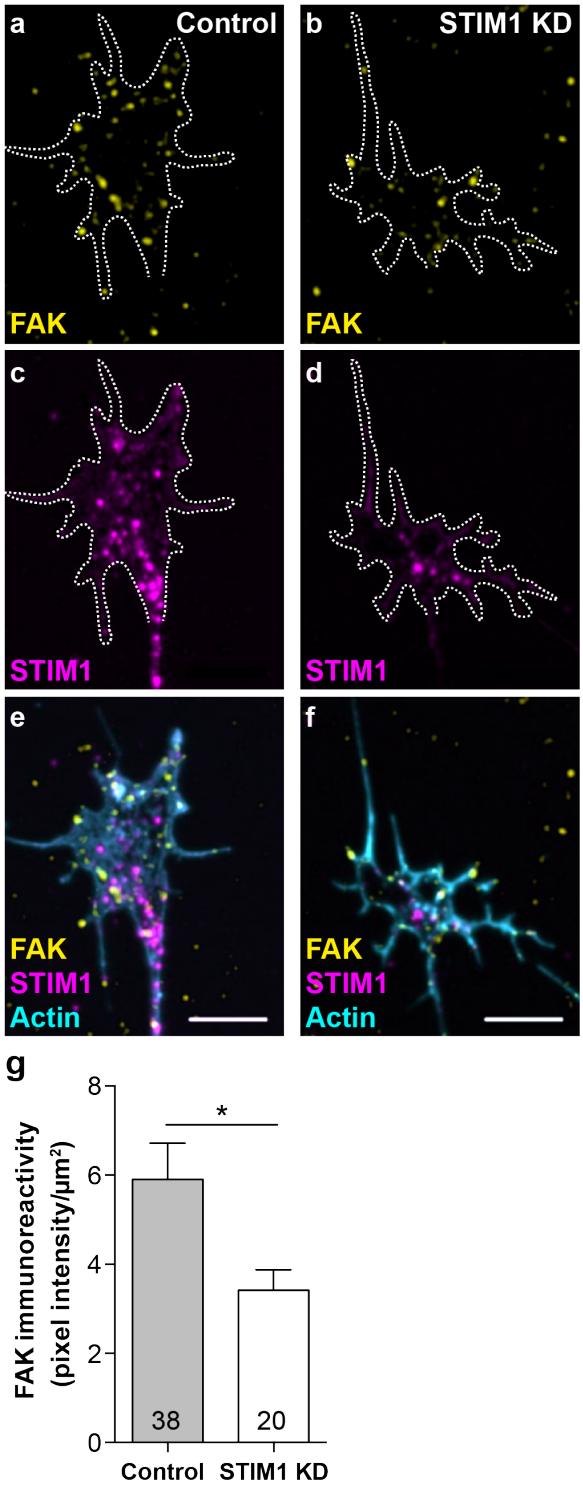
a
Control
FAK
b
STIM1 KD
FAK
c
STIM1
d
STIM1
e
FAK
STIM1
Actin
f
FAK
STIM1
Actin
g
FAK immunoreactivity
(pixel intensity/μm²)
8
6
4
2
0
*
38
20
Control
STIM1 KD

3.2.2 STIM1 regulates expression of the actin-associated protein drebrin in growth cones

Having determined that STIM1 regulates F-actin expression levels in motile growth cones, we next sought to determine the effects of STIM1 on the expression and localization of proteins that mediate actin and microtubule interactions, particularly EB3 and drebrin. In growth cones, drebrin-EB3 interactions mediate actin-microtubule dynamics through direct binding. Drebrin, an actin-binding protein, crosslinks with microtubules by binding EB3 at the base of growth cone filopodia and facilitates microtubule protrusion into filopodia (Geraldo et al., 2008). Given that EB3 binds STIM1 directly to form tip attachment complexes (Grigoriev et al., 2008), we predicted that the expression of drebrin would be disrupted in STIM1-deficient growth cones. In addition, since drebrin interacts with EB3 to mediate microtubule extension in filopodia, we also sought to determine whether STIM1 is required for the spatial localization of drebrin in growth cones.

Randomly extending control growth cones and growth cones with reduced STIM1 expression were immunolabelled for drebrin and STIM1 (Fig. 3.3.a-b). Prominent drebrin expression was observed in the peripheral zone of control and STIM1 morphant growth cones, especially at lamellipodial borders (Fig. 3.3.a-b and arrowhead). Drebrin immunoreactivity in whole growth cones (control n=21, STIM1 KD n=25; Fig. 3.3.c) and at filopodia (control n=86, STIM1 KD n=81; Fig. 3.3.d) was significantly increased in growth cones with reduced STIM1 expression, compared to control. The percentage of filopodia that were positive for drebrin or STIM1 immunoreactivity (regardless of expression level) was analysed in control growth cones (n=21) and growth cones with reduced STIM1 expression (n=25; Fig. 3.3.e). $51 \pm 5.7\%$ of filopodia in control growth cones were positive for drebrin, and 77 ± 5.3 % were positive for STIM1 expression,

Figure 3.3. Reduced expression of STIM1 increases drebrin expression at filopodial growth cones

(a) Control and (b) STIM1 morphant growth cones were immunolabelled with drebrin (green, arrowhead and inset depict prominent expression along lamellipodial border and filopodia respectively) and STIM1 (red).

(c-d) Drebrin immunoreactivity was quantified in (c) whole growth cone and in (d) filopodia of control and STIM1 morphant sensory neurons. * $p<0.05$, **** $p<0.0001$; (Students *t*-test).

(e) Proportion of filopodia that are positive for drebrin and STIM1 immunoreactivity in control and STIM1 morphant neurons. ** $p<0.01$, *** $p<0.005$, **** $p<0.0001$; (one-way ANOVA, Tukey's multiple comparison test).

(f) Drebrin-to-STIM1 pixel intensity ratio at filopodia of control and STIM1 morphant growth cones. *** $p<0.005$; (Students *t*-test). Error bars indicate $\pm$ SEM.

* $p<0.05$, ** $p<0.01$, *** $p<0.005$, **** $p<0.0001$; (Students *t*-test, one-way ANOVA, Tukey's multiple comparison test). Scale bar 5μm.

Fig 3.3

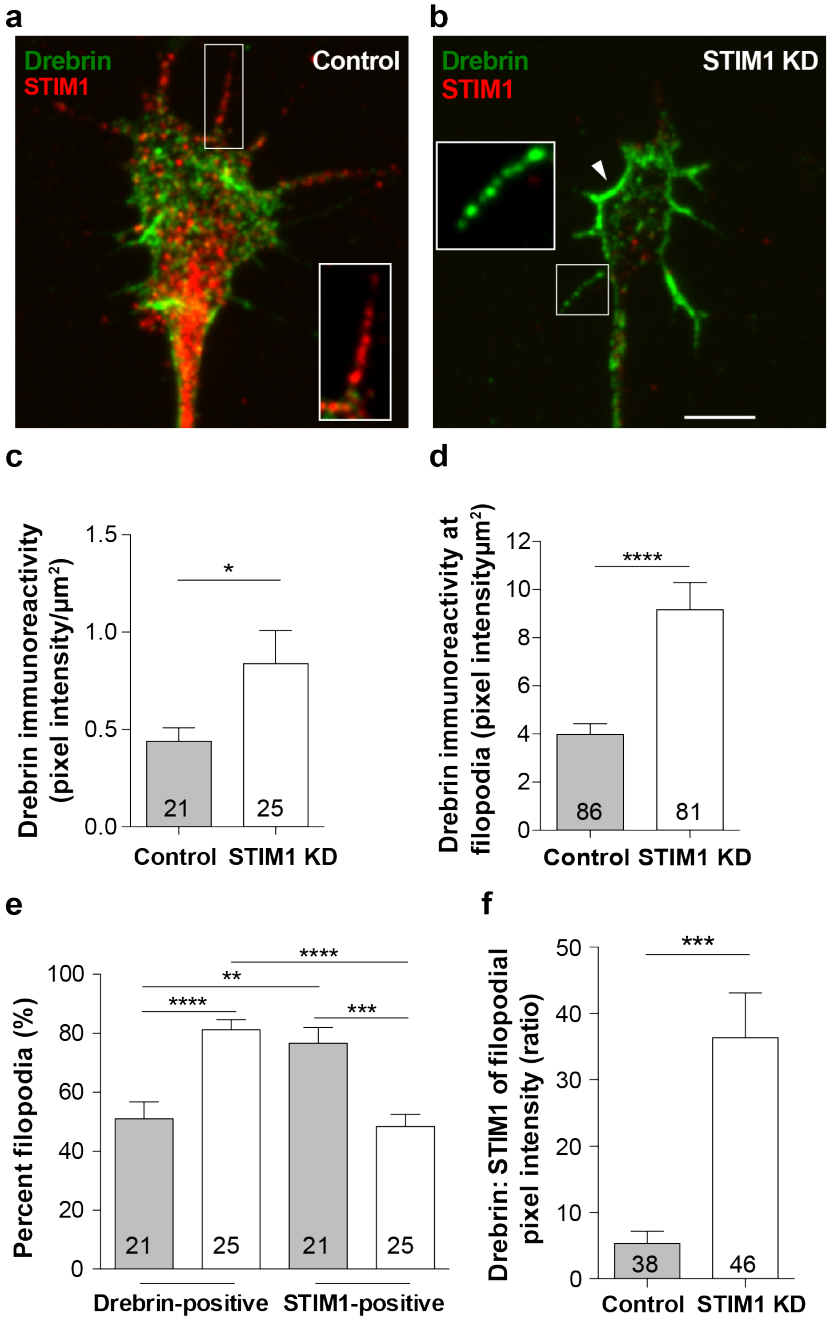
a
Drebrin
STIM1
Control
b
Drebrin
STIM1
STIM1 KD
c
Drebrin immunoreactivity (pixel intensity/µm²)
1.5
1.0
0.5
0.0
*
21
25
Control
STIM1 KD
d
Drebrin immunoreactivity at filopodia (pixel intensityµm²)
12
10
8
6
4
2
0
****
86
81
Control
STIM1 KD
e
Percent filopodia (%)
100
80
60
40
20
0
****
**
****
***
21
25
21
25
Drebrin-positive
STIM1-positive
f
Drebrin: STIM1 of filopodial pixel intensity (ratio)
50
40
30
20
10
0
***
38
46
Control
STIM1 KD

while in growth cones with reduced STIM1 expression 81 ± 3.4% of filopodia were positive for drebrin, and 48 ± 4.1% were positive for STIM1 (Fig. 3.3.e). To further demonstrate that STIM1 expression regulates filopodial drebrin levels, the ratio of filopodial drebrin and STIM1 immunoreactivity was calculated and shown to be significantly increased in filopodia of growth cones with reduced STIM1 expression (n=46) compared to control (n=38; Fig. 3.3.f). As a cross-linker of actin and microtubules and a binding partner of EB3, drebrin function was predicted to be altered in growth cones with reduced STIM1 expression. These data might potentially suggest a compensatory mechanism.

3.2.3 STIM1 localises with EB-1/3 at the periphery of randomly extending growth cones in a Ca^{2+}_{ER}-dependent manner

Having shown that STIM1 regulates the expression of actin and focal adhesion kinase and the expression and localization of the actin-microtubule cross-linker protein drebrin, we sought to determine whether STIM1 interacts with the microtubule cytoskeleton through binding to the proteins EB-1/3 and APC. The microtubule-binding proteins EB-1/3 and APC have been previously studied in neuronal growth cones (Stepanova et al., 2003; Zhou et al., 2004). Whether these proteins interact with STIM1 to form tip attachment complexes to remodel ER and activate SOCE in motile growth cones is not known. The presence of STIM1-mediated tip attachment complexes in growth cones would provide a mechanism for directly localizing ER and Ca^{2+}_{ER} signals to the cytoskeleton. Using immunocytochemistry, βIII tubulin (Fig. 3.4.a-b), EB-1/3 (Fig. 3.4.a,c), STIM1 (Fig. 3.4.b,c) and APC (Fig. 3.4.c-d) were quantified. As expected, EB-1/3 expression was localized to polymerizing microtubule plus-ends at the growth cone periphery (arrowheads Fig. 3.4.a). STIM1 immunostaining decorated the entire growth cone and closely aligned with the microtubule cytoskeleton, particularly at filopodia

Figure 3.4. STIM1 colocalises with EB-1/3 and APC at the periphery of sensory growth cones and STIM1 dissociates from EB-1/3 following Ca^{2+}_{ER} depletion.

(a-b) Images of randomly extending sensory neuron growth cones immunostained with β-III tubulin (green) and microtubule plus-end binding proteins (a) EB-1/3 (red) or (b) STIM1 (red). EB-1/3 and STIM1 align with polymerised microtubules (β-III tubulin) and extend into filopodial tips (arrowheads, insets).

(c) EB-1/3 (red) and APC (green) colocalise along microtubules in central and peripheral regions of growth cone (inset depicts colocalised proteins at base of filopodia). (d) APC (green) localizes with STIM1 (red) along filopodial compartments (arrowheads, inset). (e) Quantified ACP immunoreactivity (as represented by integrated pixel density) in whole growth cone of control (grey bars) and STIM1 morphant (clear bars) neurons. * $p<0.05$; (Students *t*-test).

(f-g) STIM1 (green) and EB-1/3 (red) colocalisation (inset) (e) before and (f) after Ca^{2+}_{ER} depletion with 50 nM thapsigargin (TG).

(h) Colocalisation of EB-1/3 and STIM1 in cells treated with vehicle or TG was analysed in the whole growth cone and the peripheral zone calculated using Mander's overlap coefficient, where 1 is complete colocalisation. (i) Colocalisation between EB-1/3 and STIM1, STIM1 and APC, and EB-1/3 and APC at the growth cone periphery of cells treated with vehicle or TG, calculated using Mander's overlap coefficient. * $p<0.05$; (One-way ANOVA, Tukey's multiple comparison test). Error bars indicate ± SEM.

* $p<0.05$; (Students *t*-test, One-way ANOVA, Tukey's multiple comparison test). Scale bar 5μm.

Fig 3.4

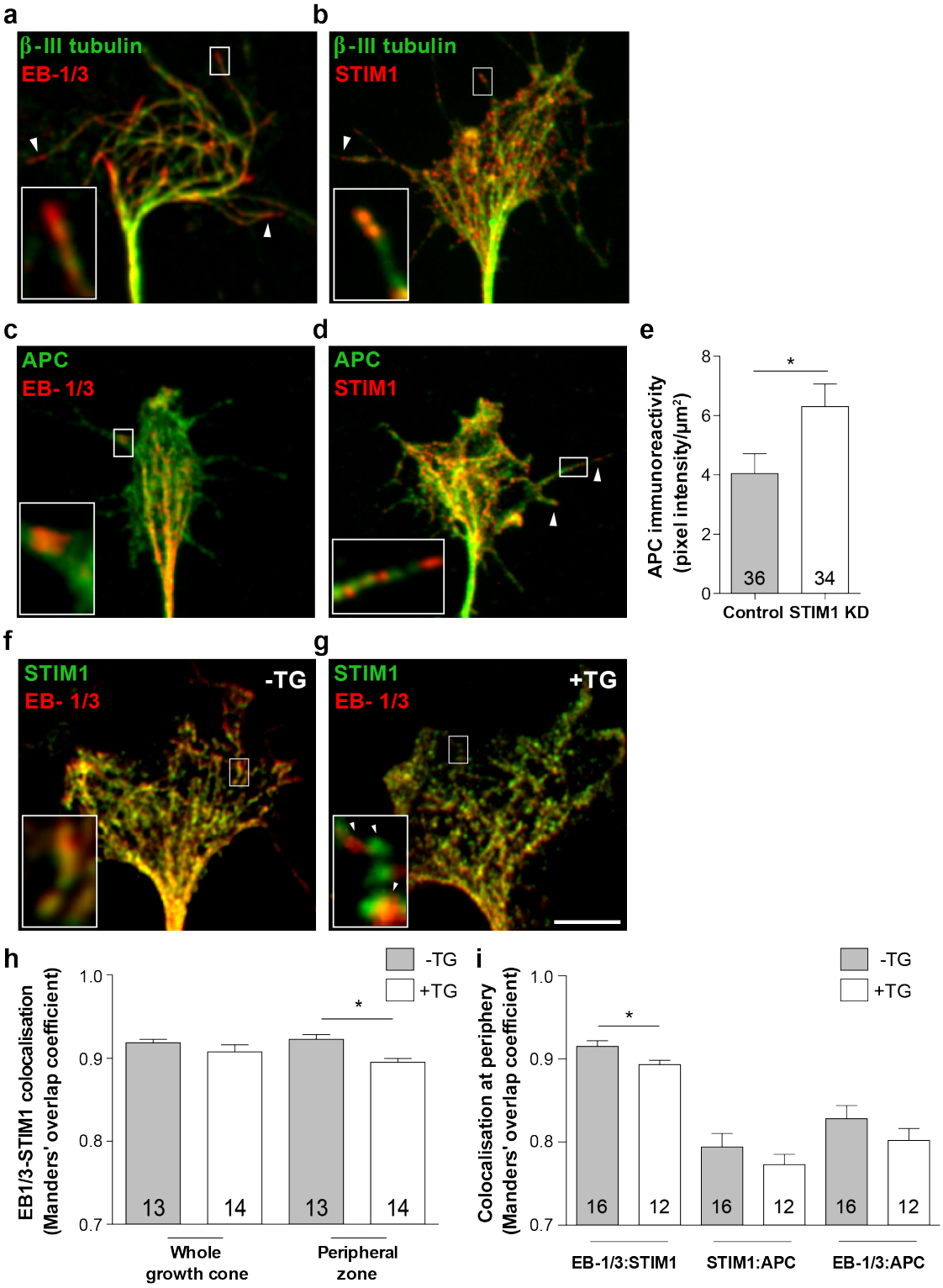
a
β-III tubulin
EB-1/3
b
β-III tubulin
STIM1
c
APC
EB- 1/3
d
APC
STIM1
e
APC immunoreactivity (pixel intensity/μm²)
8
6
4
2
0
*
36
34
Control
STIM1 KD
f
STIM1
EB- 1/3
-TG
g
STIM1
EB- 1/3
+TG
h
EB1/3-STIM1 colocalisation (Manders' overlap coefficient)
1.0
0.9
0.8
0.7
-TG
+TG
*
13
14
13
14
Whole growth cone
Peripheral zone
i
Colocalisation at periphery (Manders' overlap coefficient)
1.0
0.9
0.8
0.7
-TG
+TG
*
16
12
16
12
16
12
EB-1/3:STIM1
STIM1:APC
EB-1/3:APC

(arrowheads Fig. 3.4.c). APC interacts with EB1 via the short polypeptide motif SxIP, in the same manner as STIM1 (Honnappa et al., 2009). Colocalisation of APC with EB-1/3 (Fig. 3.4.c) and STIM1 (Fig. 3.4.d) was also observed throughout the growth cone and peripherally in filopodia (insets Fig. 3.4.c-d). Interestingly, the total expression of APC was significantly increased in growth cones with reduced STIM1 expression (n=34) compared to control growth cones (n=36; Fig. 3.4.e). This is most likely as a result of increased availability of SxIP-binding motif of EB-1/3 in growth cones with reduced STIM1 expression, since APC and STIM1 bind EB-1/3 in the same manner to the hydrophobic groove of the EB homology domain (Honnappa et al., 2009).

The close apposition of STIM1, EB-1/3 and APC in the growth cone could support the presence of a relay mechanism similar to that described previously. In non-neuronal cells, a relay mechanism occurs in a Ca^{2+}_{ER}-dependent manner, where STIM1 dissociates from EB1 upon ER store depletion to bind APC and facilitate SOCE activation (Asanov et al., 2013). To determine whether STIM1 and EB-1/3 associate in growth cones in a Ca^{2+}_{ER}-dependent manner, Ca^{2+}_{ER} depletion was induced using a sarcoendoplasmic reticulum Ca^{2+}-ATPase (SERCA) pump inhibitor, thapsigargin (TG, 50nM). Thapsigargin has been previously used to activate STIM1 oligomerisation and therefore SOCE, in DRG sensory neuron growth cones (Mitchell et al., 2012). Treatment with thapsigargin inhibits SERCA pumps, resulting in Ca^{2+}_{ER} depletion (Gomez et al., 1995). Following treatment, cells were fixed and immunostained for STIM1, EB-1/3 and APC. Significant colocalisation of STIM1 and EB-1/3 along microtubules was observed throughout the growth cone and extending into the periphery (Fig. 3.4.f); an interaction that was less apparent following treatment with TG (Fig. 3.4.g). Analysis of colocalisation using Manders' overlap coefficient (Manders et al., 1993) revealed that STIM1 and EB-1/3 colocalisation was significantly reduced in the growth cone periphery following treatment with TG (-TG n=13, +TG n=14; *p= 0.0174; Fig. 3.4.h). Colocalisation between

STIM1 and APC, or EB-1/3 and APC was not significantly changed following 5 min treatment with TG (-TG n=16, +TG n=12; Fig. 3.4.i). These data suggest STIM1 and EB-1/3 interact as tip attachment complexes at the neuronal growth cone in a manner that is dependent on Ca^{2+}_{ER}.

3.3 Discussion

This chapter investigated STIM1 interactions with the growth cone cytoskeleton, including actin and microtubule associated proteins and focal adhesion kinases, all key regulators of cell motility. Our data demonstrate that expression levels of F-actin and FAK are significantly decreased in growth cones with reduced STIM1 expression. These findings are consistent with reports that STIM1-dependent SOCE regulates actomyosin and focal adhesion turnover in migratory cancer cells (Yang et al., 2009; Chen et al., 2011; 2013). Interestingly, in growth cones with reduced STIM1 expression levels of APC and drebrin were significantly increased. Moreover, in growth cones with reduced STIM1 expression, drebrin was significantly upregulated in filopodia. A likely reason for this localised upregulation, is that reduced STIM1 expression increased filopodial drebrin levels in response to impaired EB3-microtubule protrusion in growth cones, in an attempt to promote filopodial stability. Furthermore, STIM1 was localised with the microtubule-binding proteins EB-1/3 and APC throughout the growth cone and particularly at peripheral areas of active growth/remodelling and guidance-cue signaling such as filopodia. The close apposition of STIM1 and EB-1/3 expression was dependent on Ca^{2+}_{ER} content, which is consistent with a model of ER remodelling where STIM1 associates with microtubules when ER stores are replete and dissociates from EB-1/3 upon store depletion to activate SOCE.

STIM1 has been previously reported to regulate SOCE-dependent BDNF induced growth cone attraction, as well as SOCE-independent sema-3a induced growth cone repulsion (Mitchell et al., 2012). The mechanisms of STIM1 function in sema-3a induced growth cone turning are unclear. STIM1-dependent regulation of growth cone turning in response to sema-3a may be due to the STIM1 microtubule binding function. Together with our current findings, we suggest that reducing STIM1 below a threshold level

perturbs STIM1-mediated SOCE (Mitchell et al., 2012), but also STIM1 regulation of the cytoskeleton and adhesion elements.

STIM1 is necessary for the regulation of F-actin, focal adhesions and drebrin

These data demonstrate that F-actin and FAK levels were significantly decreased in randomly extending growth cones with reduced expression of STIM1. As a result, STIM1 deficient growth cones were often smaller in area, although adhered and extended on laminin substrates normally, as axon extension rates were unchanged between controls and growth cones with reduced STIM1 expression, as previously reported (Mitchell et al., 2012). Axon extension or branching over longer cell culture periods might demonstrate that these behaviours are perturbed over time in growth cones with reduced STIM1 expression, however time did not permit these experiments. Since STIM1-dependent Ca^{2+} signaling regulates focal adhesion turnover, actomyosin organisation and cell migration of non-neuronal cells (Yang et al., 2009; Chen et al., 2011; 2013), it was not surprising to observe actin and focal adhesion kinase defects in STIM1 deficient growth cones.

Ca^{2+} signaling is a known regulator of growth cone adhesion and motility. Local calcineurin-dependent Ca^{2+} transients in *Xenopus* neuronal growth cones reduce the level of activated FAK (phosphorylated FAK) and lead to growth cone de-adhesion (Conklin et al., 2005). Calpain is another Ca^{2+}-dependent effector involved in *Xenopus* axon outgrowth, filopodial Ca^{2+} signals and growth cone steering through regulation of FAK and talin (Kerstein et al., 2017). Given that STIM1-dependent SOCE signaling is impaired in growth cones with reduced STIM1 expression (Mitchell et al., 2012) and within filopodia of STIM1-deficient *Xenopus* spinal neurons (Shim et al., 2013) it is possible that the defects observed in actin and adhesion systems in the current study

are in part the result of disrupted SOCE, but may also reflect defects in STIM1 binding of APC, EB3 and the cytoskeleton.

The multifunctional aspect of STIM1 is also supported by the finding that STIM1 expression is required for growth cone repulsion in response to the Ca^{2+}/SOCE-independent cue sema-3a. Sema-3a causes accumulation of PTEN (phosphatase and tensin homolog deleted on chromosome ten) at the growth cone leading edge, which induces growth cone collapse (Chadborn et al., 2006). The phosphatase PTEN mediates growth cone collapse or chemorepulsion in response to MAG (and likely also in response to sema-3a) by dephosphorylating PIP_3 to PIP_2 and by negatively regulating β1-integrin adhesions (Henle et al., 2013). Prior to being recruited to the growth cone leading edge, PTEN is sequestered to microtubules (Chadborn et al., 2006), where it has been shown to affect phosphorylation and association of microtubule-associated protein Tau with microtubules (Zhang et al., 2006). In light of this, it could be possible that sema-3a regulates microtubule dynamics via PTEN to induce growth cone repulsion/collapse, and in growth cones with reduced STIM1 expression where microtubule-binding function is disrupted growth cones are unable to respond. Furthermore, sema-3a signaling has also been linked to Mical-induced disassembly of F-actin *in vivo* (Hung et al., 2010). Mical is an F-actin depolymerizing protein known to function in motor axon guidance (Terman et al., 2002), and proposed to regulate complex highly-branched growth cone morphologies associated with pausing at choice points (Hung et al., 2010). Since growth cones with reduced STIM1 expression have reduced basal levels of F-actin, it is possible that Mical function is also subsequently disrupted in STIM1 deficient growth cones. Together these mechanisms might help explain the necessity of STIM1 for microtubule, F-actin and adhesion regulation necessary for appropriate turning in response to SOCE-independent guidance cue sema-3a.

Upregulation of drebrin in both growth cones and filopodia of STIM1 morphant growth cones illustrates the complex interplay of compensatory signals acting at polymerizing microtubules to maintain motility. Overexpression of drebrin has been shown to increase levels of F-actin, stabilize adhesion sites and induce axonal growth(Ikeda et al., 1996; Geraldo et al., 2008; Mizui et al., 2009), while drebrin deficiency has been correlated to reduced F-actin levels in neuronal growth cones (Mizui et al., 2009). Drebrin deficiency also inhibits SOCE in Jurkat T cells, and prevents actin rearrangements (Mercer et al., 2010). Drebrin upregulation is associated with increased microtubule invasion into filopodia which in turn stabilize filopodial protrusions and increases the number of filopodia (Geraldo et al., 2008). This mechanism likely represents the compensatory drebrin effect that was observed here. APC expression was also significantly increased in growth cones with reduced STIM1 expression. A decrease in STIM1 expression may result in increased availability of the microtubule binding SxIP motif of EB-1/3 in STIM1 morphant growth cones. This would result in increased APC binding to EB-1/3 at the SxIP motif on EB homology domain (Honnappa et al., 2009). The increase in APC binding may cause an increase in the expression of drebrin, which does not bind EB3 via the same motif as APC. This may represent a compensatory mechanism to preserve microtubule protrusion into filopodia, in agreement with the observations of Geraldo and colleagues (Geraldo et al., 2008). Another possible explanation for APC upregulation in growth cones with reduced STIM1 expression is that APC is upregulated to enhance SOCE activation with the remaining STIM1.

STIM1 regulates actin and microtubule associated proteins and interacts with EB-1/3 in a Ca^{2+}_{ER}-dependent manner

This chapter demonstrates that colocalisation between STIM1 and EB-1/3 proteins at the growth cone periphery is dependent on the level of Ca^{2+} within the ER. These observations are consistent with previously reported models of ER remodelling and SOCE in non-neuronal cells (Grigoriev et al., 2008) where STIM1 binds EB proteins

directly and this interaction is crucial for ER remodelling. Depletion of either STIM1 or EB1 perturbs ER protrusion, but is distinct from SOCE as knockdown of EB1 does not affect SOCE (Grigoriev et al., 2008). In the model proposed by Asanov and colleagues (Asanov et al., 2013), EB1 dissociates from STIM1 upon ER store depletion and STIM1 subsequently associates with APC to facilitate the formation of SOCE channels at ER-PM junctions. Our results are consistent with the STIM1-EB dissociation model, however the relay mechanism in which STIM1 associates with APC following store depletion is not supported in our system. While APC is crucial for axon growth and guidance, through the regulation of microtubule and actin assembly (Zhou et al., 2004; Koester et al., 2007), it might not play a vital role in localising calcium signals as part of a tip attachment complex with EB-1/3 and STIM1 in growth cones. Indeed the study by Asanov and colleagues (Asanov et al., 2013) reported that APC depletion diminished but did not block thapsigargin-induced calcium entry suggesting that APC is important but not crucial for SOCE. The results presented here however are limited to the resolution of confocal microscopy and it is likely that coupling between STIM1 and APC following store depletion could be better detected with more sensitive imaging. Current super-resolution imaging techniques have identified that molecules once thought to interact (using less sensitive imaging modalities) are in fact positioned in overlapping yet distinct nanodomains (Huang et al., 2009). Future experiments are necessary to re-examine the relay mechanism and address whether APC facilitates STIM1 clustering at ER-PM junctions. These experiments should consider the use of techniques which enable the visualisation of molecules at the nanometre scale or single-molecule level including super-resolution imaging (Huang et al., 2009) and electron microscopy using immunogold labelling (de Harven et al., 1984). Furthermore, experiments using overexpression of STIM1 variants that lack functional EB-1/3 and APC binding domains, in a STIM1- replete and deplete background may tease out the STIM1-EB-APC relay mechanism in growth cones.

A model in which STIM1 forms tip attachment complexes with EB-1/3 in growth cones and particularly in sub-compartments of the growth cone involved in active guidance cue transduction signaling such as the filopodia, would provide the means to localize Ca^{2+}_{ER} signals spatially and temporally. Altogether, these data strongly suggest that STIM1 is multifunctional and acts as a key regulator of instructional signals during growth cone motility by altering the cytoskeletal organisation in ways that are both SOCE-dependent and independent.

These findings prompted further investigation on the association of STIM1 with the microtubule cytoskeleton, particularly in growth cones under active control of a guidance cue in addition to randomly extending motile growth cones. We asked whether STIM1 participates in the formation of tip-attachment complexes and regulates the localization of ER (and Ca^{2+}) through direct interaction with microtubules in steering growth cones.

Chapter 4:

STIM1 is required for the spatial distribution and polymerization of microtubules in steering growth cones

Chapter 4: STIM1 is required for the spatial distribution and polymerization of microtubules in steering growth cones

4.1 Introduction

During axon pathfinding, guidance cues activate receptors on the growth cone membrane to instruct growth cone motility and steering (Tessier-Lavigne and Goodman, 1996b; Song and Poo, 1999; Dent and Gertler, 2003; Chilton, 2006). Cue-induced signal transduction regulates growth cone motility through the activity of second messengers, such as calcium (Ca^{2+}). Ca^{2+} regulates cytoskeletal rearrangements that alter growth cone motility and turning (Kater and Mills, 1991; Gomez et al., 1995; Gomez and Spitzer, 1999; Song and Poo, 1999; Hong et al., 2000; Zheng, 2000; Henley et al., 2004; Jin et al., 2005a; Gasperini et al., 2017). Understanding how Ca^{2+} signals are regulated in growth cones is of particular importance since highly spatial and localized elevations of intracellular Ca^{2+} in filopodial and lamellipodial compartments provide directional instruction for growth cone extension and steering (Zheng et al., 1994; 1996; Zheng, 2000; Gomez et al., 2001; Wen et al., 2004b; Shim et al., 2013). There are two major sources of Ca^{2+} in growth cones: extracellular and intracellular. These sources determine and regulate the cytosolic Ca^{2+} levels that instruct cytoskeletal organization and growth cone motility. Transient and localized Ca^{2+} signals are generated by channels that mobilize Ca^{2+} from the extracellular space, such as TRPC, VGCC or CRAC; or intracellular stores, such as IP_3R and RyR on the endoplasmic reticulum (Bandtlow et al., 1993; Gomez et al., 1995; Tang et al., 2003a; Shim et al., 2013). While we know the spatial dynamics of Ca^{2+} are instructional for growth cone motility, the mechanisms that regulate the spatial localization of Ca^{2+} signals remain unclear.

Store operated Ca^{2+} entry (SOCE), a STIM1-induced source of Ca^{2+} which is necessary for growth cone pathfinding (Mitchell et al., 2012), is activated to replenish depleted ER compartments (Liou et al., 2005; Roos et al., 2005; Zhang et al., 2005). STIM1

expression is necessary for growth cone attraction to the Ca^{2+}/SOCE-dependent cue BDNF, as well as repulsion to the Ca^{2+}/SOCE-independent cue sema-3a (Mitchell et al., 2012), indicating that STIM1 may have multiple functions in steering growth cones. BDNF induced growth cone attraction is likely to require STIM1 expression to sustain Ca^{2+} signals for the regulation of Ca^{2+}-dependent CaMKII/CaN switch, however the mechanisms by which STIM1 regulates sema-3a induced growth cone repulsion are less clear. STIM1 expression has been shown to regulate microtubule polymerization and organization in mast cells and HEK 293 (Smyth et al., 2007; Hájková et al., 2011b) possibly indicating a direct regulatory link between a STIM1-dependent Ca^{2+} source and the cytoskeleton. Indeed, the ER and microtubule cytoskeleton are highly interdependent structures proposed to function in close association to localize ER-derived signals within cells (Terasaki et al., 1986; Dailey and Bridgman, 1989; Waterman-Storer and Salmon, 1998). Ca^{2+} differentially stabilizes and destabilizes the microtubule and actin cytoskeleton in a localized manner to regulate axon extension, growth cone motility and steering (Gasperini et al., 2017). However, exactly how Ca^{2+} signals are spatially and temporally localized to the growth cone cytoskeleton to alter motility remains unclear. The data presented in chapter 3 suggests that STIM1 may regulate the growth cone cytoskeleton in a Ca^{2+} dependent manner.

Microtubule-associated proteins including the microtubule plus-end tracking proteins, regulate spatiotemporal microtubule dynamics by the differential stabilization of microtubule filaments (Akhmanova and Steinmetz, 2008). Microtubule plus-end tracking proteins also mediate direct interactions between the ER and the microtubule cytoskeleton through tip-attachment complexes (Waterman-Storer and Salmon, 1998; Akhmanova and Steinmetz, 2008). In chapter 3, we demonstrated that STIM1 localises with microtubule associated proteins in particular EB-1/3, and this association was dependent on Ca^{2+}_{ER} content. In non-neuronal cells, the binding of STIM1 and EB-1/3 facilitates the tracking of ER along microtubules, which in turn optimizes STIM1

localisation for SOCE (Smyth et al., 2007). We therefore asked whether the interaction between STIM1 and EB-1/3 was a mechanism used to remodel ER and SOCE in steering growth cones.

The multifunctional nature of STIM1 and particularly how STIM1 regulates both SOCE and microtubule dynamics was investigated using optogenetics, immunocytochemistry and pharmacology. The data in this chapter demonstrate the role of STIM1 on microtubule polymerisation and recruitment to the motile/steering side during growth cone turning. We also investigate whether tip-attachment complexes (comprising STIM1, EB-1/3 and APC) translocate within actively turning growth cones to areas requiring localized Ca^{2+} signals.

4.2 Results

4.2.1 STIM1 activation is sufficient to steer growth cones

STIM1 and SOCE are necessary for growth cone steering in response to guidance cues (Mitchell et al., 2012; Shim et al., 2013). While ER-derived Ca^{2+} signals and SOCE are required to sustain growth cone attraction in response to BDNF (Li et al., 2005b; Mitchell et al., 2012), Ca^{2+}-independent cues such as sema-3a elicit growth cone repulsion in an SOCE-independent manner (Mitchell et al., 2012). Growth cone repulsion in response to sema-3a however, is abolished following knockdown of STIM1 expression (Mitchell et al., 2012), suggesting a non-SOCE function of STIM1 is required for sema-3a repulsion. We therefore asked whether STIM1 was both necessary and sufficient to regulate growth cone motility, and if STIM1 and SOCE activation per se could steer growth cones in the absence of a guidance cue.

To investigate whether STIM1 activation is sufficient to steer growth cones three optogenetic variants of STIM1 were used. OptoSTIM1 contains full-length STIM1 and activates Ca^{2+}-release-activated Ca^{2+} (CRAC) channels upon stimulation with blue light (Kyung et al., 2015). The light-insensitive OptoSTIM1 variant OptoSTIM1-Cry2(D387A) was used as a control (Kyung et al., 2015). To explore the possibility that the STIM1 interaction with microtubules (Grigoriev et al., 2008) is necessary to regulate growth cone steering, a truncated optogenetic variant of STIM1 was expressed in sensory neurons: LOVS1K which lacks the SxIP microtubule-binding domain but retains CRAC activity (Pham et al., 2011) (Fig. 4.1.a). The traditional SOCE function of OptoSTIM1 was first tested for each construct in HEK293A cells. HEK293A cells transfected with OptoSTIM1 were loaded with Fura-2 AM and imaged in the presence of 5-10mM Ca^{2+}. Illumination induced transient intracellular [Ca^{2+}] increases in HEK293A cells

Figure 4.1. Activation of STIM1 is sufficient to alter growth cone motility.

(a) Schematic depiction of OptoSTIM1, OptoSTIM1-Cry2(D387A) and LOVS1K constructs. OptoSTIM1 fusion constructs are labelled with EGFP, while LOVS1K is labelled with mRFP. CC2, Coiled-coil domain 2; ERM, ezrin-radixin- moesin domain; SxIP, Ser-x-Ile-Pro domain; APC/K, adenomatous polyposis coli (APC)-binding and polybasic domain.

(b) Fluorescence image of Fura-2 intensity in HEK293A cells expressing moderate (left cell) or low (right cell) levels of OptoSTIM1, imaged before and after illumination with blue light (2 sec stimulation every 4 min). Scale bar 30μm. (c) Relative mean fluorescence of Fura-2, normalized to intensity at t=0 ($\Delta F/F$), where arrows indicate illumination time-points. n=13.

(d) OptoSTIM1 localisation in a DRG growth cone before and after illumination (2 sec stimulation every 5 min for 12 min at ROI indicated by dotted rectangle). Arrows indicate OptoSTIM1 puncta formed at the stimulated side.

(e) Change in axon trajectory evident after 12 min stimulation in OptoSTIM1-transfected growth cones stimulated with light at bounded ROI (dotted rectangle).

(f) Average angle of steering from initial trajectory exhibited by growth cones transfected with OptoSTIM1-D387A, LOVS1K and OptoSTIM1 in response to light stimulation, where positive turning angles correspond to the stimulated side. Unless indicated by bars, asterisk represents significance compared to OptoSTIM1-D387A. Error bars indicate ± SEM.

*** $p<0.0005$; (Mann-Whitney *U*-test). Scale bars b, 30μm; d-e, 5μm.

Fig 4.1

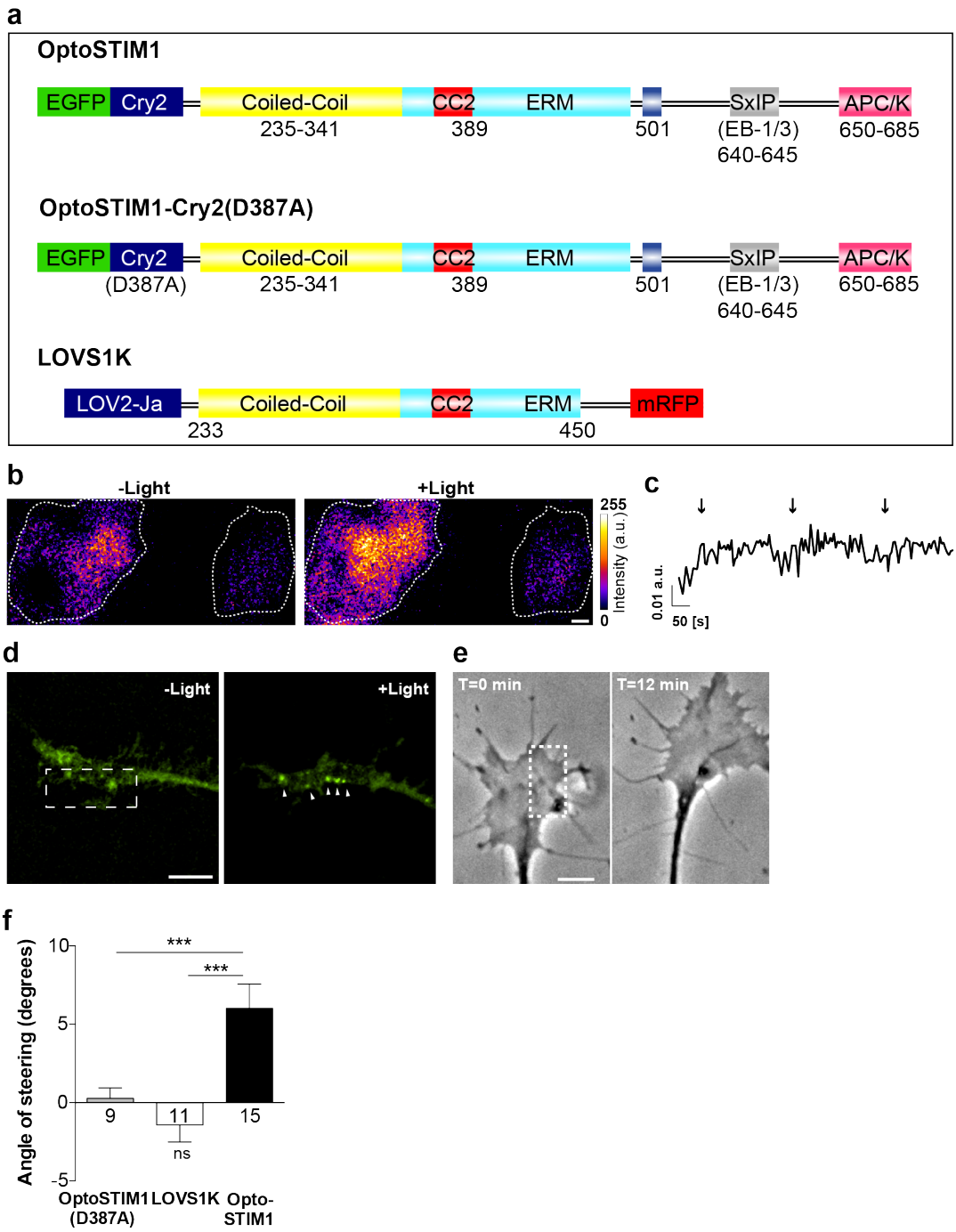
a
OptoSTIM1
EGFP
Cry2
Coiled-Coil
235-341
CC2
389
ERM
501
SxIP
(EB-1/3)
640-645
APC/K
650-685
OptoSTIM1-Cry2(D387A)
(D387A)
LOVS1K
LOV2-Ja
233
mRFP
450
b
-Light
+Light
255
Intensity (a.u.)
0
c
0.01 a.u.
50 [s]
d
e
T=0 min
T=12 min
f
Angle of steering (degrees)
10
5
0
-5
***
***
9
11
15
ns
OptoSTIM1 (D387A)
LOVS1K
Opto-STIM1

transfected with moderate levels of OptoSTIM1 compared to cells expressing little or no OptoSTIM1 (Fig. 4.1.b-c). Having validated that activation of OptoSTIM1 causes an increase in cytosolic [Ca^{2+}], we next activated OptoSTIM1 asymmetrically in growth cones. Localised illumination of OptoSTIM1-transfected growth cones caused redistribution of the eGFP-tagged protein at the stimulated area, forming aggregates or puncta (Fig. 4.1.d, arrows). These likely represented oligomerised STIM1 and potentially sites of CRAC. Asymmetric stimulation resulted in significant change in axon angle as growth cones turned towards the stimulated side (Fig. 4.1.e). This effect was not observed in growth cones expressing the light-insensitive OptoSTIM1-Cry2(D387A) (n=9; Fig. 4.1.f). Furthermore, to test whether growth cone reorientation following OptoSTIM1 activation requires STIM1 SOCE function as well as microtubule interactions, LOVS1K was transfected into neurons and activated asymmetrically in extending growth cones. Significantly, LOVS1K-transfected growth cones (n=11) exhibited variable angles of steering to asymmetric illumination, which were not significantly different from growth cones transfected with OptoSTIM1-Cry2(D387A) (Fig. 4.1.f). These data suggest that local STIM1 activation is sufficient to trigger growth cone steering when SOCE and non-SOCE functions of STIM1 are conserved, and implies that in addition to SOCE activation, STIM1 also requires interaction with polymerising microtubule tips to facilitate growth cone steering.

4.2.2 STIM1 is necessary for microtubule polymerization and growth cone turning

The close association of STIM1 and EB proteins at microtubule plus-ends (as demonstrated in Chapter 3) suggests that ER tubules interact with polymerizing microtubules in growth cones. This mechanism could remodel the ER in growth cones to spatially localize and provide a direct source of Ca^{2+} to support microtubule polymerization. Growth cones treated with mispaired (control) morpholino displayed regular microtubule distribution, with polymerized microtubules splayed from the central

domain of the growth cone into the transition and peripheral domains, as well as filopodial tips (Fig. 4.2.a). Growth cones of neurons treated with a specific STIM1 morpholino (STIM1 morphant) displayed significantly reduced numbers of polymerized microtubules (n=35; Fig. 4.2.b; quantified in Fig. 4.2.g).

We next asked whether the microtubule destabilization observed in growth cones with reduced STIM1 expression resulted from perturbed SOCE activity. We investigated the role of the binding partner of STIM1, Orai1, on microtubule polymerization. Since Orai1 does not bind microtubules, any changes to microtubule polymerization observed in growth cones with reduced Orai1 expression would result from altered SOCE signaling. Reducing the expression of Orai1 using Orai1-specific siRNA oligonucleotides did not alter microtubule polymerization in growth cones (n=19; Fig. 4.2.c; quantified in Fig. 4.2.g). Importantly, expression of polymerised and non-polymerised βIII-tubulin as measured by immunocytochemistry was unchanged in growth cones with reduced expression of STIM1 (n=50) or Orai1 (n=19), compared to control growth cones (n=46; Fig. 4.2.h).

To further investigate the mechanisms by which STIM1 regulates microtubule polymerisation, DRG neurons were transfected with a mutant STIM1: STIM1-ΔK, which retains the SxIP domain but lacks a C-terminal polybasic motif required for targeting ER to the plasma membrane (Liou et al., 2007). Overexpression of STIM1-ΔK has been previously used to separate two STIM1 processes; oligomerization following Ca^{2+}_{ER} depletion and translocation of STIM1 to ER-PM junctions for the formation of store operated Ca^{2+} channels (Liou et al., 2007). STIM1-ΔK mutant is able to oligomerise, but fails to recruit STIM1 puncta to ER-PM junctions for SOCE in HeLa cells, suggesting the polybasic motif is required for such recruitment (Liou et al., 2007). It is reasonable to infer that if microtubule polymerization was perturbed in growth cones overexpressing STIM1-

ΔK, then microtubule disruption in growth cones with reduced STIM1 expression is likely to result from failure of STIM1 to participate in SOCE. To test this idea, DRG neurons were transfected with STIM1-ΔK and growth cones were immunostained for STIM1 and microtubules. Overexpression of STIM1-ΔK in wild-type growth cones did not alter microtubule polymerization of DRG growth cones compared to control growth cones (n=21; Fig. 4.2.d; quantified in Fig. 4.2.g). However, it has been reported that STIM1-ΔK can also oligomerise with endogenous STIM1 and be recruited to the plasma membrane via the polybasic tail of wild-type STIM1 (Liou et al., 2007). We subsequently expressed STIM1-ΔK in growth cones with reduced STIM1 expression. Overexpression of STIM1-ΔK in growth cones with reduced STIM1 expression did not alter microtubule polymerization compared to control growth cones (n=11; Fig. 4.2.e; quantified in Fig. 4.2.g). Taken together, these data suggest that reduced microtubule polymerization in STIM1 morphant growth cones does not result from impaired SOCE, but it is more likely the result of disrupting the function of STIM1 at the microtubule plus-end.

We next asked whether pharmacological stabilization of microtubules might "rescue" the microtubule phenotype observed in growth cones with reduced STIM1 expression. Epothilones promote the polymerization of tubulin monomers into microtubules, and when used at higher concentrations, can cause cell cycle arrest and cytotoxicity as a result of microtubule hyperstabilisation (Bollag et al., 1995). When used at lower concentrations however, epothilone D (EpoD) has neuroprotective effects in models of Parkinson's disease (Cartelli et al., 2013) and tauopathy (Brunden et al., 2010). A low concentration of 0.1nM EpoD has been reported to promote microtubule polymerization of injured neurons *in vitro* (Brizuela et al., 2015). Using this concentration, we observed that the number of polymerized microtubules in growth cones with reduced STIM1 expression following treatment with 0.1nM EpoD was significantly increased compared to untreated STIM1 morphant growth cones (n=18; Fig. 4.2.f; quantified in Fig. 4.2.g).

Having found that microtubule polymerization in STIM1 deficient growth cones could be normalized using EpoD, we next investigated whether promoting microtubule polymerization could "rescue" the turning phenotype exhibited by growth cones with reduced STIM1 expression in response to the guidance cues BDNF and sema-3a. Consistent with our previous work (Mitchell et al., 2012), reducing STIM1 expression reversed attractive growth cone turning in response to BDNF (n=21), and abolished repulsion in response to sema-3a (n=19; Fig. 4.3.a). EpoD treatment did not rescue turning to BDNF (n=11) or sema-3a (n=13) in STIM1 morphants, which remained significantly different from controls treated with the same concentration of EpoD (Fig. 4.3.a). Axon extension was significantly increased in growth cones with reduced STIM1 expression after treatment with EpoD, as a result of enhanced microtubule polymerization (Fig. 4.3.b). EpoD-treatment groups displayed increased variability in turning data and increased axon extension during imaging, likely suggesting that EpoD enhanced axon outgrowth rather than directional behaviour of growth cones, highlighting differences between the two distinct processes. These results demonstrate that while STIM1 is required for net polymerisation at microtubule plus-ends, pharmacological stabilization of microtubules is insufficient to rescue turning in growth cones with reduced STIM1 expression. Altogether, these findings reflect a necessity for multiple STIM1 functions during turning including the regulation of SOCE and recruitment of microtubules, which is in agreement with previous reports (Mitchell et al., 2012).

4.2.3 STIM1 is required for EB3 movement and recruitment in sensory neuron growth cones

The data above demonstrates that STIM1 is required for microtubule polymerization.

Figure 4.2. STIM1 is necessary for microtubule polymerization in randomly extending sensory growth cones.

(a-f) Images of sensory neuron growth cones immunostained with β-III tubulin (green) and STIM1 (red). Growth cones were treated with (a) control morpholino, (b) STIM1 morpholino, (c) Orai1 siRNA; or were transfected with STIM1-ΔK in (d) wild type (WT) or (e) STIM1 knockdown (STIM1 KD) growth cones; or were treated with (f) STIM1 morpholino and microtubule-stabilizing drug Epothilone-D (EpoD).

(g) Number of polymerised microtubules in growth cones of all treatment groups (normalized to growth cone area). (h) Total β-III tubulin immunoreactivity measured by integrated density, in control, STIM1 morphant and Orai1 knockdown growth cones was unchanged.

* $p<0.05$, ** $p<0.01$; (One-way ANOVA, Tukey's multiple comparison test). Scale bar 5μm.

Fig 4.2

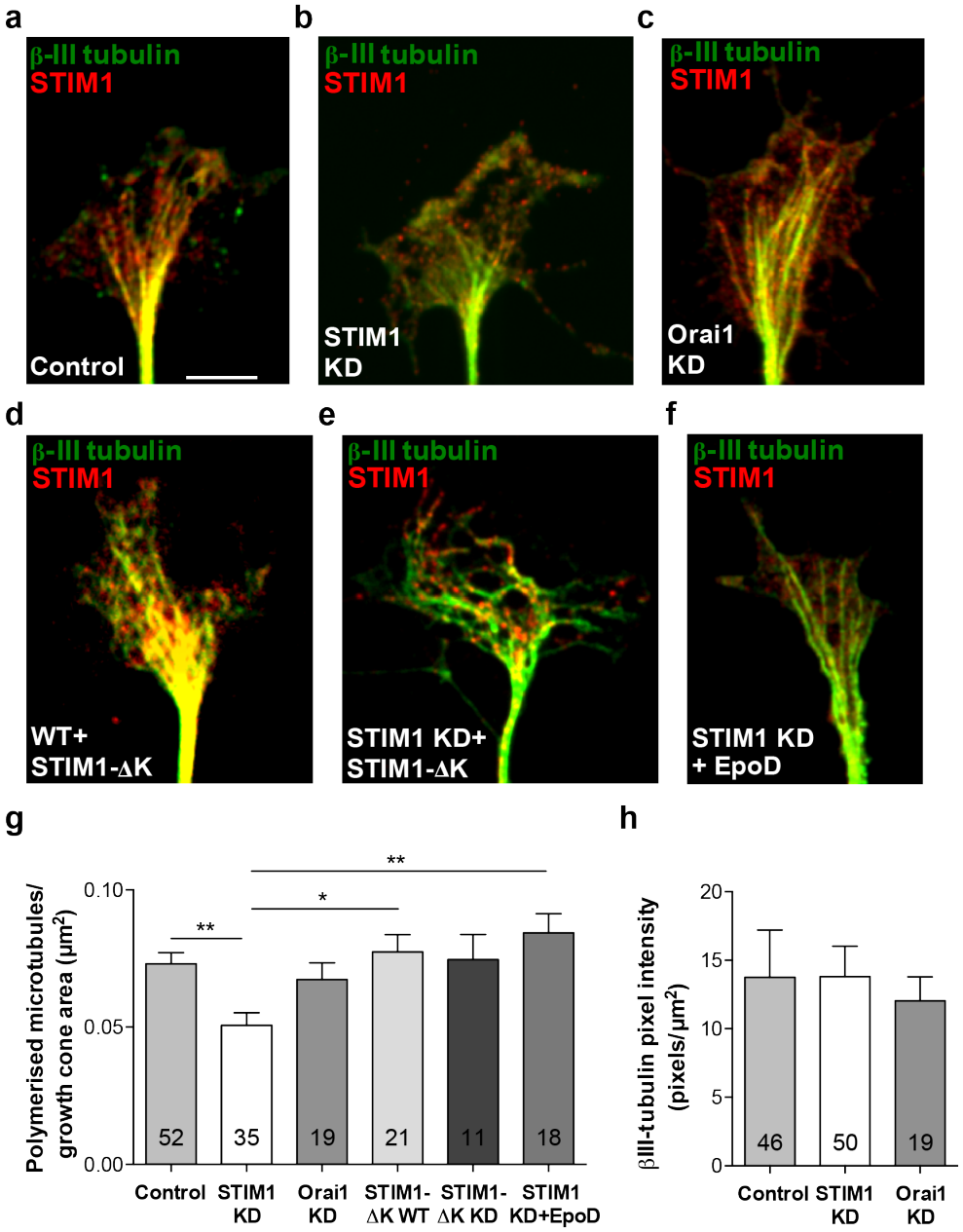
a
b
c
β-III tubulin
STIM1
Control
STIM1
KD
Orai1
KD
d
e
f
WT+
STIM1-ΔK
STIM1 KD+
STIM1-ΔK
STIM1 KD
+ EpoD
g
h
Polymerised microtubules/
growth cone area (μm²)
0.10
0.05
0.00
**
*
**
52
35
19
21
11
18
Control
STIM1
KD
Orai1
KD
STIM1-
ΔK WT
STIM1-
ΔK KD
STIM1
KD+EpoD
βIII-tubulin pixel intensity
(pixels/μm²)
20
15
10
5
0
46
50
19
Control
STIM1
KD
Orai1
KD

Figure 4.3. Microtubule-stabilization with epothilone-D does not rescue turning in STIM1 morphant growth cones.

(a) Average turning angles in response to vehicle, BDNF and sema-3a, in normal and EpoD treatment conditions for control and STIM1 morphant growth cones. Growth cone turning response was analysed following treatment with 0.1nM EpoD (bath applied). (b) Axon growth/extension during imaging was increased in most EpoD treatment groups compared to vehicle. Unless otherwise specified, asterisks represent significance compared to vehicle. * $p<0.05$, ** $p<0.01$, *** $p<0.0005$, **** $p<0.0001$; (Mann-Whitney *U*-test).

Fig 4.3

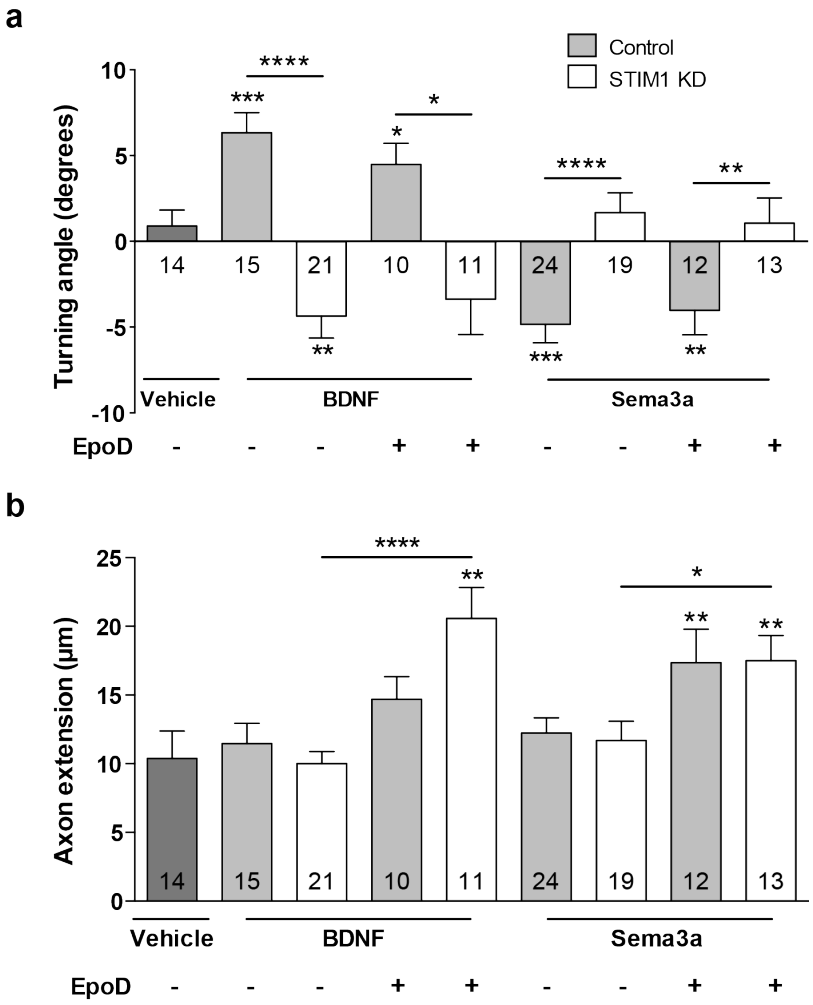
a
Control
STIM1 KD
Turning angle (degrees)
10
5
0
-5
-10
****
***
*
*
****
**
**
***
**
14
15
21
10
11
24
19
12
13
Vehicle
BDNF
Sema3a
EpoD - - - + + - - + +
b
Axon extension (µm)
25
20
15
10
5
0
****
**
*
**
**
14
15
21
10
11
24
19
12
13
Vehicle
BDNF
Sema3a
EpoD - - - + + - - + +

To determine whether STIM1 also regulates microtubule dynamics such as rate of growth and trajectory of microtubules, EB3-YFP overexpression was used to localize the polymerizing tips of microtubules in real-time. Consistent with previous reports (Stepanova et al., 2003; Geraldo et al., 2008), neurons transfected with EB3-YFP demonstrate comet-like dashes in all neuronal compartments, including the growth cone (Fig. 4.4.a-b). Live imaging of sensory neurons co-transfected with EB3-YFP and control morpholino revealed that EB3 dashes spread from the central domain of the growth cone to the peripheral domain, extending out to filopodial tips (Fig. 4.4.a, arrows and insets). The trajectories of EB3-YFP dashes at the growth cone moved from the distal axon towards the filopodial tips and reflected anterograde growth, consistent with previous reports (Stepanova et al., 2003). Sensory neurons co-transfected with EB3-YFP and STIM1 morpholino displayed disrupted EB3 dash behaviour compared to control neurons (Fig. 4.4.a-b, inset depicts distance of dash protruded into filopodia over the same time). Closer examination revealed that growth cones with reduced STIM1 expression displayed EB3 dashes which tracked shorter distances and moved at slower rates compared to control growth cones (Fig. 4.4.c-d and Table. 4.1). The number of EB3 dashes observed per single frame (acquisition every 6 sec for 10 min) was averaged and normalized to whole growth cone area (μm^2), to account for growth cone size variability. Although not significantly different, a trend was observed where average dash numbers within growth cones with reduced STIM1 expression were decreased compared to control growth cones (Table. 4.1). In control growth cones 82% of dashes could be traced for >4μm, while only 33% could be traced for >4μm in STIM1 deficient growth cones. Average EB3 dash velocity was significantly reduced in STIM1 morphant growth cones compared to control (Table. 4.1). Since average EB3 dash velocity is a measure of microtubule polymerization rate (Stepanova et al., 2003), these data suggest microtubule polymerization is perturbed in neurons with reduced STIM1 expression. We also observed that average distance travelled by a single dash was significantly reduced in

STIM1 morphant growth cones (0.71 ± 0.26μm) compared to control (1.07 ± 0.36μm) (Table. 4.1). Furthermore, average track length calculated from the sum of the distance travelled by an individual dash was also significantly reduced in STIM1 deficient growth cones (3.81 ± 1.58μm) compared to control (9 ± 5.85μm) (Table. 4.1). These results demonstrate that growth cones with reduced STIM1 expression exhibit perturbed EB3 dash dynamics, further supporting a role for STIM1 in the regulation of microtubule function.

Filopodia are key signalling domains in growth cones. Ca^{2+} regulation would be expected to have crucial functions in these peripheral structures. EB3 dashes were observed protruding to the periphery of control growth cones and often extended into filopodia, however in growth cones with reduced STIM1 expression EB3 dashes were spatially restricted to the central domain (Fig. 4.4.d), Given the importance of microtubule protrusion into filopodia during steering (Dent et al., 1999), we next examined whether STIM1 was required for EB3 dash recruitment to filopodia. First, the number of filopodia were quantified and found to be significantly increased in control growth cones overexpressing EB3-YFP (n=12) compared to non-transfected control (n=32) and STIM1 morphant growth cones (n=30; Fig. 4.4.e). Increased filopodial formation in control growth cones overexpressing EB3-YFP most likely results from enhanced recruitment of microtubules and microtubule-binding effectors such as drebrin to the growth cone periphery (Geraldo et al., 2008). Furthermore, enhanced filopodial formation in growth cones overexpressing EB3-YFP required STIM1 expression as this effect was not observed in EB3-YFP-transfected STIM1 morphant growth cones (n=17; Fig. 4.4.e). Significantly, control and STIM1 morphant growth cones that were not transfected with EB3-YFP showed comparable numbers of filopodia (Fig. 4.4.e), indicating little compensation by other microtubule-binding effectors or that STIM1 has no effect on the initial formation of filopodia.

Figure 4.4. STIM1 regulates EB3 recruitment and dynamics at the periphery of sensory growth cones.

(a-b) Microtubule dynamics were examined using EB3-YFP in (a) control and (b) STIM1 morphant growth cones. Representative images depict EB3 comet-like dashes, including movement into filopodia (arrows, insets depict movement of filopodial EB3 dash over 14 sec).

(c-d) Composite of EB3-YFP dashes in (c) control and (d) STIM1 morphant growth cones, colour-coded for dash velocity (μm/sec), comprising of 5-7 dashes from 3 growth cones per group (control and STIM1 morphant).

(e) Total number of filopodia in control and STIM1 morphant growth cones, with or without EB3-YFP overexpression. * $p<0.05$, ** $p<0.01$; (One-way ANOVA, Tukey's multiple comparison test). (f**)** Percentage of filopodia that present EB-1/3 dash immunoreactivity (endogenous) in control and STIM1 morphant growth cones. (g**)** Percentage of filopodia that present EB3 dashes in control and STIM1 morphant growth cones which overexpressed EB3-YFP. Column graphs display controls in grey bars and STIM1 morphants in clear bars. n-values are displayed within bars on graph. * $p<0.05$, *** $p<0.0005$; (Student's *t*-test).

* $p<0.05$, ** $p<0.01$, *** $p<0.0005$; (Student's *t*-test, One-way ANOVA, Tukey's multiple comparison test). Scale bar 5μm.

Fig 4.4

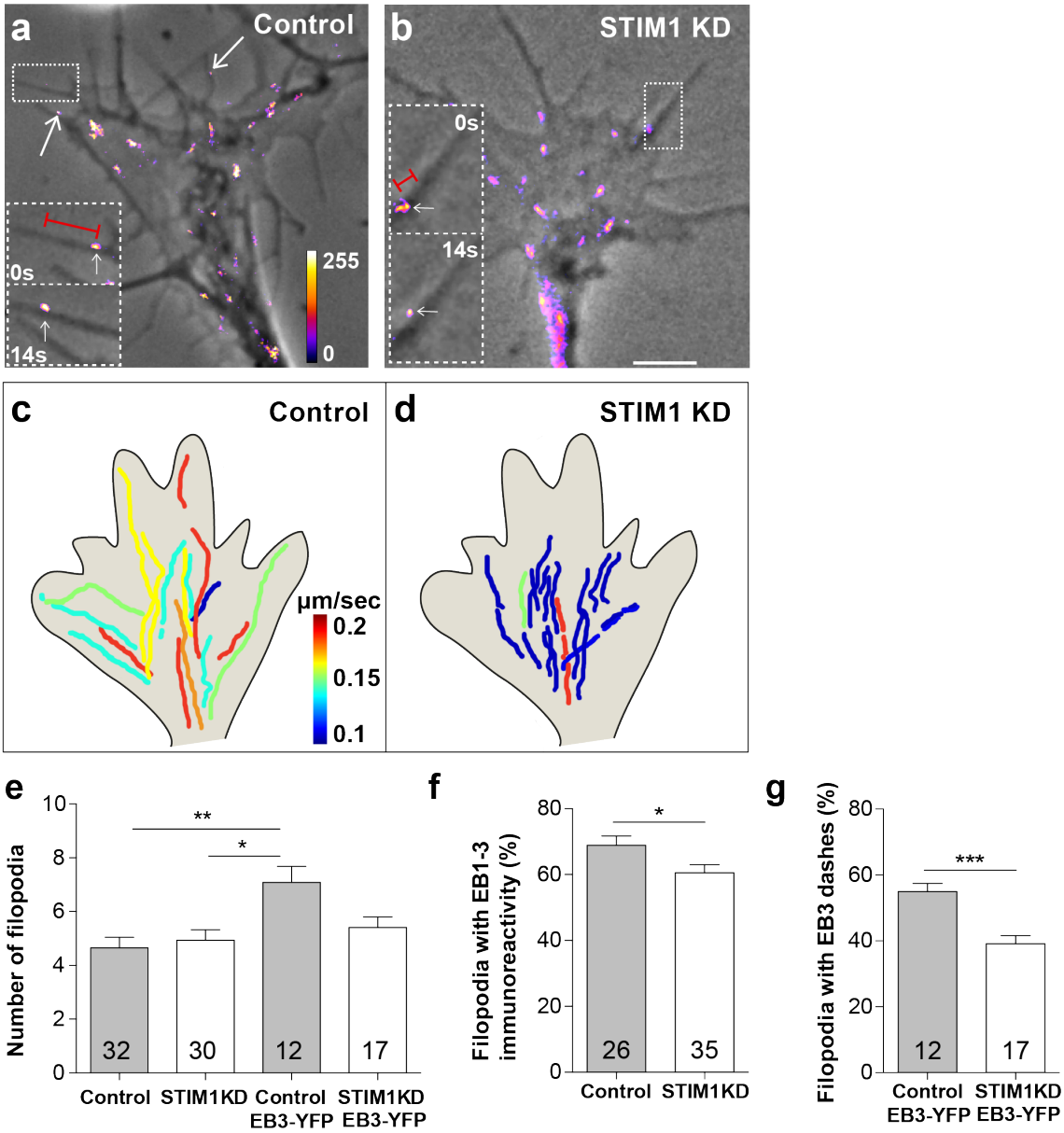
a
Control
0s
14s
255
0
b
STIM1 KD
0s
14s
c
Control
μm/sec
0.2
0.15
0.1
d
STIM1 KD
e
Number of filopodia
10
8
6
4
2
0
**
*
32
30
12
17
Control
STIM1KD
Control
EB3-YFP
STIM1KD
EB3-YFP
f
Filopodia with EB1-3 immunoreactivity (%)
80
60
40
20
0
*
26
35
Control
STIM1KD
g
Filopodia with EB3 dashes (%)
80
60
40
20
0
***
12
17
Control
EB3-YFP
STIM1KD
EB3-YFP

Table 4.1. Reduced STIM1 expression disrupts EB3 dash dynamics.

STIM1 expression	Control	STIM1 KD
Average dash number per frame[a] in whole growth cone	0.031 ± 0.0131 (9)	0.018 ± 0.0130 (6)
Average dash velocity[b] in whole growth cone	0.17 ± 0.07 (9)	0.11 ± 0.04 (6)****
Average distance[c] per dash (μm) in whole growth cone	1.07 ± 0.36 (9)	0.71 ± 0.26 (6)****
Average track length (μm) in whole growth cone	9 ± 5.85 (9)	3.81 ± 1.58 (6)****
Average filopodial dash velocity[b]	0.37 ± 0.13 (12)	0.29 ± 0.05 (13)*

[a] Images acquired every 6 seconds. Number of dashes/EB3 comets per frame, were normalized to growth cone area. [b] μm/sec ± SD. [c] Value calculated from average of distance travelled by a single dash per frame.

* $p<0.05$, **** $p<0.0001$; (Student's *t*-test).

Filopodia of STIM1 deficient growth cones (n=35) exhibited fewer endogenous EB-1/3 dash-like puncta compared to control growth cones (n=26; Fig. 4.4.f). In STIM1 morphant growth cones overexpressing EB3-YFP (n=17), filopodia were also less likely to contain EB3 dashes and when present these dashes protruded slower than EB3 dashes in filopodia of control growth cones (n=12; Fig. 4.4.g and Table. 4.1). These findings demonstrate that reducing STIM1 expression in growth cones disrupts EB3 dash velocity and track length, which in turn decreases microtubule polymerisation and disrupts organisation/protrusion of microtubules to peripheral structures of the growth cone involved in active signal transduction, such as the filopodia.

4.2.4 The spatial organization of microtubules and microtubule-associated proteins necessary for appropriate growth cone turning requires STIM1 expression

If STIM1-EB interactions are important for ER remodelling and microtubule polymerisation in pathfinding growth cones as the data presented here suggests, then reducing STIM1 expression should disrupt the recruitment of EB dashes to the motile side of turning growth cones responding to guidance cues. To test this idea, we examined the dynamics of EB3 dashes in control and STIM1 morphant growth cones in response to pulsatile microgradients of the attractive guidance cue BDNF or the repulsive guidance cue sema-3a using time-lapse imaging (Fig. 4.5). As reported previously (Mitchell et al., 2012), growth cone attraction in response to BDNF was reversed and repulsion to sema-3a was abolished in growth cones with reduced STIM1 expression (Fig. 4.5.a). By dividing growth cone images symmetrically at the midline extending from the peripheral domain to the axon, “near” and “far” side of growth cones were defined relative to the source of guidance cue (Fig. 4.5.b). Analysis of EB3-YFP dash trajectories using a near/far ratio (Fig. 4.5.c) revealed that EB3 dashes, and by

Figure 4.5. STIM1 expression regulates EB3-YFP recruitment to the steering side of turning growth cones.

(a) Average turning angles in response to vehicle, BDNF and sema-3a, in control (grey bars) and STIM1 morphant (white bars) growth cones. * $p<0.05$, ** $p<0.01$; (Mann-Whitney *U*-test).

(b) Schematic representation of turning assay depicting "near" and "far" side of growth cone used to calculate EB3-YFP-labelled tracks, where near (N) side is closest to source of guidance cue compared to far (F) side, in control and STIM1 morphant growth cones turning in response to BDNF and sema-3a. (c) Near/Far ratio of EB3-YFP-labelled tracks. (d-g) Polar plots depicting displacement and angle of trajectory of individual EB3 dashes calculated from time-lapses of control (d and f) and STIM1 morphant (e and g) growth cones (n=3 per group) responding to a gradient of (d-e) BDNF and (f-g) sema-3a. Representative control and STIM1 morphant growth cones turning to BDNF and sema-3a display EB3-YFP-labelled tracks quantified over 12 min (color-coded for average velocity per dash, μm/sec). Dash tracks displayed anterograde movement at the growth cone.

* $p<0.05$, ** $p<0.01$, *** $p<0.0005$, **** $p<0.0001$; (Student's *t*-test). Scale bar 5μm.

Fig 4.5

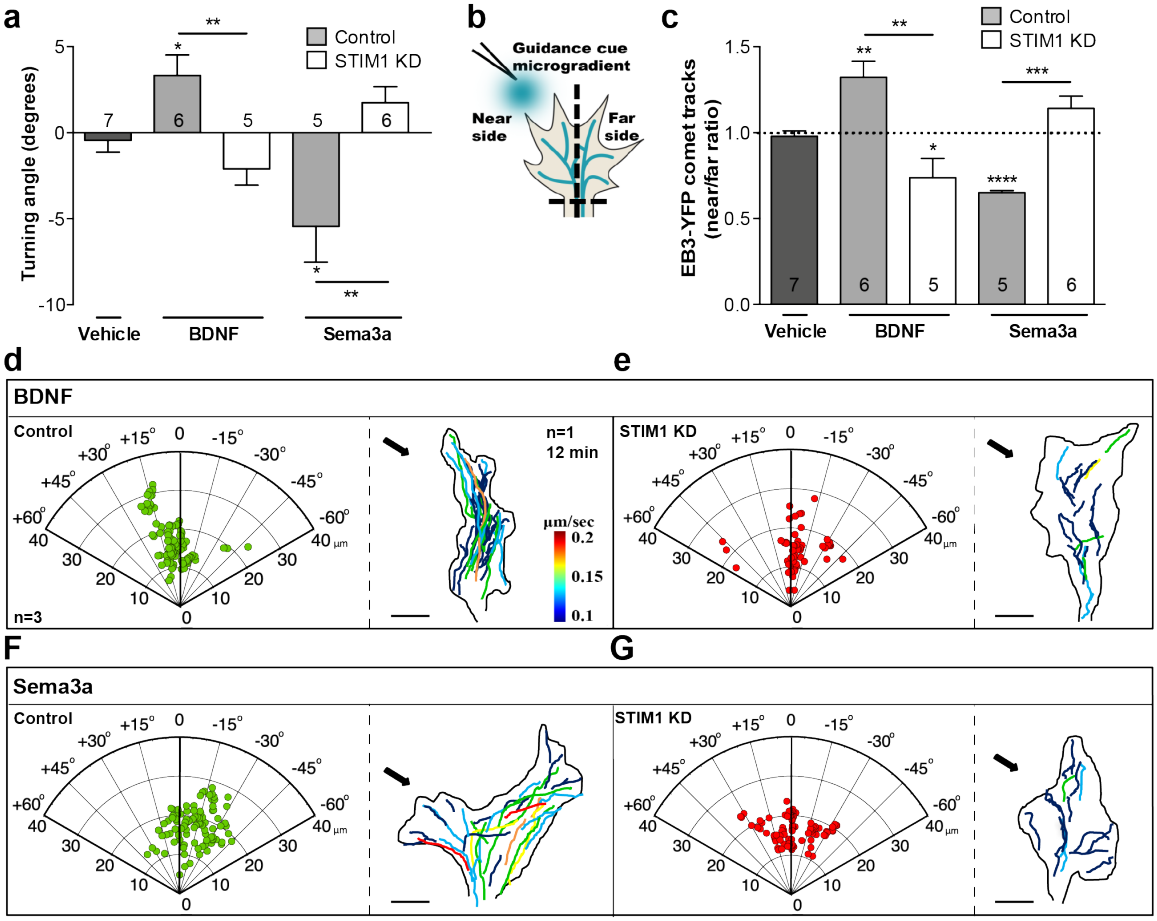
a
Turning angle (degrees)
Control
STIM1 KD
Vehicle
BDNF
Sema3a
b
Guidance cue microgradient
Near side
Far side
c
EB3-YFP comet tracks (near/far ratio)
Control
STIM1 KD
Vehicle
BDNF
Sema3a
d
BDNF
Control
n=3
n=1
12 min
µm/sec
e
STIM1 KD
F
Sema3a
Control
G
STIM1 KD

implication polymerising microtubule tips, translocate to the motile/turning side of control growth cones turning to BDNF (near or attractive side, n=6) and sema-3a (far or repulsive side, n=5). Analysis of growth cones with reduced STIM1 expression responding to BDNF (n=5) revealed that EB3 dashes translocated to the far/repulsive side and were distributed randomly in response to sema-3a (n=6; Fig. 4.5.c), consistent with the turning results (Fig. 4.5.a). Analyses of dash trajectory and displacement were also visualised using polar plots and by creating superimposed composite reconstructions of EB3 dashes in individual growth cones exposed to BDNF (Fig. 4.5.d-e) or sema-3a (Fig. 4.5.f-g). These data illustrate that EB3 dashes, representing polymerising microtubules, translocate to the steering/turning side of growth cones. Moreover, EB3 dash translocation in turning growth cones was dependent on STIM1 expression, implying a necessity of the STIM1-EB interaction for the regulation of microtubule distribution and ultimately growth cone motility in response to guidance cues.

The work above examined EB3 movement in growth cones overexpressing EB3-YFP. We next confirmed that this data extended to endogenous microtubules and the microtubule-associated proteins involved in tip-attachment complexes, in steering growth cones. To assess the endogenous distribution of these microtubule-binding proteins during steering, growth cones exposed to asymmetric gradients of vehicle (Fig. 4.6.a), BDNF (Fig. 4.6.b) and sema-3a (Fig. 4.6.c) were rapidly fixed following steering and processed for immunocytochemistry. EB-1/3, APC and βIII tubulin immunoreactivities were analysed in the near and far side of growth cones (as depicted in schematic Fig. 4.6.d) with reduced expression of STIM1 or Orai1 (as knockdown of Orai1 tests SOCE function independently of microtubule-binding). BDNF-induced growth cone turning (Fig. 4.6.e) and near/far ratio of polymerized microtubules (Fig. 4.6.f) were significantly reversed in growth cones with reduced STIM1 expression (n=17; turning angle $p<0.0001$; N/F microtubule ratio $p<0.0005$) and reduced Orai1 expression (n=10; turning angle $p<0.0001$; N/F microtubule ratio $p<0.05$) compared to controls (n=31). In

response to sema-3a, average turning angles (Fig. 4.6.e) and near/far ratio of polymerized microtubules (Fig. 4.6.f) were abolished (not significantly different from vehicle) in growth cones with reduced STIM1 levels (n=22; turning angle $p<0.0001$; N/F microtubule ratio $p<0.05$) and Orai1 levels (n=9; turning angle $p<0.0001$; N/F microtubule ratio $p<0.05$) compared to controls (n=33). These data demonstrate that STIM1 and Orai1 are required for growth cone turning in response to BDNF and sema-3a, and that disruption of SOCE-machinery results in loss of microtubule recruitment. Reduction of Orai1 expression and hence SOCE at the growth cone likely impairs STIM1 function, subsequently inhibiting the ability of STIM1 to localize the cytoskeleton. No significant changes were observed in tubulin immunoreactivity measured using pixel intensity amongst the different treatment groups (Fig. 4.6.g), suggesting the total protein level of tubulin is not affected and the likely cause of impaired growth cone turning relates to a loss of polymerization and recruitment of microtubules to the appropriate steering/turning side.

Consistent with our data demonstrating EB3-dash recruitment to the steering side of turning growth cones (Fig. 4.5), there was a significant loss of endogenous EB-1/3 recruitment, in terms of near/far ratio of EB-1/3 puncta (Fig. 4.6.h) and pixel intensity (not shown) in response to BDNF (STIM1 morphant $p<0.01$; Orai1 knockdown $p<0.0005$ compared to control) and sema-3a (STIM1 morphant $p<0.05$; Orai1 knockdown $p<0.05$ compared to control). APC localization to the turning side of growth cones (Fig. 4.6.i), was abolished in STIM1 deficient growth cones turning to BDNF (n=13; $p<0.05$ compared to control, n=6) and appeared to trend towards even distribution in growth cones with reduced STIM1 expression responding to sema-3a (n=8; $p>0.05$ compared to control, n=11). Taken together, these data support a mechanism in which EB-1/3 and APC interact with STIM1 at the polymerizing microtubule plus-end, possibly via tip-attachment complexes, to mediate microtubule-ER association in steering growth cones.

In this manner, STIM1 and microtubules coordinate the translocation of ER membranes and SOCE machinery to the steering/turning side of growth cones.

Figure 4.6. STIM1 is required for EB-1/3 and APC recruitment to the steering side of turning growth cones.

(a-c) Representative images of growth cones turning in response to microgradients of (a) vehicle, (b) BDNF, and (c) sema-3a. Growth cones fixed immediately post-turn were immunolabelled for β-III tubulin (green), EB-1/3 (red), and APC (blue). In all cases, the pipette delivering guidance cue was positioned top-left corner creating an asymmetric microgradient as depicted in (d). (e) Average turning angles in response to vehicle, BDNF and sema-3a, in growth cones treated with control morpholino (grey bars), STIM1 morpholino (white bars) and Orai1 siRNA (black bars). Key applies to (e-h). ** $p<0.01$, *** $p<0.0005$, **** $p<0.0001$; (Mann-Whitney *U*-test).

(f) Near/Far ratio of polymerized microtubules showed loss of recruitment to the appropriate turning side in response to BDNF and sema-3a in growth cones with reduced STIM1 or Orai1 expression. (g-i) Graph of (g) β-III tubulin pixel intensity near/far ratio, (H) EB-1/3 and, (i) APC puncta near/far ratio in response to vehicle (circles), BDNF (squares) and sema-3a (triangles). All treatments were compared to vehicle control, unless otherwise shown. * $p<0.05$, ** $p<0.01$, *** $p<0.0005$; (Student's *t*-test).

* $p<0.05$, ** $p<0.01$, *** $p<0.0005$, **** $p<0.0001$; (Student's *t*-test, Mann-Whitney *U*-test). Scale bar 10μm.

Fig 4.6

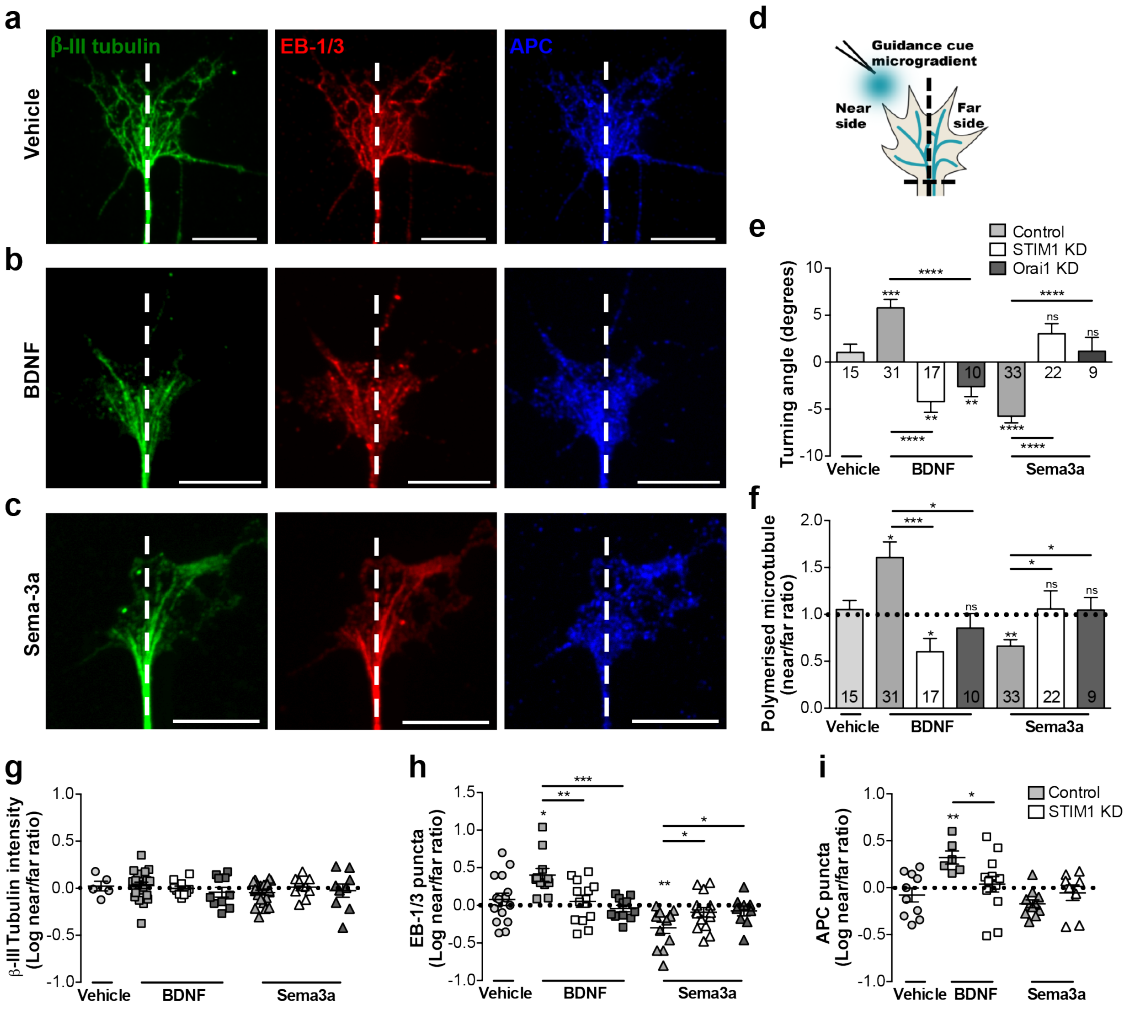
a
β-III tubulin
EB-1/3
APC
Vehicle
b
BDNF
c
Sema-3a
d
Guidance cue microgradient
Near side
Far side
e
Control
STIM1 KD
Orai1 KD
Turning angle (degrees)
15
31
17
10
33
22
9
Vehicle
BDNF
Sema3a
f
Polymerised microtubule (near/far ratio)
g
β-III Tubulin intensity (Log near/far ratio)
h
EB-1/3 puncta (Log near/far ratio)
i
APC puncta (Log near/far ratio)

4.3 Discussion

Growth cone motility is critically dependent on the spatiotemporal regulation of intracellular Ca^{2+} (Zheng, 2000) and while Ca^{2+} regulates cytoskeletal dynamics indirectly through downstream effectors, physical links between microtubules and a Ca^{2+}-source such as the ER have not been largely studied in growth cones until recently. STIM1-dependent regulation of SOCE and tip-attachment complexes is important for microtubule polymerization and is likely necessary for ER remodelling and localization of ER-derived Ca^{2+} signals within growth cones. The functional consequences of ER remodelling have, until now, been largely ignored in neuronal cells. Using STIM1 and EB-1/3 as markers of ER and microtubules, this chapter has demonstrated the close association between the ER and microtubule cytoskeleton in central and peripheral domains of steering growth cones. The components of tip-attachment complexes and cross-linkers of microtubules and ER have not been investigated at the periphery of the growth cone until now. Our previous results (chapter 3) indicated that the association of STIM1 and EB-1/3 is Ca^{2+}_{ER}-dependent. Here we also demonstrate that this association is functional and necessary for steering/turning growth cones. STIM1-mediated ER remodelling in growth cones would support the spatial localization of Ca^{2+} signals required for axon pathfinding, a mechanism that has not been previously investigated.

STIM1 regulates microtubule polymerization in steering growth cones

In this study, reduced STIM1 expression decreased the number of polymerized microtubules in randomly extending growth cones. Analysis of endogenous EB-1/3 protein distribution after steering to BDNF or sema-3a, and EB3-YFP dash trajectories were also disrupted in growth cones with reduced STIM1 expression. Significantly fewer EB-1/3 dashes were observed in filopodia of STIM1 morphant growth cones. This finding suggests that STIM1 expression is necessary for the advancement or protrusion of

polymerizing microtubules into filopodia, where they are necessary to sustain growth cone motility and extension.

Imaging experiments presented in this chapter have demonstrated that the number of filopodia remained unchanged between control growth cones and those with reduced STIM1 expression. Interestingly, control growth cones overexpressing EB3-YFP exhibited greater number of filopodia most likely through enhanced recruitment of effectors such as drebrin. Indeed, reports have demonstrated that upregulation of drebrin stabilizes filopodial protrusions and increases the number of filopodia in COS-7 cells (Geraldo et al., 2008). However, filopodial numbers were unchanged in growth cones with reduced STIM1 expression transfected with EB3-YFP despite having found in the previous chapter that filopodial drebrin is upregulated in STIM1 morphant growth cones (see chapter 3). This supports the idea that drebrin upregulation alone is insufficient to "rescue" filopodial defects.

Multifunctional role of STIM1 in the regulation of SOCE and ER-remodelling is dependent on a threshold expression level

Associations between SOCE and microtubule polymerization have been previously demonstrated. In HEK293 cells, microtubule depolymerisation using nocodazole inhibited SOCE, and this is significantly reversed in cells overexpressing STIM1-YFP (Smyth et al., 2012). It is likely that perturbing aspects of one function of STIM1, for example SOCE or microtubule regulation, can affect the ability of STIM1 to function in other signaling mechanisms. We propose that STIM1 expression but more importantly a crucial level/threshold of STIM1 expression is required for STIM1 to appropriately regulate SOCE and tip-attachment complex functions. In line with this idea, our data suggests that asymmetric activation of OptoSTIM1 but not LOVS1K induces growth cone motility, supporting the notion that both SOCE and microtubule-binding functions of STIM1 are necessary for the regulation of growth cone motility. Our findings that

LOVS1K activation does not induce a change in growth cone motility could suggest that SOCE is not necessary for growth cone pathfinding. However LOVS1K has limitations including different activation kinetics compared to OptoSTIM1 (Pham et al., 2011; Kyung et al., 2015) and the absence of a lysine-rich tail which has been shown to be necessary for SOCE activation in non-neuronal cells (Huang et al., 2006). Future experiments could include examining LOVS1K distribution post-light stimulation and simultaneously measuring calcium levels during optogenetic stimulation, in order to determine whether LOVS1K is able to oligomerise and induce SOCE in growth cones.

Our experiments predicted that if microtubule polymerization was reduced in STIM1-deficient growth cones, reduced Orai1 expression in growth cones would also perturb microtubule polymerisation. While we did not observe a significant change in the number of polymerized microtubules in growth cones with reduced Orai1 expression compared to control, such a defect could be masked by an underlying compensatory mechanism and binding of STIM1 to isoforms of Orai1 and/or TRPC channels. If that was the case, reduced Orai1 expression should not have disrupted growth cone turning in response to guidance cues. Since growth cone turning and the distribution of polymerized microtubules were disrupted in response to either STIM1 or Orai1 knockdown, we conclude that appropriate growth cone steering requires the integration of SOCE activation and organized spatiotemporal regulation of microtubules. Knockdown of Orai1 disrupts SOCE, which in turn disrupts STIM1 and hinders STIM1 function as a regulator of microtubule organization.

It is possible that for STIM1 to function appropriately as a regulator of steering, a threshold level of STIM1 and Orai1 expression is required and when either function is disrupted, dysregulation of all STIM1 functions results. This is a likely possibility, given that overexpression of the mutant STIM1-ΔK (Liou et al., 2007) in STIM1 morphant growth cones rescued the number of polymerized microtubules. In this case, STIM1-ΔK

was unable to participate in SOCE but retained microtubule-binding/tracking abilities, theoretically allowing ER to be remodelled through tip-attachment complexes. STIM1 morphants with increased expression of STIM1-ΔK exhibited normal numbers of polymerized microtubules as STIM1-ΔK retains microtubule binding function that is able to restore the functional STIM1 threshold. However, steering of STIM1 morphant growth cones expressing STIM1-ΔK (data unavailable as time did not permit) would be predicted to be perturbed as SOCE is required for growth cone turning (Mitchell et al., 2012) and microtubule dynamics (Smyth et al., 2007; Hájková et al., 2011b). In addition, the directionality of the microtubules after reducing endogenous STIM1 levels and overexpressing STIM1-ΔK, while not quantified, appeared quite different to controls, suggesting that full function of STIM1 is required to regulate microtubule orientation and recruitment. The concept that a threshold level of regulatory proteins is required to promote specific functions has been reported in many other cell systems. Examples of this include threshold levels of APC to protect against intestinal tumorigenesis (Li et al., 2005a); PKA/cAMP levels to promote fungus growth (Pereyra et al., 2000); glucocorticoid receptor levels to promote leukemic cell apoptosis (Schwartz et al., 2010); and DNA methyltransferase 1 levels to maintain genomic methylation in human cells (Spada et al., 2007). We therefore propose that a threshold level of STIM1 is crucial and necessary for the regulation of SOCE and tip-attachment complexes in steering growth cones.

Our finding that treatment of STIM1 morphant cells with the microtubule-stabilising compound EpoD, while rescuing the number of polymerized microtubules, did not rescue turning to BDNF and sema-3a, suggests that promoting microtubule polymerization alone is insufficient to restore a turning phenotype, as Ca^{2+} signal localization remains perturbed. Local and selective stabilization of microtubules has been previously shown to initiate and instruct directional growth cone steering (Buck and Zheng, 2002). Taken together, an interplay between functional microtubule growth and localization, with

appropriate Ca^{2+} signaling is necessary for instructive cytoskeletal-driven growth cone steering.

STIM1 serves as a direct link between microtubules and ER to localize Ca^{2+} signals necessary for growth cone steering

We observed that EB-1/3 was spatially redistributed to the turning side of growth cones in response to BDNF and sema-3a, consistent with our hypothesis that STIM1 forms tip-attachment complexes with EB-1/3. Significantly, the spatial reorganization of EB-1/3 was dependent on STIM1 expression. These findings indicate that STIM1 is important for the coupling of ER to microtubules and the distribution/localization of microtubules, and suggests that STIM1 participates to link instructive microtubule reorganization and Ca^{2+} signaling. This data is in concordance with reports demonstrating STIM1 translocation to the turning side of growth cones responding to Ca^{2+}-dependent guidance cues (Mitchell et al., 2012) in a manner that facilitates spatial Ca^{2+} signals to regulate growth cone steering (Zheng, 2000). Previously, asymmetric Ca^{2+} transients and microtubule reorganization have been linked by microtubule-associated protein Tau (Li et al., 2013). The morphogen Wnt5a elicits axon extension and growth cone repulsion by distinct mechanisms that either activate TRP channels and IP_3R for axon extension, or TRP channels alone for growth cone repulsion (Li et al., 2009). Li and colleagues (Li et al., 2013) showed that Wnt5a-induced growth cone chemorepulsion was facilitated by Tau-mediated microtubule organization and upon CaMKII inhibition, which inhibits Tau phosphorylation, microtubule reorganization was prevented. Our data suggests that STIM1 provides a direct link between the microtubule cytoskeleton and the ER-derived Ca^{2+} signal, rather than indirectly through downstream effectors of Ca^{2+} such as CaMKII, potentially providing a more efficient regulatory mechanism to instruct growth cone steering.

The spatial regulation of Ca^{2+} signaling to the cytoskeleton to instruct growth cone motility has been mostly studied in the context of indirect mechanisms that signal through molecules such as IP_3 (Akiyama et al., 2009), phosphatidylinositol 3-kinase (PI3K)/glycogen synthase kinase 3β (GSK-3β)/APC (Zhou et al., 2004), and $PI(3,4,5)P_3$/Akt/TRPC (Henle et al., 2011). For example, microtubule advance into the growth cone peripheral domain is facilitated by PI3K downstream of Ca^{2+} and facilitates microtubule-dependent membrane trafficking (Akiyama and Kamiguchi, 2010). Microtubule excursions into the growth cone periphery are blunted in the presence of PI3K inhibitors, which in turn also abolish vesicle transport known to occur in response to Ca^{2+} signals (Akiyama and Kamiguchi, 2010). PI3K catalyses the production of PIP_3 from $PI(4,5)P_2$ to activate a number of downstream effectors including the kinase Akt, which when activated asymmetrically, can regulate growth cone attraction (Henle et al., 2011). Growth cone attraction by PIP_3/Akt signalling requires TRP channel activation and downstream Ca^{2+} signals (Henle et al., 2011). Inhibition of PI3K is able to reduce EB1 dash speed and attenuate microtubule advance into growth cone periphery, whereas the presence of exogenous PIP_3 increases EB1 dash speed and promotes microtubule advance (Akiyama and Kamiguchi, 2010). Exactly how PIP_3/PI3K is spatially localized to the cytoskeleton remains unclear, however it could be facilitated by STIM1 localization of ER to microtubules.

For example, spatially activated PI3K and downstream inactivation of local GSK-3β, mediates nerve growth factor (NGF)-induced axon extension through phosphorylation/activation of APC (Zhou et al., 2004). Zhou and colleagues have demonstrated that spatial activation of APC in growth cones sustained extension by inducing microtubule assembly and actin stabilization through activation of the Cdc42/Rac pathway (Zhou et al., 2004). It is possible that APC supports microtubule stability in response to locally applied guidance cues in a GSK-3β-dependent manner, as cues such as sema-3a have been shown to require compartmentalized GSK-3β

signaling (Eickholt et al., 2002). Our results showing the spatial organization of microtubule binding proteins in control, and both STIM1 and Orai1 knockdown growth cones turning to BDNF revealed that EB-1/3 and APC distribution correlated to the distribution of polymerized microtubules. However unlike EB-1/3, APC distribution was not significantly organized in response to sema-3a in control and STIM1 morphants. Since APC accumulation at the distal axon is not necessary for microtubule polymerization per se (Zhou et al., 2004), it is likely that APC is not required to regulate spatial microtubule dynamics directly, but rather it stabilizes microtubules (consistent with axon extension role) and mediates microtubule-actin interactions.

Taken together and in conjunction with previous studies, the data presented in this chapter demonstrate that STIM1 is crucial for the regulation of SOCE and microtubule polymerization in steering growth cones. Our data demonstrate that STIM1-mediated cytoskeletal organization and signal transduction is necessary for growth cone steering in response to Ca^{2+} dependent and independent guidance cues. Furthermore, the findings in this chapter strongly support the function of tip-attachment complexes in growth cones, and provide a mechanism to regulate ER remodelling and the localization of Ca^{2+} signals in steering growth cones. Whether STIM1 facilitates this remodelling to localize Ca^{2+}_{ER} signals within sub-compartments of motile growth cones involved in cue-sensing and signal transduction, such as filopodia, is unknown.

Chapter 5:

STIM1 regulates ER remodelling and microtubule protrusion into filopodia

Chapter 5: STIM1 regulates ER remodelling and microtubule protrusion into filopodia

5.1 Introduction

As growth cones pathfind through the embryonic milieu they encounter a range of guideposts and extracellular guidance cues, which alter growth cone morphology and rate of migration. Changes in growth cone behaviour and axon outgrowth are initiated by receptor-mediated intracellular signalling on growth cone filopodia (Gomez and Letourneau, 1994; Gomez et al., 2001; Dent et al., 2007; Shim et al., 2013). Growth cone filopodia express receptors which support transmission of Ca^{2+} signals from filopodial tips to the growth cone (Davenport et al., 1993). Filopodia are therefore considered the "first responders" of axon guidance. Consistent with this role, early studies demonstrated that disruption of filopodia formation in embryonic grasshopper Ti1 pioneer neurons causes growth cones to become disoriented and unable to steer appropriately (Bentley and Toroian-Raymond, 1986). A single filopodial contact with a high-affinity substrate was sufficient to cause the reorientation of Ti1 pioneer growth cones steering *in situ* (O'Connor et al., 1990). Growth cone filopodia are reported to be the driving force of sensory and motor growth cone functions, and are regulated by external cues and intracellular signal amplification (Goodhill et al., 2004). Filopodia transduce guidance cues through receptor-mediated Ca^{2+} transients (Gomez et al., 2001; Shim et al., 2013) however, precisely how filopodial Ca^{2+} signals regulate the cytoskeleton to support growth cone motility is unknown at present.

Ca^{2+} is a crucial regulator of filopodial dynamics and function. Early experiments demonstrated that electric fields increase the number of growth cone filopodia and cytoplasmic spines in *Xenopus* spinal neurites (McCaig, 1986). These activity-induced filopodial changes were subsequently linked to spatially restricted increases of

intracellular Ca^{2+} in growth cones of *Helisoma* neurons (Davenport and Kater, 1992). Focal Ca^{2+} increases, using photolysis, induce filopodial extension in Ti1 neurons from F-actin patches and cause branching of new filopodia from existing ones (Lau et al., 1999). Spatially restricted Ca^{2+} transients, including in filopodia, also regulate the rate of neurite outgrowth and promote growth cone turning when stimulated asymmetrically and differentially (Gomez and Spitzer, 1999; Hong et al., 2000; Zheng, 2000; Gomez et al., 2001; Ooashi et al., 2005). However, the question of how Ca^{2+} signals are localised and regulated spatiotemporally within subcellular micro-domains of the growth cone, such as the filopodia, remains largely unanswered.

Ca^{2+} signals derived from the ER are likely to be an important component of the spatially restricted Ca^{2+} signals that regulate growth cone motility (Davenport et al., 1996; Gasperini et al., 2009; Mitchell et al., 2012). However, exactly how ER might remodel to localize Ca^{2+} signals within filopodia, in order to spatially regulate cytoskeletal dynamics for instructional growth cone steering, is unknown. Data presented in chapter 3 and 4 suggests that the interaction between EB proteins and STIM1 mediates ER tracking and remodeling along microtubules to localize Ca^{2+} and facilitate SOCE, as described in non-neuronal cells (Smyth et al., 2007; Grigoriev et al., 2008). STIM1 and microtubules share strikingly similar organisation in non-neuronal cells (Baba et al., 2006; Mercer et al., 2006) and previous work has shown that STIM1 regulates microtubule rearrangement in mast cells (Hájková et al., 2011a). Furthermore, microtubule depolymerization is linked to disrupted SOCE and I_{CRAC} signaling in non-neuronal cells (Smyth et al., 2007). Taken together these data demonstrate that ER and microtubules are interdependent and that STIM1 regulates ER-microtubule interactions as a microtubule binding protein as well as a regulator of SOCE. Since ER functions to sequester and release Ca^{2+} (Somlyo, 1984), and Ca^{2+} is a known local regulator of microtubule stability (Schliwa et al., 1981), a direct interaction with microtubules would likely facilitate Ca^{2+}_{ER} localization. Filopodia and

growth cone behaviors are spatially regulated by distinct local Ca^{2+} microdomains, and these domains depend on the source and availability of Ca^{2+} stores (Davenport et al., 1996). Significantly, STIM1 regulates filopodial Ca^{2+} transients in *Xenopus* growth cones which are necessary for appropriate growth cone turning in response to Netrin-1 (Shim et al., 2013). Thus, STIM1 is required for filopodial (Shim et al., 2013) and whole growth cone (Mitchell et al., 2012) Ca^{2+} dynamics in response to guidance cues.

Experiments previously described in chapter 4, demonstrated that filopodial numbers were reduced in STIM1 deficient growth cones overexpressing EB3-YFP compared to control EB3-YFP-transfected growth cones. These data suggest that STIM1 morphant growth cones have a disrupted ability to induce or sustain filopodia. Given the crucial role of filopodia in growth cone navigation (Bentley and Toroian-Raymond, 1986; O'Connor et al., 1990), this would likely result in axon pathfinding defects. Regulation of growth cone filopodial dynamics have been previously linked to changes in intracellular Ca^{2+} (Davenport and Kater, 1992; Lau et al., 1999; Gomez et al., 2001) and the cytoskeleton (Schaefer et al., 2002; Zhou et al., 2002). Therefore, given the role of STIM1 as a $Ca^{2+}{}_{ER}$ sensor, regulator of SOCE and microtubule-binding protein, it was hypothesised that STIM1 functions as a crucial regulator of Ca^{2+} transduction in growth cone filopodia.

5.2 Results

5.2.1 STIM1 expression is required for microtubule protrusion and ER remodeling into growth cone filopodia

The ER and microtubule cytoskeleton are highly interdependent structures, likely functioning closely to localize signals, proteins, vesicles and membrane trafficking within cells (Terasaki et al., 1986; Dailey and Bridgman, 1989; Cole and Lippincott-Schwartz, 1995; Waterman-Storer and Salmon, 1998; Wada et al., 2016). Given that in a range of non-neuronal cells, microtubules support ER remodeling and SOCE in a STIM1-dependent manner (Baba et al., 2006; Smyth et al., 2007; Hájková et al., 2011a), we hypothesized that ER is remodeled by microtubules to facilitate spatial Ca^{2+} signals in steering growth cones. In the previous chapter, we used STIM1 expression as a proxy of ER localisation. To confirm the presence and localisation of ER within growth cones, and determine whether ER membranes are closely associated with microtubules, randomly extending growth cones (Fig. 5.1.a) were imaged using tubulin-GFP (Fig. 5.1.b), and ER-RFP (Fig. 5.1.c) reporters, to label microtubules and ER respectively. Microtubule and ER structures redistributed in parallel within the central and peripheral zones of growth cones (Fig. 5.1.d), consistent with results in chapters 3 and 4 which used STIM1 and βIII-tubulin as measures of ER and microtubule localisation. These data suggest ER colocalises with microtubules in DRG sensory neuron growth cones. Taken together with data in chapter 4, STIM1 functions as both a microtubule binding protein and SOCE regulator to possibly localise Ca^{2+} signals to the cytoskeleton directly through EB3. We sought to determine whether ER remodeling occurs in a STIM1 and EB3 dependent manner in areas of instructive Ca^{2+} signaling, such as growth cone filopodia.

While the peripheral domains of extending growth cones are relatively organelle-poor and dominated by actin filaments, the presence of microtubules and ER-like membranes

in growth cones has been previously demonstrated by electron microscopy (Dailey and Bridgman, 1989; 1991). Since our baculovirus-transfected tubulin-GFP and ER-RFP experiments provided initial confirmation of ER remodeling in sensory growth cones, we next utilized more sensitive constructs that allowed visualization and spatiotemporal analysis of ER and microtubule structures in the small filopodial sub-compartments. To determine whether remodelling of the ER occurs in growth cone filopodia, DRGs were co-transfected with BiP-mCherry-KDEL (Zurek et al., 2011) and EB3-YFP (Fig. 5.2), to localise ER and microtubules respectively. Consistent with previous reports that ER-like membranes extend along microtubules and appear to interact via cross-bridging elements at electron dense microtubule tips (Dailey and Bridgman, 1991), ER (KDEL-mCherry) co-localised with EB3-YFP at microtubule-tips, extending towards and into filopodia (Fig. 5.2.a-b). Growth cones with reduced STIM1 expression exhibited significantly fewer filopodia that contained both ER and EB3 protrusions (Fig. 5.2.c; quantified in Fig. 5.2.e). Interestingly, while in control growth cones (n=7) many of the observed EB3 dashes (80.1 $\pm$ 5.8%) were localized with KDEL-mCherry, this number was significantly reduced (54.13 $\pm$ 5.4%) in growth cones with reduced STIM1 expression (n=12; Fig. 5.2.f). This could account for the reduced number of ER-protrusions in filopodia of STIM1 deficient growth cones. Furthermore, the distance and velocity of ER and EB3 protrusions in filopodia (quantified in Fig. 5.2.g) was significantly reduced in growth cones with reduced STIM1 expression compared to control (as reflected in time-scale of kymographs, Fig. 5.2.b,d). Taken together, these findings demonstrate that STIM1 is required for the tethering and remodelling of ER into protruding filopodia by microtubules.

Figure 5.1. Remodeling of the ER parallels the distribution of tubulin

(a-d) Time-lapse images of randomly extending DRG sensory neuron growth cones imaged over 2 min (phase images in a) transfected with fluorescent reporters for (b) tubulin (GFP, green) and (c) endoplasmic reticulum (ER; RFP, red). Arrows depict ER protrusions extending into the leading edge of the growth cone over time, which co-localize with polymerized microtubules (merged images in d).

Scale bars a, 10μm; b-d, 5μm.

Fig 5.1

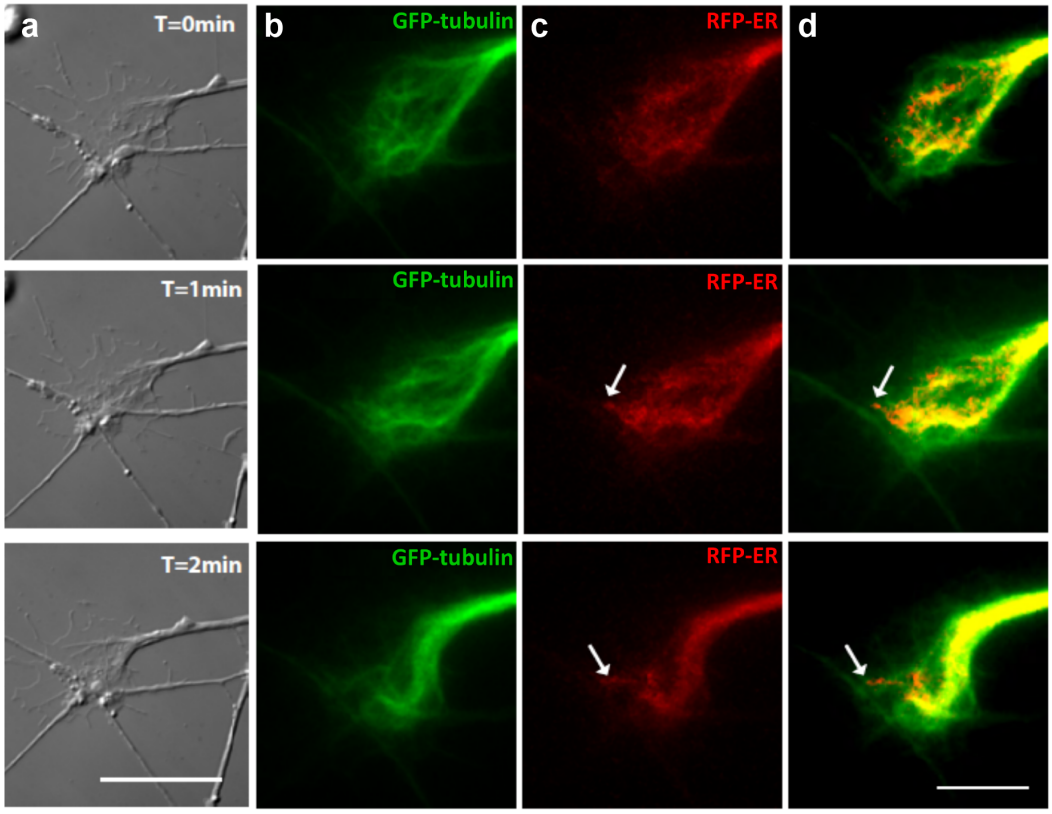
a
T=0min
b
GFP-tubulin
c
RFP-ER
d
T=1min
GFP-tubulin
RFP-ER
T=2min
GFP-tubulin
RFP-ER

Figure 5.2. STIM1 is required for the remodeling of microtubules and ER at growth cone filopodia

(a-d) Images of randomly extending DRG sensory neurons co-transfected with BiP-mCherry-KDEL (ER marker, red) and EB3-YFP (green). (a, c) Merged images depict ER and EB3 distribution in (a) control (inset depicts filopodial expression) and (c) STIM1 knockdown (STIM1 KD) growth cones.

(b, d) Left: KDEL (red) and EB3 (green) localisation in filopodia (outlined on phase images). Right: Representative kymograph of KDEL (red) and EB3 (green) as an EB3-dash extends into filopodial tip, displayed over 20sec in (b) control and 40sec in (d) STIM1 morphant.

(e) Percent of filopodia with KDEL signal, (f) percent of filopodia with EB3-KDEL signal and (g) the distance of EB3-KDEL protrusion into filopodia of control and STIM1 morphant growth cones (distance of protrusion normalized to entire filopodial length). n-values displayed. Error bars indicate ± SEM. * $p<0.05$, **** $p<0.0001$; (Student's *t*-test).

* $p<0.05$, **** $p<0.0001$; (Student's *t*-test). Scale bars a and c, 5μm; b and d, 500nm.

Fig 5.2

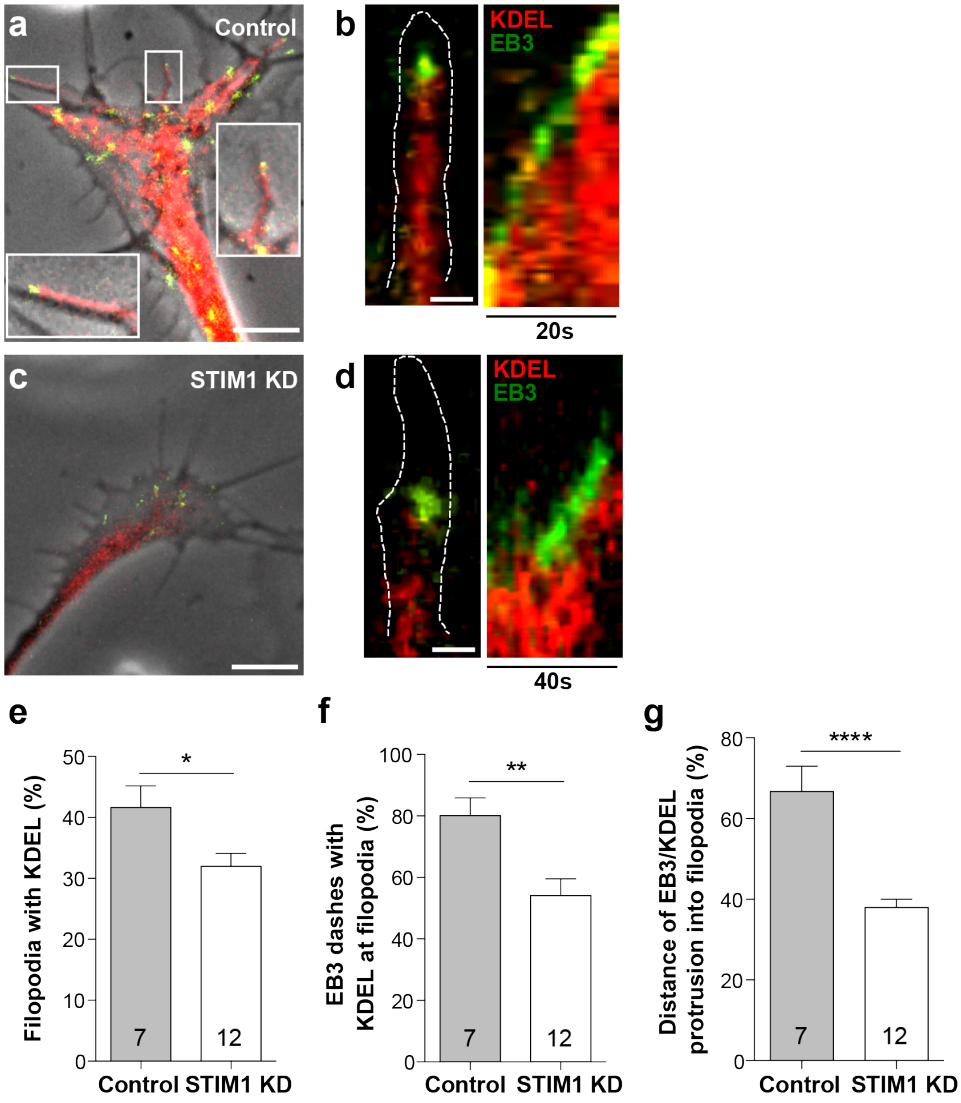
a
Control
b
KDEL
EB3
20s
c
STIM1 KD
d
KDEL
EB3
40s
e
Filopodia with KDEL (%)
*
7
12
Control STIM1 KD
f
EB3 dashes with KDEL at filopodia (%)
**
7
12
Control STIM1 KD
g
Distance of EB3/KDEL protrusion into filopodia (%)
****
7
12
Control STIM1 KD

5.2.2 STIM1 regulates endoplasmic reticulum-derived Ca^{2+} signals in growth cone filopodia

STIM1 has been shown to mediate filopodial Ca^{2+} transients in *Xenopus* spinal neurons through activation of SOCE (Shim et al., 2013). Given that STIM1 functions as a regulator of luminal Ca^{2+}_{ER} content, we next asked if knockdown of STIM1 expression was able to perturb Ca^{2+}_{ER} in filopodia in addition to disrupting ER remodelling. To quantitate Ca^{2+}_{ER} in filopodia, a genetically-encoded Ca^{2+}_{ER} sensor ER-GCaMP6-150 was used. ER-GCaMP6-150 has a Ca^{2+} affinity that closely resembles resting Ca^{2+}_{ER} levels, and is capable of measuring changes in axonal Ca^{2+}_{ER} (de Juan-Sanz et al., 2017). These properties make ER-GCaMP6 a good candidate for measuring filopodial Ca^{2+}_{ER} compared to alternative Ca^{2+}_{ER} sensors.

Consistent with findings that ER and EB3 protrusion into growth cone filopodia (Fig. 5.2), Ca^{2+}_{ER} dynamics were perturbed in filopodia with reduced STIM1 expression (Figs. 5.3-5.5). The speed at which EB3 and Ca^{2+}-replete ER membrane protruded to the tip of growth cone filopodia was decreased in STIM1 morphant growth cones (as reflected in time-scale of kymographs Fig. 5.3.b and Fig. 5.3.e) compared to control growth cones (Fig. 5.3.a and Fig. 5.3.d). Similarly, the distance protruded by EB3 and Ca^{2+}-replete ER membrane was also reduced in STIM1 morphant filopodia compared to control (quantified in Fig. 5.4.c), as ER protrusion was reduced in filopodia of STIM1 morphants (Fig. 5.2). Interestingly, in control growth cones (n=12) 74.5 $\pm$ 3.5% of EB3 dashes in filopodia were localized with a Ca^{2+}_{ER} signal, while in growth cones with reduced STIM1 expression (n=12) this number was significantly reduced (59.01 $\pm$ 2.7%) (Fig. 5.4.a). This result was specific to filopodia and was not significantly different between control and STIM1 morphants in transition or central domains of growth cones (Fig. 5.4.a). Importantly, this figure represents EB3 dashes associated with any fluorescent signal

Figure 5.3. STIM1 is required for the regulation of Ca^{2+}_{ER} signals at growth cone filopodia

(a-b) Time-lapse images of randomly extending growth cone filopodia co-transfected with ER-GCaMP6-150 (Ca^{2+}_{ER} reporter, green) and EB3-tdTomato (red), imaged over 10sec in (a) control and 25sec (b) STIM1 morphant.

(c) Schematic illustrates STIM1-EB3-mediated protrusion of microtubules and endoplasmic reticulum into filopodia, where ER-GCaMP6 fluorescence was used to report Ca^{2+}_{ER}.

(d-e) Left: Ca^{2+}_{ER} (green) and EB3 (red) in filopodia (outlined using phase images). Middle: Representative kymograph of Ca^{2+}_{ER} (green) and EB3 (red) as EB3-dash extends towards filopodial tip, displayed over 20sec in (d) control and 40sec (e) STIM1 morphant. Right: Representative kymograph of Ca^{2+}_{ER} (ER-GCaMP6 pseudocoloured for intensity, colours corresponding to level of Ca^{2+} as indicated by heat-map). Asterisks depict Ca^{2+}_{ER} "hotspots" likely to represent sites of ER-refilling.

Scale bars a-b, 1µm; d-e, 500nm.

Fig 5.3

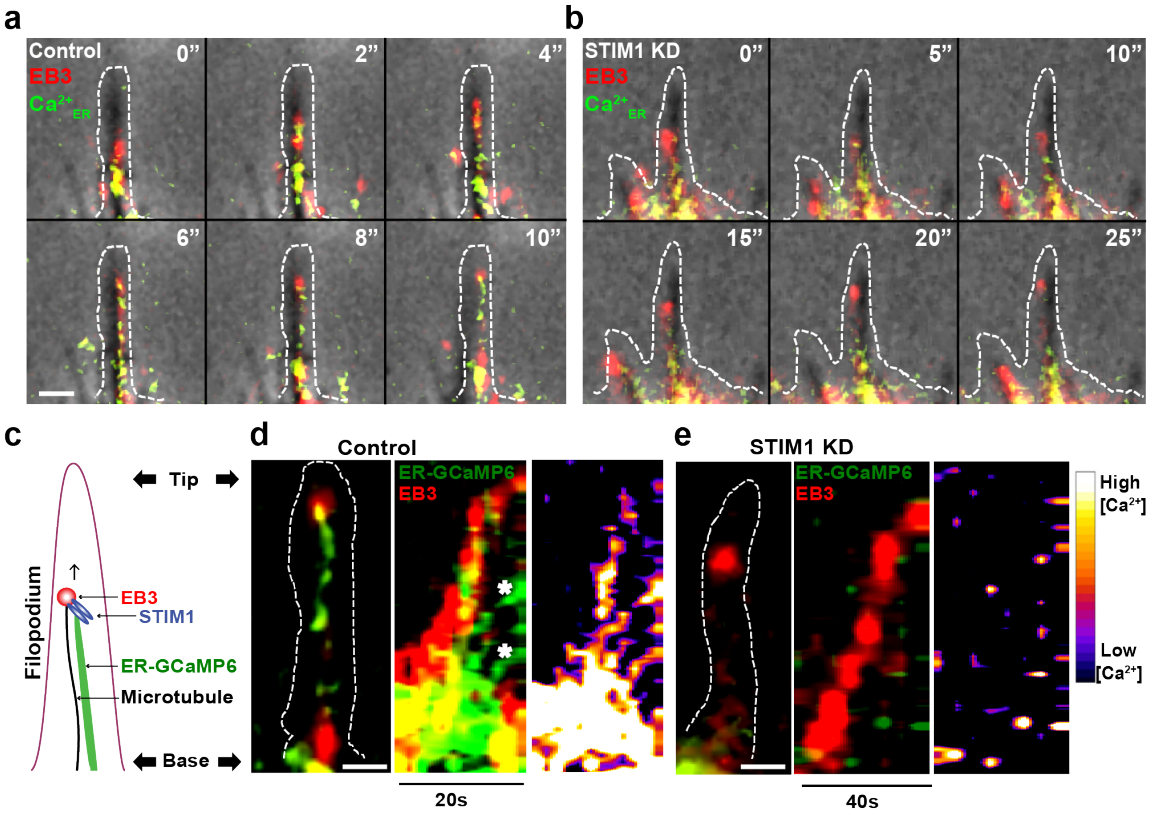
a
b
Control
EB3
Ca2+ ER
0”
2”
4”
6”
8”
10”
STIM1 KD
EB3
Ca2+ ER
0”
5”
10”
15”
20”
25”
c
Tip
Filopodium
EB3
STIM1
ER-GCaMP6
Microtubule
Base
d
Control
ER-GCaMP6
EB3
20s
e
STIM1 KD
ER-GCaMP6
EB3
40s
High [Ca2+]
Low [Ca2+]

Figure 5.4. STIM1 is required for localisation of ER-derived Ca^{2+} signals at growth cone filopodia

(a) Percent of EB3 dashes that were co-expressed with any detectable ER-GCaMP6 (Ca^{2+}_{ER}) signal at filopodia, transition zone and central zone in control (grey bars) and STIM1 morphant (clear bars) growth cones. (b) Percent of filopodia with any detectable Ca^{2+}_{ER} signal and (c) the distance of EB3-Ca^{2+}_{ER} protrusion into filopodia of control (grey bars) and STIM1 morphant (grey bars) growth cones (normalized to entire filopodial length). * $p<0.05$, ** $p<0.01$; (Student's *t*-test).

Fig 5.4

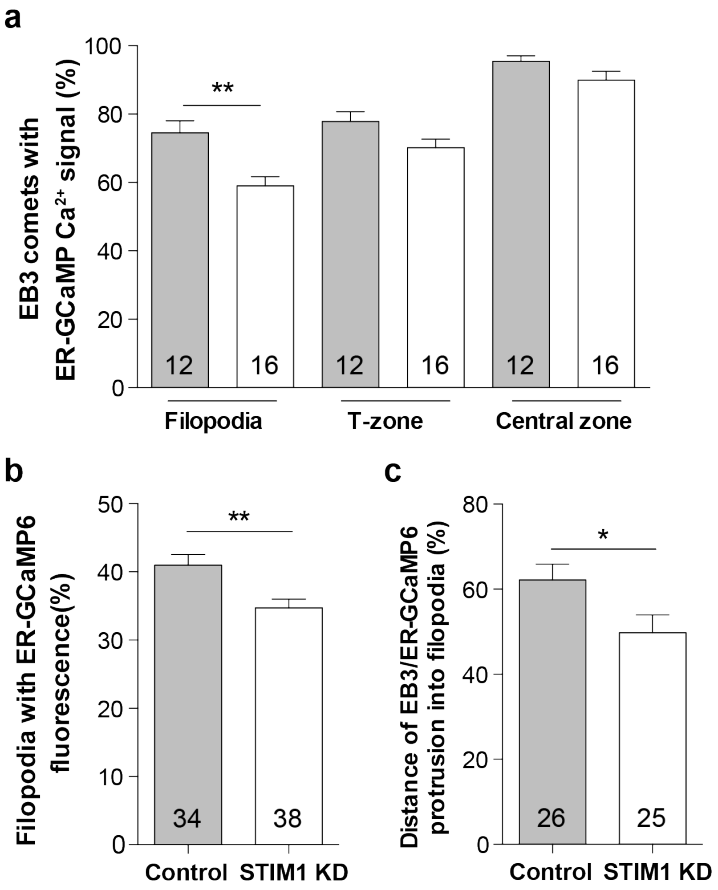
a
EB3 comets with ER-GCaMP Ca2+ signal (%)
100
80
60
40
20
0
**
12
16
12
16
12
16
Filopodia
T-zone
Central zone
b
Filopodia with ER-GCaMP6 fluorescence(%)
50
40
30
20
10
0
**
34
38
Control
STIM1 KD
c
Distance of EB3/ER-GCaMP6 protrusion into filopodia (%)
80
60
40
20
0
*
26
25
Control
STIM1 KD

from the ER-GCaMP6-150, regardless of how weak the signal. As illustrated in Fig. 5.3.e, the Ca^{2+}_{ER} signal was extremely weak (quantified in Fig. 5.5.c). In both control and STIM1 deficient growth cones, the percentage of filopodia exhibiting a Ca^{2+}_{ER} signal (Fig. 5.4.b, signals quantified irrespective of magnitude) correlated with the percentage of filopodia containing ER (Fig. 5.2.e). Interestingly, Ca^{2+}_{ER} signal was highly localised with the EB3 signal in control growth cones as EB3 dash protruded to the tip of the filopodia (see kymograph Fig. 5.3.d), suggesting interaction between microtubules and replete stores, consistent with the Ca^{2+}_{ER}-dependent tip-attachment complex model. Focal Ca^{2+}_{ER} signals were detected at stationary "hot-spots" (Fig. 5.3.d) which followed periods of low Ca^{2+}_{ER} signals (emptied stores) and likely represent sites of ER-refilling. Taken together, these results demonstrate that reduced STIM1 expression disrupts both the level of Ca^{2+}_{ER}, SOCE signalling and ER remodelling in filopodia.

Quantitation of Ca^{2+}_{ER} flux in filopodia confirmed how these are spatially regulated in filopodia of control and STIM1 morphant growth cones. The spatial kinetics of Ca^{2+}_{ER} concentration in filopodia were analysed by measuring Ca^{2+}_{ER} at the base, middle and tip of filopodia as EB3 dashes protruded towards the filopodial tip (Fig. 5.5.a-b), as previously we had only quantitated the percentage of filopodia expression any Ca^{2+}_{ER} signal, regardless of spatial location and concentration. Focal increases in filopodial Ca^{2+}_{ER}, observed in control growth cones were not evident in STIM1 morphant growth cones. Notably, these focally-elevated Ca^{2+}_{ER} signals were evident at or near EB3 dashes in control filopodia (Fig. 5.5.b), further indicating that Ca^{2+}_{ER} signals within replete and actively-remodelling ER were closely associated with protruding microtubules in filopodia. The level of Ca^{2+}_{ER}, assessed using the change in relative fluorescence of ER-GCaMP6-150, was dramatically reduced in STIM1 morphant filopodia (n=39; 0.08 $\pm$ 0.02) compared to control filopodia (n=36; 0.38 $\pm$ 0.07) (Fig. 5.5.c), correlated to the expressions presented earlier (Fig. 5.3). These findings support a model where STIM1

expression is necessary for the regulation of Ca^{2+}_{ER} levels and localisation of ER-derived Ca^{2+} signals within subcellular compartments such as filopodia (Fig. 5.5.d). Altogether these data demonstrate a necessity for STIM1 in the spatial localisation of ER Ca^{2+} flux in filopodia.

Figure 5.5. STIM1 is required for the spatial regulation of ER-derived Ca^{2+} signals at growth cone filopodia

(a) Schematic illustrating STIM1- and EB3-mediated microtubule and ER protrusion into filopodia, and demarks regions at the base, middle and tip of filopodia. (b) ER-GCaMP6 relative fluorescence ($\Delta F/F$) was measured at these points in control (grey circles) and STIM1 morphant (open circles) filopodia. Arrowheads depict point of peak EB3 intensity at tip, middle and base of filopodia. * $p<0.05$; (Two-way ANOVA, Sidak's multiple comparison test).

(c) Relative filopodial Ca^{2+}_{ER} signal in control (n=12) and STIM1 morphant (n=13) filopodia (integrated over the entire imaging period). **** $p<0.0001$; (Student's *t*-test).

(d) Schematic illustrates proposed model of STIM1-EB3-mediated microtubule and ER protrusion in control and STIM1 morphant filopodia where STIM1 expression facilitates ER-protrusion and sustains ER-derived Ca^{2+} signals.

* $p<0.05$, **** $p<0.0001$; (Student's *t*-test, Two-way ANOVA, Sidak's multiple comparison test))

Fig 5.5

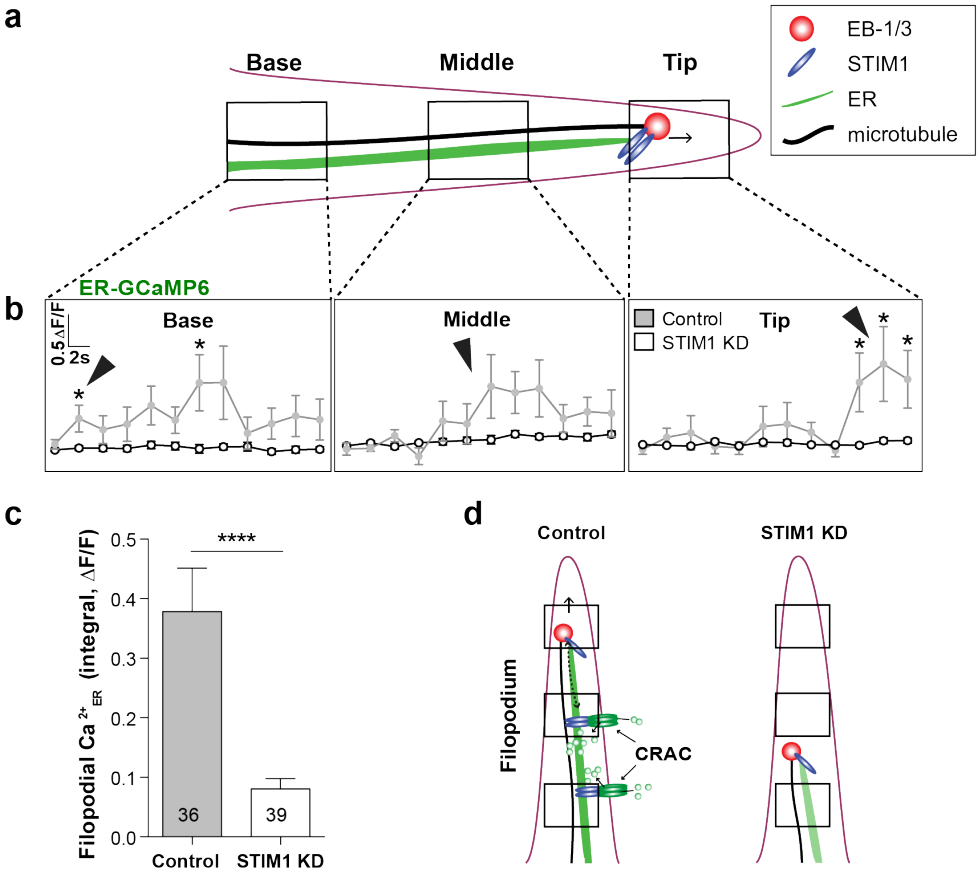
a
Base
Middle
Tip
EB-1/3
STIM1
ER
microtubule
b
ER-GCaMP6
0.5 ΔF/F
2s
Base
Middle
Tip
Control
STIM1 KD
c
Filopodial Ca2+ ER (integral, ΔF/F)
0.5
0.4
0.3
0.2
0.1
0.0
****
36
39
Control
STIM1 KD
d
Control
STIM1 KD
Filopodium
CRAC

5.3 Discussion

This is the first study to demonstrate active ER remodeling in growth cone filopodia. The data presented in this chapter suggest that ER networks are dynamically mobile within growth cones and that ER remodeling at central and peripheral domains of growth cones is facilitated by microtubules. The dynamic interaction between polymerizing microtubules observed using EB3 dashes, and ER membranes at the growth cone periphery was disrupted when STIM1 expression was reduced. The data presented here suggests that STIM1 is necessary for both protrusion of microtubules and remodeling of Ca^{2+}-replete ER at growth cone filopodia, mediating the spatiotemporal dynamics of Ca^{2+}_{ER} in filopodia. These data strongly suggest that STIM1 regulates Ca^{2+}_{ER} and microtubule stability in filopodia and represents a possible mechanism to sustain instructional Ca^{2+} transients. Since filopodia are the crucial initiators of growth cone motility and instructors of axon navigation, it is not surprising that STIM1 morphant growth cones exhibit axon pathfinding defects when filopodial Ca^{2+}_{ER} signal localization is disrupted.

STIM1 is necessary for the remodeling of microtubules and ER into filopodia

Tubular ER is thought to be a wholly interconnected and continuous membrane structure in neurons (Terasaki et al., 1994). This Ca^{2+}-rich network could facilitate the transduction of Ca^{2+} signals throughout growth cones through a tunnel-like system of interconnected tubules. In this manner, Ca^{2+}_{ER} depletion in areas of active motility such as the growth cone periphery could activate SOCE and sustain Ca^{2+} signals spatially and temporally. Work in this chapter supports the notion that STIM1 is crucial for the transduction of such Ca^{2+} signals to areas that are critical for growth cone steering such as growth cone filopodia, by directly regulating ER-microtubule remodeling. Interactions between microtubules and ER associated proteins, including p600 and myosin Va, are known to

occur in neurons and are important for neuronal function (Shim et al., 2008; Wada et al., 2016). This chapter demonstrates that STIM1 is also crucial for microtubule-ER remodeling and the localization of Ca^{2+}_{ER} in filopodia, a mechanism that is likely to sustain instructional Ca^{2+} transients necessary during pathfinding.

Here we demonstrate that microtubules remodel ER in growth cones and filopodia. These findings support the early work of Dailey and Bridgman who demonstrated striking colocalisation between ER-like membranes and microtubules at the growth cone periphery using electron microscopy (Dailey and Bridgman, 1989). The colocalisation between microtubules and a Ca^{2+} sequestering store such as the ER was proposed to coordinate Ca^{2+} signals and cytoskeletal reorganization in growth cones (Dailey and Bridgman, 1989). Since then, mechanisms that regulate direct interaction between the ER and microtubule cytoskeleton have been explored in various cell types.

The microtubule and ER associated protein, p600 (or ZUBR1), has been shown to colocalise with microtubules and ER in various compartments of neurons (Shim et al., 2008). Reducing the expression of p600 disrupts migration and positioning of cortical neurons in the developing mouse neocortex, likely resulting from destabilization of microtubules and reduced ER localization at leading processes (Shim et al., 2008). While STIM1 links ER and microtubules through a tip attachment complex with EB proteins (Grigoriev et al., 2008), p600 is likely implicated in ER-microtubule transport through sliding via motors, or microtubule-based movement (Waterman-Storer and Salmon, 1998; Shim et al., 2008). In a manner similar to STIM1 morphant growth cones however, leading processes of p600-depleted neurons contained few weakly stained ER-membranes, exhibited perturbed microtubule stability and presented defects in motility, migration and positioning. Although there is no evidence that STIM1 and p600 interact to regulate ER and microtubule interactions in growth cones, these ER-proteins appear

to share functions and cause similar defects in neurons when absent. Together with the results demonstrated in this chapter, it is clear that growth cone motility is heavily dependent on the interplay between cytoskeletal dynamics and ER function, including Ca^{2+}_{ER} signaling.

In endothelial cells, direct interaction between microtubules and ER occur through EB3 binding to IP_3Rs (Geyer et al., 2015). Microtubules assist in the clustering of IP_3Rs within the ER membrane, and this clustering is required for Ca^{2+} to be released from the stores to generate spatially-organized Ca^{2+} domains (Geyer et al., 2015). In this manner, microtubules support the generation of IP_3-induced Ca^{2+} micro-domains (Geyer et al., 2015), reflecting how microtubule tip-attachment complexe localizes STIM1 to activate SOCE upon store depletion.

Microtubule-ER interactions are also regulated by the Ca^{2+}-dependent motor protein myosin Va (MyoVa) which binds to RyR and IP_3R to tether VAMP2-positive vesicles to ER membranes to regulate vesicle transport in a Ca^{2+}-dependent manner (Wada et al., 2016). Activation of CICR causes MyoVa to dissociate from RyR and IP_3R and facilitates asymmetric vesicle transport and membrane exocytosis which supports attractive growth cone turning. Growth cone attraction is reversed to repulsion when the MyoVa pathway is impaired (Wada et al., 2016). It is likely that dissociation of MyoVa from the ER facilitates vesicle recruitment and downstream microtubule-dependent membrane transport to the cell periphery in a mechanism assisted by kinesin-driven transport (Akiyama et al., 2016; Wada et al., 2016). Such localized membrane and organelle trafficking is crucial for axon motility and further highlights the importance of understanding the mechanisms that localize Ca^{2+} signals within motile growth cones.

STIM1 is required for the spatial regulation of Ca^{2+}_{ER} at growth cone filopodia

The findings presented here demonstrate that STIM1 is necessary for the protrusion of microtubules, ER, and importantly, Ca^{2+}_{ER} to distal filopodia. These results provide novel insights into the processes underlying the generation and maintenance of filopodial Ca^{2+} signals. Calcium is a vital regulator of filopodial protrusion and stabilisation, as demonstrated in grasshopper axons, where increasing intracellular calcium levels to approximately 1μM using photolysis, results in the formation of new filopodial protrusions which persist for up to 15 minutes (Lau et al., 1999). At rest, the concentration of cytosolic calcium is in the nM scale, while the luminal Ca^{2+}_{ER} concentration in sensory DRG neurons has been shown to range from 100-200μM (Solovyova et al., 2002). Solovyova and colleagues also calculated the maximum rate of calcium release from the ER to be 90μM/min, where the amplitude of calcium release depends on the level of luminal Ca^{2+}_{ER}, and the maximum rate of uptake was 360μM/min (Solovyova et al., 2002). Given that the ER can remodel to localise calcium signals, it provides the ideal means to maintain calcium signals necessary for the generation and stabilisation of filopodia. In support of this, while not quantified, collapsing filopodia are devoid of microtubules and ER, although it is unclear whether retraction of microtubules and ER result in the collapse of an unstable filopodia, or whether the retraction of these organelles and the filopodium itself occur simultaneously. Such experiments would be of interest to improve our understanding of filopodial protrusion and stabilisation.

Previously, the frequency of Ca^{2+} transients in filopodia of *Xenopus* spinal neurons was shown to be unaffected by store depletion (Gomez et al., 2001). Gomez and colleagues (Gomez et al., 2001) demonstrated that spatially-localized filopodial Ca^{2+} transients resulting from Ca^{2+} influx through non-VGCC, propagated back to the parent growth cone and assisted in directing growth cone motility when stimulated asymmetrically. However,

the frequency of filopodial transients was unchanged with thapsigargin treatment (ER depletion) and it was thought that filopodial Ca^{2+} transients did not require signal amplification from store-derived Ca^{2+} release. This is at odds with more recent reports which have demonstrated that STIM1-dependent SOCE operates in growth cone filopodia of *Xenopus* spinal neurons *in vitro* and *in vivo* where STIM1 expression was vital for the generation of oscillatory filopodial Ca^{2+} transients (Shim et al., 2013). The results outlined in this study are in broad agreement with Shim and colleagues, in that we demonstrate protrusion of ER membranes as well as filopodial Ca^{2+}_{ER} dynamics require STIM1. We demonstrate that STIM1-deficient growth cones exhibit fewer EB3 dashes associated with any Ca^{2+}_{ER} signal, regardless of localisation and concentration. Our findings that Ca^{2+}_{ER} dynamics were reduced in STIM1 morphant filopodia, even at the base of filopodia where ER membranes were still observed (Fig. 5.5), suggests that not only is STIM1 necessary for ER-microtubule protrusion at the periphery of growth cones, but it is also required for the maintenance of Ca^{2+}_{ER} content (as illustrated in model Fig. 5.5.c). This is also illustrated by the absence of Ca^{2+}_{ER} fluctuations over time in STIM1-deficient filopodia as EB3 dashes protrude to the filopodial tip. The results in this chapter also showed that the distance and velocity of ER and EB3 protrusions in filopodia are significantly reduced in STIM1 knockdown growth cones. These findings are consistent with the results presented in the previous chapter, and agree with the notion that a threshold level of STIM1 is necessary to sustain STIM1-microtubule interactions and SOCE. Perturbing this threshold level reduces the rate of protrusion of both ER and microtubules in filopodia as both depend on STIM1 to function correctly.

Our data, together with the observation that STIM1-dependent SOCE is required for filopodial Ca^{2+} transients and for growth cone turning to netrin-1 (Shim et al., 2013), suggest that STIM1 likely regulates filopodial Ca^{2+} through two parallel mechanisms: firstly, STIM1 interactions with polymerizing microtubules via tip-attachment complexes

remodels ER and ER-derived Ca^{2+} signals into filopodia, and secondly STIM1 dissociates from EB-1/3 upon store depletion to trigger SOCE. It is likely that Ca^{2+} transients initiated at distal filopodial tips require signal amplification, from both CICR and SOCE, in order to effectively propagate back to the growth cone and areas of motile reorganization, such as lamellipodia. A local and sustained Ca^{2+} signal that is directly linked to the microtubule cytoskeleton at growth cone filopodia would be predicted to reduce microtubule catastrophe and therefore enhance filopodial stabilization (Buck and Zheng, 2002). The spatiotemporal regulation of ER remodeling in filopodia, and subsequent formation of CRAC at ER-PM junctions following store depletion, would also provide a localized source of Ca^{2+} to enhance filopodial stability for growth cone consolidation and extension.

Whilst STIM1-dependent SOCE is necessary for the generation of filopodial Ca^{2+} transients in *Xenopus* spinal neurons (Shim et al., 2013), SOCE has also been shown to remain unchanged in STIM1 knockout rodent cortical neurons where STIM2 appears to be the main SOCE-regulator (Berna-Erro et al., 2009). For this reason, and given the abundant expression of other Ca^{2+} channels in neurons such as VGCCs, which are well-known correlates of prominent Ca^{2+} signals and neuronal activity, the function of STIM1 in neuronal cells has until recently been largely unexplored. Most studies investigating the function of STIM proteins in the nervous system report on their regulation of Ca^{2+} signaling in synaptic activity (Berna-Erro et al., 2009; Hartmann et al., 2014; Sun et al., 2014; de Juan-Sanz et al., 2017), with some reporting on SOCE-independent functions either at the synapse or growth cone (Mitchell et al., 2012; Garcia-Alvarez et al., 2015). The work in this chapter demonstrates that the SOCE-independent function of STIM1 acts to remodel ER into filopodia, and this is crucial for the delivery of ER cargo to distal filopodial tips. In rodent hippocampal neurons, Ca^{2+}_{ER} content drives changes in exocytosis at the presynaptic compartment, where natural fluctuations in Ca^{2+}_{ER} content

act in a feedback loop to drive synapse activity through regulation of plasma membrane function. This Ca^{2+}_{ER}-plasma membrane feedback loop is regulated by STIM1 expression (de Juan-Sanz et al., 2017). The work of de Juan-Sanz and colleagues provided a novel link between ER and synapse function, in a mechanism that is STIM1-dependent. Since the growth cone specializes to become the presynaptic compartment of the synapse, it may not be surprising that STIM1-regulated Ca^{2+}_{ER} machinery is vitally important in both structures. Furthermore, given the necessity of STIM1 in the Ca^{2+}_{ER}-plasma membrane feedback loop at the synapse, it would be expected that growth cone pathfinding is disrupted when STIM1-regulated exocytosis is perturbed in STIM1 morphant growth cones (Tojima et al., 2007; 2010).

Chapter 6:

Conclusions and future directions

Chapter 6: Conclusions and future directions

In addition to the canonical role of STIM proteins in store-operated Ca^{2+} entry, STIM1 is multifunctional, being required for a range of cellular processes. STIM proteins are crucial determinants of neuronal function, through regulation of Ca^{2+} homeostasis and synaptic activity (Berna-Erro et al., 2009; Hartmann et al., 2014; Sun et al., 2014; de Juan-Sanz et al., 2017), or via SOCE-independent functions either at the synapse or growth cone (Mitchell et al., 2012; Garcia-Alvarez et al., 2015). STIM1 regulates axon pathfinding, synaptic plasticity, axon branching and neuropathic pain (Baba et al., 2003; Gemes et al., 2011; Steinbeck et al., 2011; Mitchell et al., 2012; Shim et al., 2013), as well as inhibition of L-type VGCC in neurons (Park et al., 2010; Wang et al., 2010), and activation of second messenger cAMP in non-neuronal cell lines (Lefkimmiatis et al., 2009). STIM1-dependent SOCE regulates growth cone motility and Ca^{2+} dynamics in response to various guidance cues (Mitchell et al., 2012; Shim et al., 2013). A substantial amount of work mostly derived from non-neuronal cells, has demonstrated that STIM1 can regulate SOCE-dependent and –independent mechanisms, including the formation of tip-attachment complexes (Grigoriev et al., 2008; Honnappa et al., 2009). This thesis has investigated how STIM1 associates with the cytoskeleton, particularly with microtubules through tip-attachment complexes to facilitate ER remodelling and activate SOCE signalling in neuronal growth cones. The work presented here supports the hypothesis that STIM1 is not only a SOCE regulator, it also regulates ER-microtubule remodelling and localises instructive Ca^{2+} signals in a spatiotemporal and compartmentalised manner at the growth cone and at actively protruding structures such as filopodia.

Previously, STIM1 has been shown to be a key regulator of Ca^{2+}_{ER} in mouse cerebellar Purkinje neurons (Hartmann et al., 2014), and more recently, Ca^{2+}_{ER} content has been shown to regulate exocytosis and synapse activity in a STIM1-dependent manner at the

presynaptic compartment of rodent hippocampal neurons via a Ca^{2+}_{ER}-plasma membrane feedback loop (de Juan-Sanz et al., 2017). The work of de Juan-Sanz and colleagues provided novel insights into the intersection between ER and synapse dysfunction, and an understanding of the function of presynaptic STIM1. Indeed, a number of studies have demonstrated ER dysfunction in neurodevelopmental disorders such as autism, spastic paraplegias and neurodegenerative diseases including Alzheimer's, Parkinson's and amyotrophic lateral sclerosis (ALS) (Katayama et al., 1999; Atkin et al., 2008; Saxena et al., 2009; Beetz et al., 2013; Hetz and Mollereau, 2014; Schmunk et al., 2015; 2017; Yalçın et al., 2017). In order to target neurological disorders where ER dysfunction occurs, we need to better understand ER regulation in neurons.

This thesis demonstrates that as a microtubule-associated protein, STIM1 localizes with the microtubule tracking proteins EB-1/3 and APC throughout the growth cone and particularly at peripheral areas such as filopodia. The association of STIM1 and EB-1/3 was dependent on Ca^{2+}_{ER} content, suggesting that when ER stores are replete ER associates and remodels with microtubules via a tip-attachment complex formed by STIM1 and EB-1/3. This complex dissociates upon store depletion to activate SOCE. These two functions of STIM1 (formation of tip attachment complexes and SOCE activation) previously thought to be unrelated (Bola and Allan, 2009) are crucial for growth cone steering. STIM1 regulates ER remodelling and the localisation of ER-induced Ca^{2+} signals in a spatial and temporal manner in growth cone filopodia, where Ca^{2+} signals are instructional for steering (Fig. 6.1). Our data showed that both functions of STIM1, as microtubule-binding protein and SOCE activator, are necessary and sufficient to steer growth cones. Optogenetic activation of STIM1 which preserves SOCE and microtubule-binding functions, induced directed-growth. However, stimulation of the STIM1-variant lacking a microtubule binding domain, was unable to trigger directed growth. In addition, knockdown of Orai1 expression had no effect on

Figure 6.1. STIM1 functions as SOCE-regulator and microtubule-binding protein in growth cones in a Ca^{2+}_{ER}-dependent manner, and facilitates compartmentalised spatiotemporal Ca^{2+} signals at filopodia

Schematic of proposed mechanism featuring STIM1 and EB-1/3 tip attachment complex-mediated remodeling of ER and microtubules in filopodia. In response to receptor mediated Ca^{2+} signals, tip attachment complexes recruit microtubules and ER to sustain Ca^{2+} flux. STIM1 orchestrates ER remodeling into growth cone periphery through tip attachment complexes, while also functioning in store operated Ca^{2+} entry (SOCE). ER remodelling to growth cone filopodia is crucial for regulating local ER-derived and ER-induced Ca^{2+} signals in a spatiotemporal manner at the actively-protruding growth cone periphery (arrowheads depict local Ca^{2+} microgradients).

(i) Under Ca^{2+} replete conditions monomers of the endoplasmic reticulum-(ER) protein STIM1 are uniformly distributed along the ER membrane, in a state where STIM1 can interact with the microtubule-binding proteins EB-1/3 to facilitate ER-microtubule remodelling. As ER Ca^{2+} is released from the stores through IP_3R/RyR, (ii) Ca^{2+} depletion causes STIM1 monomers to dissociate from EB-1/3, oligomerise and translocate into larger complexes at ER-PM junctions (arrowhead). STIM1 interacts with Orai1, causing Orai1 dimerisation and the formation of a Ca^{2+} release-activated Ca^{2+} (CRAC) channel that facilitates store operated Ca^{2+} entry (SOCE) into the cytoplasm. Ca^{2+} entering the cytosol through SOC channels is rapidly sequestered to the ER via the sarco/endoplasmic reticulum Ca^{2+}-ATPase (SERCA) pump, facilitating store repletion.

Fig 6.1

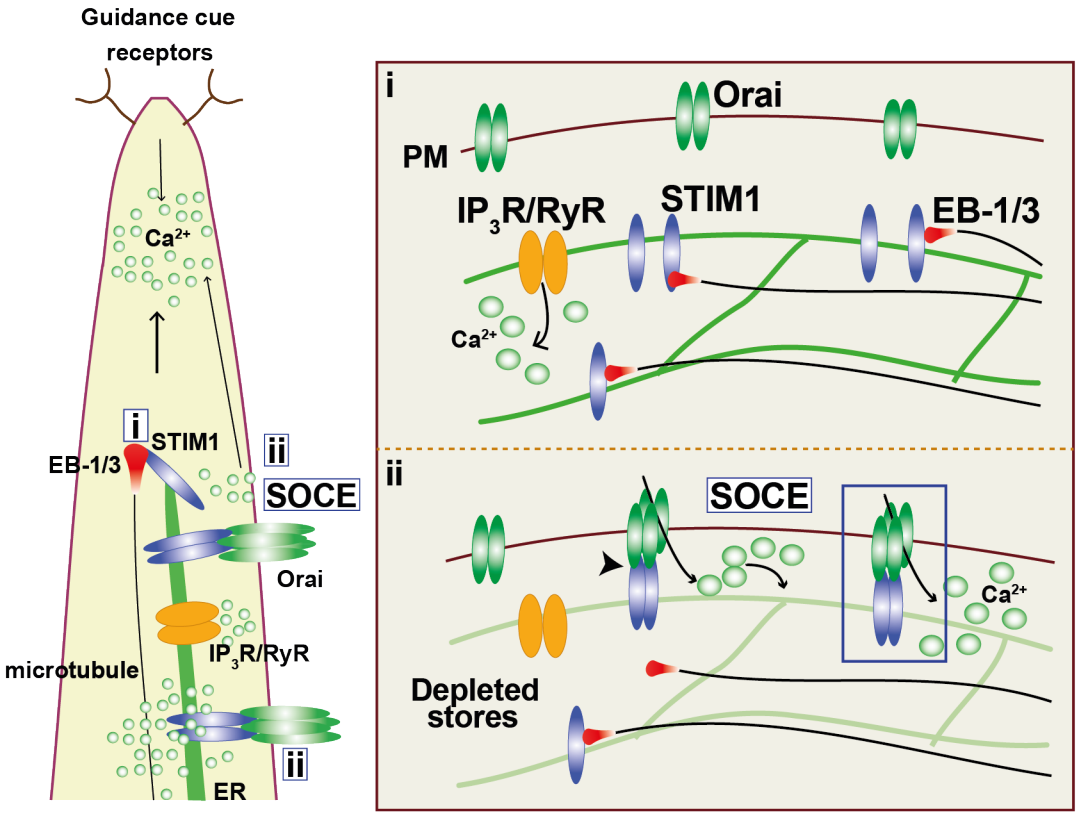
Guidance cue
receptors
Ca2+
i
STIM1
EB-1/3
ii
SOCE
Orai
IP3R/RyR
microtubule
ER
i
Orai
PM
IP3R/RyR
STIM1
EB-1/3
Ca2+
ii
SOCE
Ca2+
Depleted
stores

microtubule polymerisation but significantly impaired growth cone turning to BDNF and sema-3a, demonstrating that a threshold level of STIM1 and SOCE activity are required to carry out SOCE dependent and independent functions. These findings suggest that STIM1 regulates growth cone steering through both SOCE and microtubule-binding functions.

However, there are limitations that remain to be addressed in order to dissect out these functions and better understand how they instruct growth cone motility. While both OptoSTIM1 and LOVS1K trigger Ca^{2+} influx upon light stimulation, OptoSTIM1 has been reported to be more efficient and have higher dynamic range than LOVS1K (Pham et al., 2011; Kyung et al., 2015). This is not surprising, given that OptoSTIM1 and LOVS1K use different light-activated domain systems and LOVS1K is also significantly truncated and lacks not only the EB-1/3 binding domain but also the polybasic polyphosphoinositide binding motif that binds APC. In future work, a potential better control would be "OptoSTIM1-NN" which would combine the light-inducing activity of OptoSTIM1 with a STIM1-NN construct. STIM1-NN has two mutations within EB-1/3-binding motif that render the protein incapable of binding microtubules; 2 amino acids (IP from SxIP motif) are mutated to NN (ie. I644N and P645N point mutations (Honnappa et al., 2009)). This experiment would serve to confirm the microtubule-binding function of STIM1 from SOCE activation. Regardless, our work demonstrates that both SOCE and microtubule-binding functions of STIM1 are necessary for the regulation of growth cone steering.

The ER and microtubule cytoskeleton are interdependent structures. This thesis supports the hypothesis that ER remodels into peripheral regions of the growth cone including filopodia, and demonstrates that this remodelling is mediated by STIM1. As outlined in chapters four and five, STIM1 regulates the spatial localisation of ER, microtubules, microtubule-associated proteins and Ca^{2+}_{ER} within actively protruding growth cones. Interactions between the ER and microtubules are crucial for ER

translocation and organisation, which in itself, is vital for cell migration and motility (Bola and Allan, 2009). Previously, a direct interaction between microtubules and ER via EB-3 and IP_3R had been reported to occur in endothelial cells (also through S/TxIP motif) (Geyer et al., 2015). This interaction is required for the activation of IP_3-induced Ca^{2+} release from the stores and helps to provide a localised Ca^{2+} signal in endothelial cells (Geyer et al., 2015). Microtubules also localise Ca^{2+}_{ER} signals through binding of the Ca^{2+}-dependent motor protein myosin Va to IP_3R/RyR, thus facilitating vesicle-transport and localise membrane trafficking in neuronal growth cones (Wada et al., 2016).

There is clear evidence that microtubules are required to regulate ER-derived Ca^{2+} signals such as those mediated by IP_3R, as well as ER-induced Ca^{2+} signals (ie. SOCE). Disruption of either ER or microtubule function can significantly affect the function of the other organelle. For example, pharmacological disruption of microtubules has been shown to inhibit IP_3R-induced Ca^{2+} activity (Fogarty et al., 2000; Béliveau and Guillemette, 2009), SOCE and I_{CRAC} in non-neuronal cells (Smyth et al., 2007). Perhaps not surprisingly, IP_3R has also been reported to interact with STIM proteins in bovine aortic endothelial cells. In these cells, reduced STIM1 expression disrupts IP_3R-induced Ca^{2+} release from the stores, effectively regulating Ca^{2+} mobilisation by altering both SOCE and IP_3R-mediated Ca^{2+} mobilisation (Béliveau et al., 2014). In addition, it is also likely that STIM1 regulates IP_3R-induced Ca^{2+} release indirectly through calnexin and calreticulin which directly interact with IP_3R (Camacho and Lechleiter, 1995; Joseph et al., 1999). Taken together with the findings presented in this thesis, STIM1 functions as a microtubule-binding protein and activator of SOCE to regulate instructive ER-microtubule remodelling and sustain both Ca^{2+} homeostasis and cytoskeletal dynamics in motile cells and pathfinding growth cones.

Microtubules and ER can associate directly through microtubule and ER crosslinking proteins, such as STIM1. This study has demonstrated that STIM1 functions as a

microtubule-binding protein to mediate ER-microtubule remodelling in pathfinding growth cones *in vitro*. One of the first microtubule-associated proteins demonstrated to interact with ER in neurons was p600 (Shim et al., 2008). p600 is necessary for the migration and localisation of cortical neurons in developing mouse neocortex; a process regulated by direct polymerisation of microtubules (Shim et al., 2008). Unlike STIM1 which is ubiquitously expressed throughout the body, p600 expression is reported in developing and adult neurons of the CNS (Shim et al., 2008). The findings presented in this thesis demonstrate that microtubule polymerisation as well as spatial organisation, were regulated by the microtubule and ER associated protein STIM1. Interestingly, p600 is a calmodulin-binding protein required for membrane-ruffle formation and activation of FAK, and therefore regulation of integrin-mediated signalling in fibroblasts (Nakatani et al., 2005). It is likely that as a calmodulin-binding protein, p600 participates in Ca^{2+} signalling and either directly or indirectly promotes microtubule stabilisation and focal adhesion disassembly at the leading edge of motile neurons, however these speculative p600-mediated mechanisms remain largely unclear. STIM1 on the other hand, forms tip-attachment complexes with EB-1/3 and APC, proteins which stabilise microtubule ends by forming complexes with the formin mDia2 (downstream of Rho) (Wen et al., 2004a) to facilitate filopodial formation, growth and maintenance (Schirenbeck et al., 2005).

The cytoskeleton and cytoskeletal-associated proteins are also crucial regulators of focal adhesions. In fibroblasts, microtubule targeting at the leading edge precedes focal adhesion site remodelling and dissociation (Kaverina et al., 1999). Local tensile stress at adhesion sites within the leading-edge, signal to microtubules to grow towards these sites in various cell types (Kaverina et al., 2002). Of interest, in addition to being a microtubule-associated protein, APC is also involved in the nucleation or assembly of actin in directed cell migration of non-neuronal cells where APC promotes actin nucleation at focal adhesion sites to promote microtubule-induced focal adhesion turnover (Juanes et al., 2017). The findings presented in this thesis demonstrate that

STIM1 regulates cytoskeletal-associated proteins including APC and the levels of focal adhesion kinase, an element of adhesion complexes. Given that STIM1 is crucial for the regulation of cytoskeletal and adhesion systems in growth cones, it is not surprising that microtubules are unable to protrude and become stabilised at the growth cone periphery despite possible compensatory mechanisms taking place such as drebrin upregulation. Several other ER-resident proteins, including calreticulin and protein tyrosine phosphatase 1B (PTP1B) regulate aspects of focal adhesion components (Arregui et al., 1998; Papp et al., 2008; Bola and Allan, 2009) which further support the idea that STIM1 is multifunctional and also necessary for focal adhesion turnover. The data presented here, together with previous reports, demonstrate that STIM1 is multifunctional and necessary for a range of cellular functions including SOCE, ER-remodelling, formation of tip-attachment complexes, and regulation of actin and focal adhesions (Fig. 6.2).

Growth cones specialise to form the presynaptic compartments of synapses, hence many of the mechanisms that regulate function at the growth cone also correlate to presynaptic activity. Ca^{2+} signalling for example, regulates cytoskeletal dynamics at the pre- and post-synaptic structures during synaptogenesis and synapse maturation (Dillon and Goda, 2005; Poo, 2007), as it regulates growth cone pathfinding and extension. Synaptic plasticity, the process that represents the basis for learning and memory, is also regulated by Ca^{2+} (Zucker, 1999). Changes in the magnitude and spatiotemporal organisation of Ca^{2+} signals are proposed to regulate synaptic plasticity and direct a bidirectional switch between long-term potentiation and long-term depression (Berridge, 1998). This bidirectional switch mirrors the attraction/repulsion switch which directs growth cone turning, supporting the notion that Ca^{2+} signalling is

Figure 6.2. STIM1 is a multifunctional protein involved in the regulation of several signalling pathways

Schematic illustrates a number of proposed STIM1 functions, some which remain to be demonstrated in neuronal growth cones. Functions of STIM1 in neurons include store operated Ca^{2+} entry (SOCE), STIM1-mediated inhibition of L-type voltage-gated Ca^{2+} channels (L-VGCC), and tip-attachment complex formation with EB-1/3 to remodel ER and microtubules. Ca^{2+} influx from STIM1/Orai-mediated SOCE is crucial for actomyosin formation and contractile force generation; for focal adhesion turnover through activation of Rac1/Ras1 and Pyk2; and for focal adhesion cleavage through calpain activity on focal adhesion components talin and focal adhesion kinase (FAK). STIM1 has also been shown to interact with ER-buffer calnexin (Cnx), which in turn interacts with calreticulin (Crt) to regulate Ca^{2+}_{ER} capacity, Ca^{2+}_{ER} mobilisation and SOCE activation. Lastly, store-operated cAMP signaling has been shown to couple Ca^{2+}_{ER} directly with cAMP production, through adenylate cyclase (AC). Cyclic nucleotides exert reciprocal inhibition over each other, and regulate the rate of Ca^{2+} flux from the ER by facilitating or inhibiting mobilisation through IP_3R/RyR. A large rise of Ca^{2+} activates Ca^{2+}-calmodulin dependent protein kinase II (CaMKII), which mediates cytoskeletal polymerisation resulting in axon extension or attractive turning if activated asymmetrically in response to a guidance cue such as BDNF.

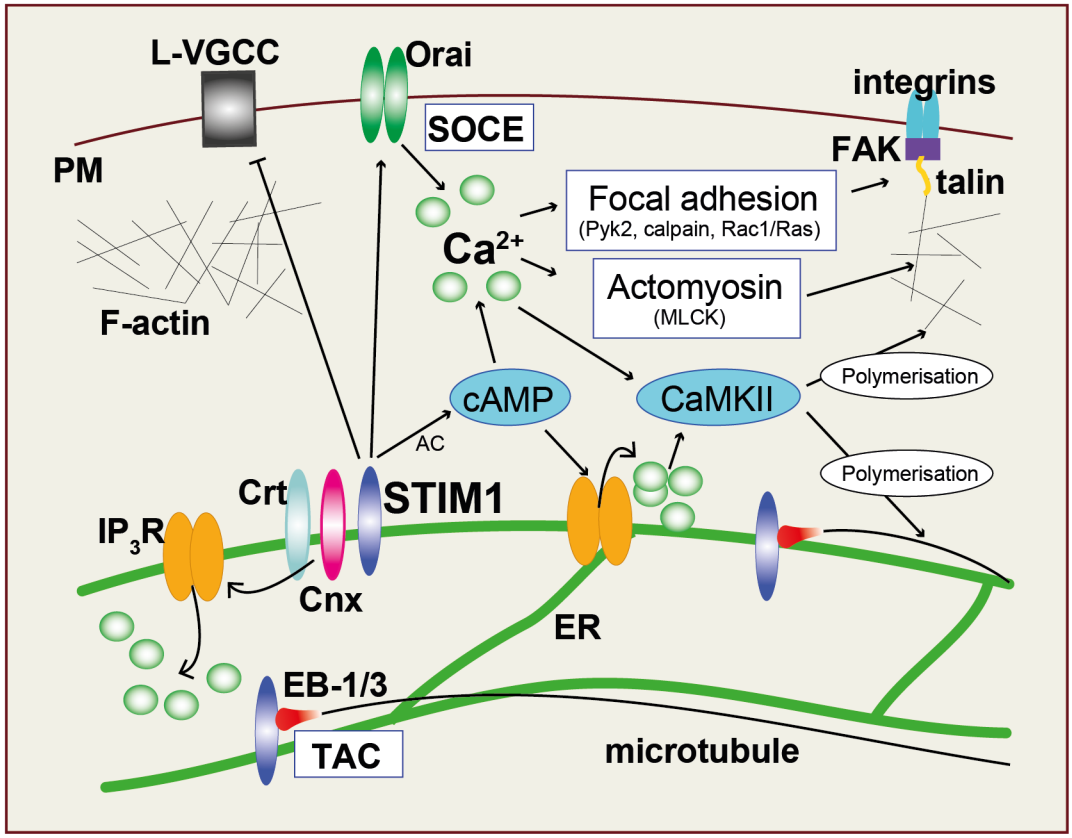
L-VGCC
Orai
integrins
SOCE
FAK
talin
PM
Focal adhesion
(Pyk2, calpain, Rac1/Ras)
Ca2+
Actomyosin
(MLCK)
F-actin
Polymerisation
cAMP
CaMKII
AC
Polymerisation
Crt
STIM1
IP3R
Cnx
ER
EB-1/3
TAC
microtubule

crucial for the regulation of bidirectional responses during axon guidance and synaptic plasticity (Poo, 2007). Given the necessity of STIM1 in the Ca^{2+}_{ER}-plasma membrane feedback loop at the synapse (de Juan-Sanz et al., 2017), it is likely via the microtubule-ER association that STIM1 also regulates exocytosis in growth cones which is vital for pathfinding (Tojima et al., 2007; 2010). In mouse cerebellar Purkinje neurons STIM1 regulation of Ca^{2+}_{ER} is required for metabotropic glutamate receptor type 1 (mGluR1) and IP_3R-dependent Ca^{2+} signals (Hartmann et al., 2014). mGluR1 is abundantly expressed in the CNS and regulates activity-dependent synaptic plasticity (Nakanishi, 1992), thus the finding that STIM1 regulates mGluR1 activity has significant implications for neuronal function in learning and memory.

The function of STIM1 in neurons has been greatly debated, and for a long time was dismissed, given the abundant nature of non-SOCE channels involved in Ca^{2+} signalling in excitable cells, including VGCC. VGCC are activated by depolarisations associated with action potentials or subthreshold stimuli and trigger the influx of Ca^{2+} necessary for neurotransmitter release and synaptic input integration (Furukawa, 2013). Ca^{2+} influx through VGCC and the generation of Ca^{2+} spikes and transients or prolonged global rise of intracellular Ca^{2+}, have been shown to halt growth cone and filopodial extension (Tang et al., 2003b; Lohmann et al., 2005; Gomez and Zheng, 2006). This suggests that a relatively large influx of Ca^{2+} through VGCC is more likely to sustain coordinated and activity-dependent events such as synaptogenesis, whilst alternate sources of Ca^{2+} may be recruited during dynamically motile events, such as axon pathfinding, where activity is spontaneous. Supporting the idea that VGCC drive coordinated events while non-VGCC sources drive spontaneous pathfinding events, is evidence that L- and N-type VGCC are significantly upregulated in foetal and adult synaptosomal membrane subfractions (Vigers and Pfenninger, 1991). Additionally, early stages of development known to support processes such as growth cone motility are mediated by spontaneous Ca^{2+} transients through non-VGCC (Gomez et al., 1995), and attractive growth cone

turning to BDNF and netrin-1 occurs largely independently of L-type VGCC activation in rodent DRG growth cones (Gasperini et al., 2017). STIM1 is necessary for growth cone turning (Mitchell et al., 2012; Shim et al., 2013), and has also been shown to reciprocally inhibit L-type VGCC in neurons while activating Orai1 (Park et al., 2010; Wang et al., 2010). Given this, the function of STIM1 as growth cones specialise to form synapses might be to switch the main source of Ca^{2+} from spontaneous to coordinated (via VGCC), to drive pathfinding and synaptic activity respectively.

The notion that SOCE is a crucial source of Ca^{2+} in developing neurons is intriguing, given the spectrum of Ca^{2+} channels involved in the regulation of neuronal processes such as axon guidance and synaptic plasticity (Luebke et al., 1993; Takahashi and Momiyama, 1993; Wheeler et al., 1994; Iwasaki et al., 2000; Gomez and Zheng, 2006). Crosstalk between different sources of Ca^{2+} signalling is likely to be important for the regulation of synaptic activity. Ca^{2+} resulting from SOCE and NMDA-induced transients and the involvement of NMDA receptor-induced SOCE in long-term potentiation, suggest these sources may function in cooperation to amplify signals (Baba et al., 2003). It is possible that the main source of Ca^{2+} necessary for driving processes such as growth cone navigation change as growth cones specialise into presynaptic structures. Although the role of Ca^{2+} signalling in regulating cytoskeletal dynamics and membrane trafficking at the growth cone and in synaptic function are well described (Zheng and Poo, 2007), the Ca^{2+} signals that direct the transition from growth cone to synapse are unclear. Investigating whether the source of Ca^{2+} at the growth cone shifts from CRAC to VGCC by means of STIM1 reciprocal inhibition as the growth cone transitions into a presynaptic structure, would provide great insights into the regulatory mechanisms that direct synaptogenesis. The source of Ca^{2+} determines the amplitude change in $[Ca^{2+}]_i$ which is important for the regulation of growth cone behaviours (Ooashi et al., 2005; Arie et al., 2009). While an initial Ca^{2+} signal through the plasma membrane can trigger growth cone repulsion, an additional release of Ca^{2+} from internal stores can shift this response to

attraction (Ooashi et al., 2005). Internal stores provide a necessary additional source of Ca^{2+}, which is not only crucial for modulating growth cone behaviour, but also for the regulation of synaptic activity (Peng, 1996; Llano et al., 2000; Galante and Marty, 2003; Sharma and Vijayaraghavan, 2003). Not only are stores necessary to sustain Ca^{2+} signals, but as the work in this thesis has shown, ER stores also regulate the spatial localisation of Ca^{2+} signals within nanostructures.

The work presented here demonstrates that STIM1 is multifunctional and regulates the function of various systems involved in steering growth cones, including the dynamics of the cytoskeleton, tip-attachment complexes, cytoskeletal-associated proteins and focal adhesion complexes. We have demonstrated that STIM1 is necessary and sufficient to steer growth cones, and that a threshold level of STIM1 expression is required to regulate the various aspects of STIM1 function. STIM1-mediated ER-remodelling and association with microtubules is likely to mediate spatially restricted Ca^{2+}_{ER} signals within the pathfinding growth cone, which is vital for growth cone motility and axon pathfinding.

Appendix 1. KEY RESOURCES

REAGENT or RESOURCE	SOURCE	IDENTIFIER
Antibodies		
Rabbit anti-STIM1 (N-terminal, 1:500)	Sigma-Aldrich (USA)	Cat#S6072; RRID: AB_1079008
Rabbit anti-MAPRE1 (EB-1 with limited homology to human EB-3; 1:1000)	Abcam (UK)	Cat#ab50188; RRID: AB_880911
Mouse anti-β3-tubulin (1:1200)	Promega (USA)	Cat#G7121; RRID: AB_430874
Mouse APC-NT (1:400)	Generous gift from Maree Faux, Elliott et al., 2013	N/A
Mouse anti-Drebrin (MF26, 1:1000)	Enzo Life Sciences (USA)	Cat#ADI-NBA-110-E; RRID: AB_2039073
Mouse anti-FAK (1:1000)	Millipore (USA)	Cat#05-537; RRID: AB_2173817
Alexafluor 488 Phalloidin	Invitrogen (USA)	Cat#A12379; RRID: AB_2315147
Alexafluor 405/488/568/647 secondary antibodies (1:1000)	Invitrogen (USA)	
Bacterial and Virus Strains		

CellLight Tubulin-GFP, BacMam 2.0	Thermo Fisher Scientific (USA)	Cat#C10509
CellLight ER-RFP, BacMam 2.0	Thermo Fisher Scientific (USA)	Cat#C10591
plenti-hsyn-EB3-YFP		N/A
Chemicals, Peptides, and Recombinant Proteins		
Laminin Mouse Protein, Natural	Invitrogen (USA)	Cat#23017015
Poly-L-ornithine hydrochloride	Sigma-Aldrich (USA)	Cat#P2533; CAS: 26982-21-8
Brain-derived neurotrophic factor human	Sigma-Aldrich (USA)	Cat#B3795
Recombinant Human Semaphorin 3A Fc Chimera Protein	R&D Systems (USA)	Cat#1250-S3
Epothilone D	Abcam (UK)	ab143616; CAS: 189453-10-9
Thapsigargin	Santa Cruz Biotechnology (USA)	Cat#sc-24017A; CAS: 67526-95-8
Fura-2, AM, cell permeant	Invitrogen (USA)	Cat#F1225
Effectene transfection reagent	Qiagen (Germany)	Cat#301425
Rat Neuron Nucleofector ® Kit	Lonza (Switzerland)	Cat#VPG-1003
NeuroMag transfection reagent	Oz Biosciences (France)	Cat#NM50200

Experimental Models: Cell Lines		
HEK293A	Cryosite	CRL-11268
Experimental Models: Organisms/Strains		
Sprague-Dawley Rat	University of Tasmania	
Oligonucleotides		
Morpholino-targeting sequence: STIM1 control (5'-GGCCAACACCAGCCACAGATCCAT)	Gene Tools LLC (USA)	
Morpholino-targeting sequence: STIM1-specific (5'-GGGCAAGACGAGCGCACACATCCAT)	Gene Tools LLC (USA)	
siRNA targeting sequence: Orai1-specific and control non-targeting siRNA	Dharmacon (USA)	304496, Alias: RGD1311873
Recombinant DNA		
pCMV-OptoSTIM1	Kyung et al. 2015	Addgene plasmid #70159
pCMV-OptoSTIM1(Cry2(D387A))	Kyung et al. 2015	Addgene plasmid #70160

LOVS1K	Pham et al. 2011	Addgene plasmid #31981
pclink-EB1-RFP and pclink-EB3-YFP	Generous gift from John Chilton	N/A
pclink-BiP-mCherry-KDEL	Generous gift from John Chilton, Based on Zurek et al. 2011	N/A
pEX-YFP-STIM1 delta K	Liou et al., 2007	Addgene plasmid #18861
EB3-tdTomato	Merriam et al., 2013	Addgene plasmid #50708
ER-GCaMP6-150/210	Generous gift from Timothy Ryan, de Juan-Sanz et al., 2017	N/A
Software and Algorithms		
ImageJ	NIH (USA)	https://imagej.nih.gov/ij/
GraphPad Prism 6	GraphPad Software Inc. (USA)	https://www.graphpad.com
NIS-Elements AR 4.00.12 software	Nikon (Japan)	https://www.nikoninstruments.com
Volocity Image Analysis Software	Perkin Elmer (USA)	http://www.perkinelmer.com
MATLAB	MathWorks (USA)	https://www.mathworks.com

References:

Akhmanova A, Steinmetz MO (2008) Tracking the ends: a dynamic protein network controls the fate of microtubule tips. Nat Rev Mol Cell Biol 9:309–322.

Akiyama H, Fukuda T, Tojima T, Nikolaev VO, Kamiguchi H (2016) Cyclic Nucleotide Control of Microtubule Dynamics for Axon Guidance. Journal of Neuroscience 36:5636–5649.

Akiyama H, Kamiguchi H (2010) Phosphatidylinositol 3-kinase facilitates microtubule-dependent membrane transport for neuronal growth cone guidance. Journal of Biological Chemistry 285:41740–41748.

Akiyama H, Matsu-ura T, Mikoshiba K, Kamiguchi H (2009) Control of neuronal growth cone navigation by asymmetric inositol 1,4,5-trisphosphate signals. Science Signaling 2:ra34–ra34.

Allan V, Vale R (1994) Movement of membrane tubules along microtubules in vitro: evidence for specialised sites of motor attachment. J Cell Sci 107 (Pt 7):1885–1897.

Allan VJ, Vale RD (1991) Cell cycle control of microtubule-based membrane transport and tubule formation in vitro. The Journal of Cell Biology 113:347–359.

Argiro V, Bunge MB, Johnson MI (1984) Correlation between growth form and movement and their dependence on neuronal age. J Neurosci 4:3051–3062.

Arie Y, Iketani M, Takamatsu K, Mikoshiba K, Goshima Y, Takei K (2009) Biochemical and Biophysical Research Communications. Biochem Biophys Res Commun 379:11–15.

Arregui CO, Balsamo J, Lilien J (1998) Impaired integrin-mediated adhesion and signaling in fibroblasts expressing a dominant-negative mutant PTP1B. The Journal of Cell Biology 143:861–873.

Asanov A, Sherry R, Sampieri A, Vaca L (2013) A relay mechanism between EB1 and APC facilitate STIM1 puncta assembly at endoplasmic reticulum–plasma membrane junctions. Cell Calcium 54:246–256.

Atkin JD, Farg MA, Walker AK, McLean C, Tomas D, Horne MK (2008) Endoplasmic reticulum stress and induction of the unfolded protein response in human sporadic amyotrophic lateral sclerosis. Neurobiology of Disease 30:400–407.

Augustine GJ, Santamaria F, Tanaka K (2003) Local calcium signaling in neurons. Neuron 40:331–346.

Baas PW, Deitch JS, Black MM, Banker GA (1988) Polarity orientation of microtubules in hippocampal neurons: uniformity in the axon and nonuniformity in the dendrite. Proc Natl Acad Sci USA 85:8335–8339.

Baba A, Yasui T, Fujisawa S, Yamada RX, Yamada MK, Nishiyama N, Matsuki N, Ikegaya Y (2003) Activity-evoked capacitative Ca2+ entry: implications in synaptic plasticity. J Neurosci 23:7737–7741.

Baba Y, Hayashi K, Fujii Y, Mizushima A, Watarai H, Wakamori M, Numaga T, Mori Y,

Iino M, Hikida M, Kurosaki T (2006) Coupling of STIM1 to store-operated Ca2+ entry through its constitutive and inducible movement in the endoplasmic reticulum. Proc Natl Acad Sci USA 103:16704–16709.

Bamburg JR, Bray D, Chapman K (1986) Assembly of microtubules at the tip of growing axons. Nature 321:788–790.

Bandtlow CE, Schmidt MF, Hassinger TD, Schwab ME, Kater SB (1993) Role of intracellular calcium in NI-35-evoked collapse of neuronal growth cones. Science 259:80–83.

Barallobre MJ, Del Río JA, Alcántara S, Borrell V, Aguado F, Ruiz M, Carmona MA, Martín M, Fabre M, Yuste R, Tessier-Lavigne M, Soriano E (2000) Aberrant development of hippocampal circuits and altered neural activity in netrin 1-deficient mice. Development 127:4797–4810.

Beetz C et al. (2013) A spastic paraplegia mouse model reveals REEP1-dependent ER shaping. J Clin Invest 123:4273–4282.

Bentley D, Toroian-Raymond A (1986) Disoriented pathfinding by pioneer neurone growth cones deprived of filopodia by cytochalasin treatment. Nature 323:712–715.

Berna-Erro A, Braun A, Kraft R, Kleinschnitz C (2009) STIM2 regulates capacitive Ca2+ entry in neurons and plays a key role in hypoxic neuronal cell death. Sci Signal ….

Berridge MJ (1998) Neuronal calcium signaling. Neuron 21:13–26.

Berridge MJ, Bootman MD, Roderick HL (2003) Calcium signalling: dynamics, homeostasis and remodelling. Nat Rev Mol Cell Biol 4:517–529.

Béliveau É, Guillemette G (2009) Microfilament and microtubule assembly is required for the propagation of inositol trisphosphate receptor-induced Ca2+ waves in bovine aortic endothelial cells. J Cell Biochem 106:344–352.

Béliveau É, Lessard V, Guillemette G (2014) STIM1 Positively Regulates the Ca2+ Release Activity of the Inositol 1,4,5-Trisphosphate Receptor in Bovine Aortic Endothelial Cells Abe K, ed. PLoS ONE 9:e114718–15.

Bola B, Allan V (2009) How and why does the endoplasmic reticulum move? Biochem Soc Trans 37:961–965.

Bollag DM, McQueney PA, Zhu J, Hensens O, Koupal L, Liesch J, Goetz M, Lazarides E, Woods CM (1995) Epothilones, a new class of microtubule-stabilizing agents with a taxol-like mechanism of action. Cancer Res 55:2325–2333.

Bootman MD, Collins TJ, Peppiatt CM, Prothero LS, MacKenzie L, De Smet P, Travers M, Tovey SC, Seo JT, Berridge MJ, Ciccolini F, Lipp P (2001) Calcium signalling—an overview. Seminars in Cell & Developmental Biology 12:3–10.

Breuss MW, Leca I, Gstrein T, Hansen AH, Keays DA (2017) Tubulins and brain development - The origins of functional specification. Molecular and cellular neurosciences 84:58–67.

Brizuela M, Blizzard CA, Chuckowree JA, Dawkins E, Gasperini RJ, Young KM, Dickson TC (2015) The microtubule-stabilizing drug Epothilone D increases axonal sprouting following transection injury in vitro. Molecular and Cellular Neuroscience 66:129–

140.

Brunden KR, Zhang B, Carroll J, Yao Y, Potuzak JS, Hogan AML, Iba M, James MJ, Xie SX, Ballatore C, Smith AB, Lee VMY, Trojanowski JQ (2010) Epothilone D Improves Microtubule Density, Axonal Integrity, and Cognition in a Transgenic Mouse Model of Tauopathy. Journal of Neuroscience 30:13861–13866.

Buck KB, Zheng JQ (2002) Growth cone turning induced by direct local modification of microtubule dynamics. Journal of Neuroscience 22:9358–9367.

Camacho P, Lechleiter JD (1995) Calreticulin inhibits repetitive intracellular Ca2+ waves. Cell 82:765–771.

Carlier MF, Laurent V, Santolini J, Melki R, Didry D, Xia GX, Hong Y, Chua NH, Pantaloni D (1997) Actin depolymerizing factor (ADF/cofilin) enhances the rate of filament turnover: implication in actin-based motility. The Journal of Cell Biology 136:1307–1322.

Carrasco S, Meyer T (2011) STIM proteins and the endoplasmic reticulum-plasma membrane junctions. Annu Rev Biochem 80:973–1000.

Cartelli D, Casagrande F, Busceti CL, Bucci D, Molinaro G, Traficante A, Passarella D, Giavini E, Pezzoli G, Battaglia G, Cappelletti G (2013) Microtubule Alterations Occur Early in Experimental Parkinsonism and The Microtubule Stabilizer Epothilone D Is Neuroprotective. Sci Rep 3.

Catterall WA (2000) Structure and regulation of voltage-gated Ca2+ channels. Annu Rev Cell Dev Biol 16:521–555.

Catterall WA (2011) Voltage-gated calcium channels. Cold Spring Harb Perspect Biol 3:a003947.

Chadborn NH, Ahmed AI, Holt MR, Prinjha R, Dunn GA, Jones GE, Eickholt BJ (2006) PTEN couples Sema3A signalling to growth cone collapse. J Cell Sci 119:951–957.

Chen YF, Chiu WT, Chen YT, Lin PY, Huang HJ, Chou CY, Chang HC, Tang MJ, Shen MR (2011) Calcium store sensor stromal-interaction molecule 1-dependent signaling plays an important role in cervical cancer growth, migration, and angiogenesis. Proc Natl Acad Sci USA 108:15225–15230.

Chen YT, Chen YF, Chiu WT, Wang YK, Chang HC, Shen MR (2013) The ER Ca2+ sensor STIM1 regulates actomyosin contractility of migratory cells. J Cell Sci 126:1260–1267.

Chien CB, Rosenthal DE, Harris WA, Holt CE (1993) Navigational errors made by growth cones without filopodia in the embryonic Xenopus brain. Neuron 11:237–251.

Chilton JK (2006) Molecular mechanisms of axon guidance. Dev Biol 292:13–24.

Clapham DE (2003) TRP channels as cellular sensors. Nature 426:517–524.

Colamarino SA, Tessier-Lavigne M (1995) The axonal chemoattractant netrin-1 is also a chemorepellent for trochlear motor axons. Cell 81:621–629.

Cole NB, Lippincott-Schwartz J (1995) Organization of organelles and membrane traffic by microtubules. Curr Opin Cell Biol 7:55–64.

Conklin MW, Lin MS, Spitzer NC (2005) Local calcium transients contribute to disappearance of pFAK, focal complex removal and deadhesion of neuronal growth cones and fibroblasts. Dev Biol 287:201–212.

Dailey ME, Bridgman PC (1989) Dynamics of the endoplasmic reticulum and other membranous organelles in growth cones of cultured neurons. J Neurosci 9:1897–1909.

Dailey ME, Bridgman PC (1991) Structure and organization of membrane organelles along distal microtubule segments in growth cones. Journal of Neuroscience Research.

Davenport RW, Dou P, Mills LR, Kater SB (1996) Distinct calcium signaling within neuronal growth cones and filopodia. J Neurobiol 31:1–15.

Davenport RW, Dou P, Rehder V, Kater SB (1993) A sensory role for neuronal growth cone filopodia. Nature 361:721–724.

Davenport RW, Kater SB (1992) Local increases in intracellular calcium elicit local filopodial responses in helisoma neuronal growth cages. Neuron 9:405–416.

de Castro F, López-Mascaraque L, De Carlos JA (2007) Cajal: Lessons on brain development. Brain Research Reviews 55:481–489.

de Harven E, Leung R, Christensen H (1984) A novel approach for scanning electron microscopy of colloidal gold-labeled cell surfaces. The Journal of Cell Biology 99:53–57.

de Juan-Sanz J, Holt GT, Schreiter ER, de Juan F, Kim DS, Ryan TA (2017) Axonal Endoplasmic Reticulum Ca2+ Content Controls Release Probability in CNS Nerve Terminals. :1–22.

Dent EW, Callaway JL, Szebenyi G, Baas PW, Kalil K (1999) Reorganization and movement of microtubules in axonal growth cones and developing interstitial branches. J Neurosci 19:8894–8908.

Dent EW, Gertler FB (2003) Cytoskeletal dynamics and transport in growth cone motility and axon guidance. Neuron 40:209–227.

Dent EW, Kalil K (2001) Axon branching requires interactions between dynamic microtubules and actin filaments. J Neurosci 21:9757–9769.

Dent EW, Kwiatkowski AV, Mebane LM, Philippar U, Barzik M, Rubinson DA, Gupton S, Van Veen JE, Furman C, Zhang J, Alberts AS, Mori S, Gertler FB (2007) Filopodia are required for cortical neurite initiation. Nature Publishing Group 9:1347–1359.

Dickson BJ (2001) Rho GTPases in growth cone guidance. Current Opinion in Neurobiology 11:103–110.

Didry D, Carlier MF, Pantaloni D (1998) Synergy between actin depolymerizing factor/cofilin and profilin in increasing actin filament turnover. J Biol Chem 273:25602–25611.

Dillon C, Goda Y (2005) The actin cytoskeleton: integrating form and function at the synapse. Annu Rev Neurosci 28:25–55.

Dominguez R, Holmes KC (2011) Actin Structure and Function. Annu Rev Biophys

40:169–186.

Dziadek MA, Johnstone LS (2007) Biochemical properties and cellular localisation of STIM proteins. Cell Calcium 42:123–132.

Eickholt BJ, Walsh FS, Doherty P (2002) An inactive pool of GSK-3 at the leading edge of growth cones is implicated in Semaphorin 3A signaling. The Journal of Cell Biology 157:211–217.

Etienne-Manneville S (2004) Actin and microtubules in cell motility: which one is in control? Traffic 5:470–477.

Feske S, Gwack Y, Prakriya M, Srikanth S, Puppel S-H, Tanasa B, Hogan PG, Lewis RS, Daly M, Rao A (2006) A mutation in Orai1 causes immune deficiency by abrogating CRAC channel function. Nature Publishing Group 441:179–185.

Fogarty KE, Kidd JF, Turner A, Skepper JN, Carmichael J, Thorn P (2000) Microtubules regulate local Ca2+ spiking in secretory epithelial cells. J Biol Chem 275:22487–22494.

Forscher P, Smith SJ (1988) Actions of cytochalasins on the organization of actin filaments and microtubules in a neuronal growth cone. The Journal of Cell Biology 107:1505–1516.

Foskett JK, White C, Cheung KH, Mak DOD (2007) Inositol Trisphosphate Receptor Ca2+ Release Channels. Physiol Rev 87:593–658.

Friedman JR, Voeltz GK (2011) The ER in 3D: a multifunctional dynamic membrane network. Trends Cell Biol 21:709–717.

Friedman JR, Webster BM, Mastronarde DN, Verhey KJ, Voeltz GK (2010) ER sliding dynamics and ER–mitochondrial contacts occur on acetylated microtubules. The Journal of Cell Biology 190:363–375.

Fukata M, Watanabe T, Noritake J, Nakagawa M, Yamaga M, Kuroda S, Matsuura Y, Iwamatsu A, Perez F, Kaibuchi K (2002) Rac1 and Cdc42 capture microtubules through IQGAP1 and CLIP-170. Cell 109:873–885.

Furukawa T (2013) Types of voltage-gated calcium channels: molecular and electrophysiological views. Curr Hypertens Rev 9:170–181.

Gabso M, Neher E, Spira ME (1997) Low mobility of the Ca2+ buffers in axons of cultured Aplysia neurons. Neuron 18:473–481.

Galante M, Marty A (2003) Presynaptic ryanodine-sensitive calcium stores contribute to evoked neurotransmitter release at the basket cell-Purkinje cell synapse. J Neurosci 23:11229–11234.

Gallo G, Yee HF, Letourneau PC (2002) Actin turnover is required to prevent axon retraction driven by endogenous actomyosin contractility. The Journal of Cell Biology 158:1219–1228.

Garcia-Alvarez G, Shetty MS, Lu B, Yap KAF, Oh-Hora M, Sajikumar S, Bichler Z, Fivaz M (2015) Impaired spatial memory and enhanced long-term potentiation in mice with forebrain-specific ablation of the Stim genes. Front Behav Neurosci 9:1–12.

Gasperini R, Choi-Lundberg D, Thompson MJ, Mitchell CB, Foa L (2009) Homer regulates calcium signalling in growth cone turning. Neural Dev 4:29.

Gasperini RJ, Pavez M, Thompson AC, Mitchell CB, Hardy H, Young KM, Chilton JK, Foa L (2017) How does calcium interact with the cytoskeleton to regulate growth cone motility during axon pathfinding? Molecular and Cellular Neuroscience:1–33.

Gemes G, Bangaru MLY, Wu H-E, Tang Q, Weihrauch D, Koopmeiners AS, Cruikshank JM, Kwok W-M, Hogan QH (2011) Store-operated Ca2+ entry in sensory neurons: functional role and the effect of painful nerve injury. J Neurosci 31:3536–3549.

Geraldo S, Gordon-Weeks PR (2009) Cytoskeletal dynamics in growth-cone steering. J Cell Sci 122:3595–3604.

Geraldo S, Khanzada UK, Parsons M, Chilton JK, Gordon-Weeks PR (2008) Targeting of the F-actin-binding protein drebrin by the microtubule plus-tip protein EB3 is required for neuritogenesis. Nature 10:1181–1189.

Geyer M, Huang F, Sun Y, Vogel SM, Malik AB, Taylor CW, Komarova YA (2015) Microtubule-Associated Protein EB3 Regulates IP. CellReports 12:79–89.

Godement P, Wang LC, Mason CA (1994) Retinal Axon Divergence in the Optic Chiasm - Dynamics of Growth Cone Behavior at the Midline. J Neurosci 14:7024–7039.

Goldberg DJ, Burmeister DW (1986) Stages in axon formation: observations of growth of Aplysia axons in culture using video-enhanced contrast-differential interference contrast microscopy. The Journal of Cell Biology 103:1921–1931.

Gomez TM, Letourneau PC (1994) Filopodia initiate choices made by sensory neuron growth cones at laminin/fibronectin borders in vitro. J Neurosci 14:5959–5972.

Gomez TM, Robles E, Poo MM, Spitzer NC (2001) Filopodial calcium transients promote substrate-dependent growth cone turning. Science 291:1983–1987.

Gomez TM, Snow DM, Letourneau PC (1995) Characterization of spontaneous calcium transients in nerve growth cones and their effect on growth cone migration. Neuron 14:1233–1246.

Gomez TM, Spitzer NC (1999) In vivo regulation of axon extension and pathfinding by growth-cone calcium transients. Nature 397:350–355.

Gomez TM, Zheng JQ (2006) The molecular basis for calcium-dependent axon pathfinding. Nat Rev Neurosci 7:115–125.

Gonzalez-Billault C, Muñoz-Llancao P, Henriquez DR, Wojnacki J, Conde C, Caceres A (2012) The role of small GTPases in neuronal morphogenesis and polarity. Bass PW, Gonzalez-Billault C, eds. Cytoskeleton (Hoboken) 69:464–485.

Goodhill GJ, Gu M, Urbach JS (2004) Predicting axonal response to molecular gradients with a computational model of filopodial dynamics. Neural Comput 16:2221–2243.

Gordon-Weeks PR (1991) Evidence for microtubule capture by filopodial actin filaments in growth cones. Neuroreport 2:573–576.

Goto S, Yamamoto H, Fukunaga K, Iwasa T, Matsukado Y, Miyamoto E (1985) Dephosphorylation of microtubule-associated protein 2, tau factor, and tubulin by

calcineurin. J Neurochem 45:276–283.

Greka A, Navarro B, Oancea E, Duggan A, Clapham DE (2003) TRPC5 is a regulator of hippocampal neurite length and growth cone morphology. Nat Neurosci 6:837–845.

Grigoriev I, Gouveia SM, van der Vaart B, Demmers J, Smyth JT, Honnappa S, Splinter D, Steinmetz MO, Putney JW, Hoogenraad CC, Akhmanova A (2008) STIM1 is a MT-plus-end-tracking protein involved in remodeling of the ER. Current Biology 18:177–182.

Gundersen RW, Barrett JN (1979) Neuronal chemotaxis: chick dorsal-root axons turn toward high concentrations of nerve growth factor. Science 206:1079–1080.

Hall A (1998) Rho GTPases and the actin cytoskeleton. Science 279:509–514.

Halloran MC, Kalil K (1994) Dynamic Behaviors of Growth Cones Extending in the Corpus-Callosum of Living Cortical Brain-Slices Observed with Video Microscopy. J Neurosci 14:2161–2177.

Harraz OF, Altier C (2014) STIM1-mediated bidirectional regulation of Ca(2+) entry through voltage-gated calcium channels (VGCC) and calcium-release activated channels (CRAC). Front Cell Neurosci 8:43.

Hartmann J, Karl RM, Alexander RPD, Adelsberger H, Brill MS, Rühlmann C, Ansel A, Sakimura K, Baba Y, Kurosaki T, Misgeld T, Konnerth A (2014) STIM1 controls neuronal Ca^{2+} signaling, mGluR1-dependent synaptic transmission, and cerebellar motor behavior. Neuron 82:635–644.

Hájková Z, Bugajev V, Dráberová E, Vinopal S, Dráberová L, Janáček J, Dráber P, Dráber P (2011a) STIM1-directed reorganization of microtubules in activated mast cells. J Immunol 186:913–923.

Hájková Z, Bugajev V, Dráberová E, Vinopal S, Dráberová L, Janáček J, Dráber P, Dráber P (2011b) STIM1-directed reorganization of microtubules in activated mast cells. J Immunol 186:913–923.

Henle SJ, Carlstrom LP, Cheever TR, Henley JR (2013) Differential Role of PTEN Phosphatase in Chemotactic Growth Cone Guidance. J Biol Chem 288:20837–20842.

Henle SJ, Wang G, Liang E, Wu M, Poo MM, Henley JR (2011) Asymmetric PI(3,4,5)P3 and Akt Signaling Mediates Chemotaxis of Axonal Growth Cones. J Neurosci 31:7016–7027.

Henley JR, Huang K-H, Wang D, Poo M-M (2004) Calcium mediates bidirectional growth cone turning induced by myelin-associated glycoprotein. Neuron 44:909–916.

Hetz C, Mollereau B (2014) Disturbance of endoplasmic reticulum proteostasis in neurodegenerative diseases. Nat Rev Neurosci 15:233–249.

Higgins ER, Cannell MB, Sneyd J (2006) A Buffering SERCA Pump in Models of Calcium Dynamics. Biophysical Journal 91:151–163.

Holy TE, Leibler S (1994) Dynamic instability of microtubules as an efficient way to search in space. Proc Natl Acad Sci USA 91:5682–5685.

Hong K, Nishiyama M, Henley J, Tessier-Lavigne M, Poo M (2000) Calcium signalling in the guidance of nerve growth by netrin-1. Nature 403:93–98.

Honnappa S, Gouveia SM, Weisbrich A, Damberger FF, Bhavesh NS, Jawhari H, Grigoriev I, van Rijssel FJA, Buey RM, Lawera A, Jelesarov I, Winkler FK, Wuthrich K, Akhmanova A, Steinmetz MO (2009) An EB1-Binding Motif Acts as a Microtubule Tip Localization Signal. Cell 138:366–376.

Hoth M, Penner R (1992) Depletion of intracellular calcium stores activates a calcium current in mast cells. Nature 355:353–356.

Huang GN, Zeng W, Kim JY, Yuan JP, Han L, Muallem S, Worley PF (2006) STIM1 carboxyl-terminus activates native SOC, I(crac) and TRPC1 channels. Nat Cell Biol 8:1003–1010.

Huang B, Bates M, Zhuang X (2009) Super-resolution fluorescence microscopy. Annu Rev Biochem 78:993-1016

Hung R-J, Yazdani U, Yoon J, Wu H, Yang T, Gupta N, Huang Z, van Berkel WJH, Terman JR (2010) Mical links semaphorins to F-actin disassembly. Nature 463:823–827.

Hur E-M, Saijilafu, Zhou F-Q (2012) Growing the growth cone: remodeling the cytoskeleton to promote axon regeneration. Trends Neurosci 35:164–174.

Huttenlocher A, Palecek SP, Lu Q, Zhang W, Mellgren RL, Lauffenburger DA, Ginsberg MH, Horwitz AF (1997) Regulation of cell migration by the calcium-dependent protease calpain. J Biol Chem 272:32719–32722.

Ikeda K, Kaub PA, Asada H, Uyemura K, Toya S, Shirao T (1996) Stabilization of adhesion plaques by the expression of drebrin A in fibroblasts. Brain Res Dev Brain Res 91:227–236.

Iwasaki S, Momiyama A, Uchitel OD, Takahashi T (2000) Developmental changes in calcium channel types mediating central synaptic transmission. J Neurosci 20:59–65.

Jaffe AB, Hall A (2005) Rho GTPases: biochemistry and biology. Annu Rev Cell Dev Biol 21:247–269.

Jin M, Guan C-B, Jiang Y-A, Chen G, Zhao C-T, Cui K, Song Y-Q, Wu C-P, Poo M-M, Yuan X-B (2005a) Ca2+-dependent regulation of rho GTPases triggers turning of nerve growth cones. J Neurosci 25:2338–2347.

Jin M, Guan C-B, Jiang Y-A, Chen G, Zhao C-T, Cui K, Song Y-Q, Wu C-P, Poo M-M, Yuan X-B (2005b) Ca2+-dependent regulation of rho GTPases triggers turning of nerve growth cones. J Neurosci 25:2338–2347.

Joseph SK, Boehning D, Bokkala S, Watkins R, Widjaja J (1999) Biosynthesis of inositol trisphosphate receptors: selective association with the molecular chaperone calnexin. Biochem J 342 (Pt 1):153–161.

Juanes MA, Bouguenina H, Eskin JA, Jaiswal R, Badache A, Goode BL (2017) Adenomatous polyposis coli nucleates actin assembly to drive cell migration and microtubule-induced focal adhesion turnover. The Journal of Cell Biology 54:jcb.201702007–jcb.201702017.

Kalil K, Dent EW (2005) Touch and go: guidance cues signal to the growth cone cytoskeleton. Current Opinion in Neurobiology 15:521–526.

Katayama T, Imaizumi K, Sato N, Miyoshi K, Kudo T, Hitomi J, Morihara T, Yoneda T, Gomi F, Mori Y, Nakano Y, Takeda J, Tsuda T, Itoyama Y, Murayama O, Takashima A, St George-Hyslop P, Takeda M, Tohyama M (1999) Presenilin-1 mutations downregulate the signalling pathway of the unfolded-protein response. Nat Cell Biol 1:479–485.

Kater SB, Mattson MP, Cohan C, Connor J (1988) Calcium regulation of the neuronal growth cone. Trends Neurosci 11:315–321.

Kater SB, Mills LR (1991) Regulation of growth cone behavior by calcium. J Neurosci 11:891–899.

Kaverina I, Krylyshkina O, Beningo K, Anderson K, Wang Y-L, Small JV (2002) Tensile stress stimulates microtubule outgrowth in living cells. J Cell Sci 115:2283–2291.

Kaverina I, Krylyshkina O, Small JV (1999) Microtubule targeting of substrate contacts promotes their relaxation and dissociation. The Journal of Cell Biology 146:1033–1044.

Kawasaki Y, Sato R, Akiyama T (2003) Mutated APC and Asef are involved in the migration of colorectal tumour cells. Nat Cell Biol 5:211–215.

Kawasaki Y, Senda T, Ishidate T, Koyama R, Morishita T, Iwayama Y, Higuchi O, Akiyama T (2000) Asef, a link between the tumor suppressor APC and G-protein signaling. Science 289:1194–1197.

Kennedy TE, Serafini T, la Torre de JR, Tessier-Lavigne M (1994) Netrins are diffusible chemotropic factors for commissural axons in the embryonic spinal cord. Cell 78:425–435.

Kerstein PC, Patel KM, Gomez TM (2017) Calpain-Mediated Proteolysis of Talin and FAK Regulates Adhesion Dynamics Necessary for Axon Guidance. J Neurosci 37:1568–1580.

Kim YT, Wu CF (1996) Reduced growth cone motility in cultured neurons from Drosophila memory mutants with a defective cAMP cascade. J Neurosci 16:5593–5602.

Koester MP, Muller O, Pollerberg GE (2007) Adenomatous Polyposis Coli Is Differentially Distributed in Growth Cones and Modulates Their Steering. J Neurosci 27:12590–12600.

Komarova Y, De Groot CO, Grigoriev I, Gouveia SM, Munteanu EL, Schober JM, Honnappa S, Buey RM, Hoogenraad CC, Dogterom M, Borisy GG, Steinmetz MO, Akhmanova A (2009) Mammalian end binding proteins control persistent microtubule growth. The Journal of Cell Biology 184:691–706.

Kozma R, Ahmed S, Best A, Lim L (1995) The Ras-related protein Cdc42Hs and bradykinin promote formation of peripheral actin microspikes and filopodia in Swiss 3T3 fibroblasts. Mol Cell Biol 15:1942–1952.

Krendel M, Zenke FT, Bokoch GM (2002) Nucleotide exchange factor GEF-H1 mediates cross-talk between microtubules and the actin cytoskeleton. Nat Cell Biol 4:294–301.

Kumar P, Wittmann T (2012) +TIPs: SxIPping along microtubule ends. Trends Cell Biol 22:418–428.

Kyung T, Lee S, Kim JE, Cho T, Park H, Jeong Y-M, Kim D, Shin A, Kim S, Baek J, Kim J, Kim NY, Woo D, Chae S, Kim C-H, Shin H-S, Han Y-M, Kim D, Do Heo W (2015) Optogenetic control of endogenous Ca. :1–8.

Lankford KL, Letourneau PC (1989) Evidence that calcium may control neurite outgrowth by regulating the stability of actin filaments. The Journal of Cell Biology 109:1229–1243.

Lau PM, Zucker RS, Bentley D (1999) Induction of filopodia by direct local elevation of intracellular calcium ion concentration. The Journal of Cell Biology 145:1265–1275.

Le Clainche C, Carlier MF (2008) Regulation of Actin Assembly Associated With Protrusion and Adhesion in Cell Migration. Physiol Rev 88:489–513.

Lebrand C, Dent EW, Strasser GA, Lanier LM, Krause M, Svitkina TM, Borisy GG, Gertler FB (2004) Critical role of Ena/VASP proteins for filopodia formation in neurons and in function downstream of netrin-1. Neuron 42:37–49.

Lefkimmiatis K, Srikanthan M, Maiellaro I, Moyer MP, Curci S, Hofer AM (2009) Store-operated cyclic AMP signalling mediated by STIM1. Nat Cell Biol 11:433–442.

Letourneau PC (1983) Differences in the organization of actin in the growth cones compared with the neurites of cultured neurons from chick embryos. The Journal of Cell Biology 97:963–973.

Levi-Montalcini R (1987) The nerve growth factor: thirty-five years later. Biosci Rep 7:681–699.

Lewis RS (2007) The molecular choreography of a store-operated calcium channel. Nature 446:284–287.

Li L, Fothergill T, Hutchins BI, Dent EW, Kalil K (2013) Wnt5a evokes cortical axon outgrowth and repulsive guidance by tau mediated reorganization of dynamic microtubules Zou Y, Salinas PC, eds. Dev Neurobiol 74:797–817.

Li L, Hutchins BI, Kalil K (2009) Wnt5a Induces Simultaneous Cortical Axon Outgrowth and Repulsive Axon Guidance through Distinct Signaling Mechanisms. J Neurosci 29:5873–5883.

Li Q, Ishikawa T-O, Oshima M, Taketo MM (2005a) The Threshold Level of Adenomatous Polyposis Coli Protein for Mouse Intestinal Tumorigenesis. Cancer Res 65:8622–8627.

Li Y, Jia Y-C, Cui K, Li N, Zheng Z-Y, Wang Y-Z, Yuan X-B (2005b) Essential role of TRPC channels in the guidance of nerve growth cones by brain-derived neurotrophic factor. Nature 434:894–898.

Lin CH, Thompson CA, Forscher P (1994) Cytoskeletal reorganization underlying growth cone motility. Current Opinion in Neurobiology 4:640–647.

Lin JY, Knutsen PM, Muller A, Kleinfeld D, Tsien RY (2013) ReaChR: a red-shifted variant of channelrhodopsin enables deep transcranial optogenetic excitation. Nat Neurosci 16:1499–1508.

Liou J, Fivaz M, Inoue T, Meyer T (2007) Live-cell imaging reveals sequential oligomerization and local plasma membrane targeting of stromal interaction molecule 1 after Ca2+ store depletion. Proc Natl Acad Sci USA 104:9301–9306.

Liou J, Kim ML, Heo WD, Jones JT, Myers JW, Ferrell JE, Meyer T (2005) STIM is a Ca2+ sensor essential for Ca2+-store-depletion-triggered Ca2+ influx. Current Biology 15:1235–1241.

Lis A, Peinelt C, Beck A, Parvez S, Monteilh-Zoller M, Fleig A, Penner R (2007) CRACM1, CRACM2, and CRACM3 Are Store-Operated Ca2+ Channels with Distinct Functional Properties. Current Biology 17:794–800.

Llano I, González J, Caputo C, Lai FA, Blayney LM, Tan YP, Marty A (2000) Presynaptic calcium stores underlie large-amplitude miniature IPSCs and spontaneous calcium transients. Nat Neurosci 3:1256–1265.

Lohmann C, Finski A, Bonhoeffer T (2005) Local calcium transients regulate the spontaneous motility of dendritic filopodia. Nat Neurosci 8:305–312.

Lohof AM, Quillan M, Dan Y, Poo MM (1992) Asymmetric modulation of cytosolic cAMP activity induces growth cone turning. J Neurosci 12:1253–1261.

Luebke JI, Dunlap K, Turner TJ (1993) Multiple calcium channel types control glutamatergic synaptic transmission in the hippocampus. Neuron 11:895–902.

Luik RM, Wang B, Prakriya M, Wu MM, Lewis RS (2008) Oligomerization of STIM1 couples ER calcium depletion to CRAC channel activation. Nature 454:538–542.

Luo L, Jan LY, Jan Y-N (1997) Rho family small GTP-binding proteins in growth cone signalling. Current Opinion in Neurobiology 7:81–86.

Luo Y, Raible D, Raper JA (1993) Collapsin: a protein in brain that induces the collapse and paralysis of neuronal growth cones. Cell 75:217–227.

Manders EMM, Verbeek FJ, Aten JA (1993) Measurement of co-localization of objects in dual-colour confocal images. Journal of Microscopy 169:375–382.

Marsh L, Letourneau PC (1984) Growth of neurites without filopodial or lamellipodial activity in the presence of cytochalasin B. The Journal of Cell Biology 99:2041–2047.

Mattila PK, Lappalainen P (2008) Filopodia: molecular architecture and cellular functions. Nat Rev Mol Cell Biol 9:446–454.

McCaig CD (1986) Dynamic aspects of amphibian neurite growth and the effects of an applied electric field. J Physiol (Lond) 375:55–69.

Mercer JC, DeHaven WI, Smyth JT, Wedel B, Boyles RR, Bird GS, Putney JW (2006) Large Store-operated Calcium Selective Currents Due to Co-expression of Orai1 or Orai2 with the Intracellular Calcium Sensor, Stim1. Journal of Biological Chemistry 281:24979–24990.

Mercer JC, Qi Q, Mottram LF, Law M, Bruce D, Iyer A, Morales JL, Yamazaki H, Shirao T, Peterson BR, August A (2010) Chemico-genetic identification of drebrin as a regulator of calcium responses. The International Journal of Biochemistry & Cell Biology 42:337–345.

Ming G, Henley J, Tessier-Lavigne M, Song H, Poo M (2001) Electrical activity modulates growth cone guidance by diffusible factors. Neuron 29:441–452.

Ming GL, Song HJ, Berninger B, Holt CE, Tessier-Lavigne M, Poo MM (1997) cAMP-dependent growth cone guidance by netrin-1. Neuron 19:1225–1235.

Mitchell CB, Gasperini RJ, Small DH, Foa L (2012) STIM1 is necessary for store-operated calcium entry in turning growth cones. J Neurochem 122:1155–1166.

Mitchison T, Kirschner M (1984) Dynamic instability of microtubule growth. Nature 312:237–242.

Mizui T, Kojima N, Yamazaki H, Katayama M, Hanamura K, Shirao T (2009) Drebrin E is involved in the regulation of axonal growth through actin-myosin interactions. J Neurochem 109:611–622.

Moore SW, Zhang X, Lynch CD, Sheetz MP (2012) Netrin-1 Attracts Axons through FAK-Dependent Mechanotransduction. Journal of Neuroscience 32:11574–11585.

Mori MX, Itsuki K, Hase H, Sawamura S, Kurokawa T, Mori Y, Inoue R (2015) Dynamics of receptor-operated Ca(2+) currents through TRPC channels controlled via the PI(4,5)P2-PLC signaling pathway. Front Pharmacol 6:22.

Mortimer D, Feldner J, Vaughan T, Vetter I, Pujic Z, Rosoff WJ, Burrage K, Dayan P, Richards LJ, Goodhill GJ (2009) Bayesian model predicts the response of axons to molecular gradients. Proc Natl Acad Sci USA 106:10296–10301.

Mortimer D, Fothergill T, Pujic Z, Richards LJ, Goodhill GJ (2008) Growth cone chemotaxis. Trends Neurosci 31:90–98.

Myers JP, Gomez TM (2011) Focal Adhesion Kinase Promotes Integrin Adhesion Dynamics Necessary for Chemotropic Turning of Nerve Growth Cones. J Neurosci 31:13585–13595.

Nakanishi S (1992) Molecular diversity of glutamate receptors and implications for brain function. Science 258:597–603.

Nakatani Y, Konishi H, Vassilev A, Kurooka H, Ishiguro K, Sawada J, Ikura T, Korsmeyer SJ, Qin J, Herlitz AM (2005) p600, a unique protein required for membrane morphogenesis and cell survival. Proc Natl Acad Sci USA 102:15093–15098.

Näthke IS, Adams CL, Polakis P, Sellin JH, Nelson WJ (1996) The adenomatous polyposis coli tumor suppressor protein localizes to plasma membrane sites involved in active cell migration. The Journal of Cell Biology 134:165–179.

Nishiyama M, Hoshino A, Tsai L, Henley JR, Goshima Y, Tessier-Lavigne M, Poo MM, Hong KS (2003) Cyclic AMP/GMP-dependent modulation of Ca2+ channels sets the polarity of nerve growth-cone turning. Nature 423:990–995.

Nishiyama M, Schimmelmann von MJ, Togashi K, Findley WM, Hong K (2008) Membrane potential shifts caused by diffusible guidance signals direct growth-cone turning. Nat Neurosci 11:762–771.

Nobes CD, Hall A (1995) Rho, rac, and cdc42 GTPases regulate the assembly of multimolecular focal complexes associated with actin stress fibers, lamellipodia, and filopodia. Cell 81:53–62.

Noritake J, Watanabe T, Sato K, Wang S, Kaibuchi K (2005) IQGAP1: a key regulator of adhesion and migration. J Cell Sci 118:2085–2092.

O'Connor TP, Duerr JS, Bentley D (1990) Pioneer growth cone steering decisions mediated by single filopodial contacts in situ. J Neurosci 10:3935–3946.

Ooashi N, Futatsugi A, Yoshihara F, Mikoshiba K, Kamiguchi H (2005) Cell adhesion molecules regulate Ca2+-mediated steering of growth cones via cyclic AMP and ryanodine receptor type 3. The Journal of Cell Biology 170:1159–1167.

Pak CW, Flynn KC, Bamburg JR (2008) Actin-binding proteins take the reins in growth cones. Nature Publishing Group 9:136–147.

Pantaloni D, Le Clainche C, Carlier MF (2001) Mechanism of actin-based motility. Science 292:1502–1506.

Papp S, Szabo E, Kim H, McCulloch CA, Opas M (2008) Kinase-dependent adhesion to fibronectin: Regulation by calreticulin. Experimental cell research 314:1313–1326.

Park CY, Shcheglovitov A, Dolmetsch R (2010) The CRAC channel activator STIM1 binds and inhibits L-type voltage-gated calcium channels. Science 330:101–105.

Patterson RL, van Rossum DB, Gill DL (1999) Store-operated Ca2+ entry: evidence for a secretion-like coupling model. Cell 98:487–499.

Paves H, Saarma M (1997) Neurotrophins as in vitro growth cone guidance molecules for embryonic sensory neurons. Cell Tissue Res 290:285–297.

Peng Y (1996) Ryanodine-sensitive component of calcium transients evoked by nerve firing at presynaptic nerve terminals. J Neurosci 16:6703–6712.

Pereyra E, Mizyrycki C, Moreno S (2000) Threshold level of protein kinase A activity and polarized growth in Mucor rouxii. Microbiology (Reading, Engl) 146 (Pt 8):1949–1958.

Pham E, Mills E, Truong K (2011) A Synthetic Photoactivated Proteinto Generate Local or Global Ca. Chemistry & Biology 18:880–890.

Pollard TD, Borisy GG (2003) Cellular motility driven by assembly and disassembly of actin filaments. Cell 112:453–465.

Poo JQZAM-M (2007) Calcium Signaling in Neuronal Motility. :1–30.

Prakriya M, Feske S, Gwack Y, Srikanth S, Rao A, Hogan PG (2006) Orai1 is an essential pore subunit of the CRAC channel. Nature 443:230–233.

Putney JW (1986) A model for receptor-regulated calcium entry. Cell Calcium 7:1–12.

Ramsey IS, Delling M, Clapham DE (2006) An introduction to TRP channels. Annu Rev Physiol 68:619–647.

Ren XD, Kiosses WB, Schwartz MA (1999) Regulation of the small GTP-binding protein Rho by cell adhesion and the cytoskeleton. The EMBO Journal 18:578–585.

Ribeiro CM, Reece J, Putney JW (1997) Role of the cytoskeleton in calcium signaling in NIH 3T3 cells. An intact cytoskeleton is required for agonist-induced [Ca2+]i

signaling, but not for capacitative calcium entry. J Biol Chem 272:26555–26561.

Ridley AJ (2001) Rho GTPases and cell migration. J Cell Sci 114:2713–2722.

Ridley AJ, Hall A (1992) The small GTP-binding protein rho regulates the assembly of focal adhesions and actin stress fibers in response to growth factors. Cell 70:389–399.

Ridley AJ, Paterson HF, Johnston CL, Diekmann D, Hall A (1992) The small GTP-binding protein rac regulates growth factor-induced membrane ruffling. Cell 70:401–410.

Robles E, Gomez TM (2006) Focal adhesion kinase signaling at sites of integrin-mediated adhesion controls axon pathfinding. Nat Neurosci 9:1274–1283.

Rodriguez OC, Schaefer AW, Mandato CA, Forscher P, Bement WM, Waterman-Storer CM (2003) Conserved microtubule-actin interactions in cell movement and morphogenesis. Nat Cell Biol 5:599–609.

Roos J, DiGregorio PJ, Yeromin AV, Ohlsen K, Lioudyno M, Zhang S, Safrina O, Kozak JA, Wagner SL, Cahalan MD, Veliçelebi G, Stauderman KA (2005) STIM1, an essential and conserved component of store-operated Ca2+ channel function. The Journal of Cell Biology 169:435–445.

Rosoff WJ, Urbach JS, Esrick MA, McAllister RG, Richards LJ, Goodhill GJ (2004) A new chemotaxis assay shows the extreme sensitivity of axons to molecular gradients. Nat Neurosci 7:678–682.

Saxena S, Cabuy E, Caroni P (2009) A role for motoneuron subtype–selective ER stress in disease manifestations of FALS mice. Nat Neurosci 12:627–636.

Schaefer AW, Kabir N, Forscher P (2002) Filopodia and actin arcs guide the assembly and transport of two populations of microtubules with unique dynamic parameters in neuronal growth cones. The Journal of Cell Biology 158:139–152.

Schafer DA, Cooper JA (1995) Control of actin assembly at filament ends. Annu Rev Cell Dev Biol 11:497–518.

Schirenbeck A, Bretschneider T, Arasada R, Schleicher M, Faix J (2005) The Diaphanous-related formin dDia2 is required for the formation and maintenance of filopodia. Nat Cell Biol 7:619–625.

Schliwa M, Euteneuer U, Bulinski JC, Izant JG (1981) Calcium lability of cytoplasmic microtubules and its modulation by microtubule-associated proteins. Proc Natl Acad Sci USA 78:1037–1041.

Schmunk G, Boubion BJ, Smith IF, Parker I, Gargus JJ (2015) Shared functional defect in IP3R-mediated calcium signaling in diverse monogenic autism syndromes. 5:e643–10.

Schmunk G, Nguyen RL, Ferguson DL, Kumar K, Parker I, Gargus JJ (2017) High-throughput screen detects calcium signaling dysfunction in typical sporadic autism spectrum disorder. Sci Rep 7:40740–40749.

Schroer TA, Sheetz MP (1991) Two activators of microtubule-based vesicle transport. The Journal of Cell Biology 115:1309–1318.

Schultz J, Ponting CP, Hofmann K, Bork P (1997) SAM as a protein interaction domain involved in developmental regulation. Protein Sci 6:249–253.

Schwartz JR, Sarvaiya PJ, Vedeckis WV (2010) Glucocorticoid receptor knock down reveals a similar apoptotic threshold but differing gene regulation patterns in T-cell and pre-B-cell acute lymphoblastic leukemia. Molecular and Cellular Endocrinology 320:76–86.

Sharma G, Vijayaraghavan S (2003) Modulation of presynaptic store calcium induces release of glutamate and postsynaptic firing. Neuron 38:929–939.

Shelly M, Lim BK, Cancedda L, Heilshorn SC, Gao H, Poo MM (2010) Local and Long-Range Reciprocal Regulation of cAMP and cGMP in Axon/Dendrite Formation. Science 327:547–552.

Shim S, Goh EL, Ge S, Sailor K, Yuan JP, Roderick HL, Bootman MD, Worley PF, Song H, Ming G-L (2005) XTRPC1-dependent chemotropic guidance of neuronal growth cones. Nat Neurosci 8:730–735.

Shim S, Zheng JQ, Ming G-L (2013) A critical role for STIM1 in filopodial calcium entry and axon guidance. Mol Brain 6:51.

Shim SY, Wang J, Asada N, Neumayer G, Tran HC, Ishiguro KI, Sanada K, Nakatani Y, Nguyen MD (2008) Protein 600 Is a Microtubule/Endoplasmic Reticulum-Associated Protein in CNS Neurons. J Neurosci 28:3604–3614.

Smyth JT, Beg AM, Wu S, Putney JW, Rusan NM (2012) Phosphoregulation of STIM1 leads to exclusion of the endoplasmic reticulum from the mitotic spindle. Curr Biol 22:1487–1493.

Smyth JT, DeHaven WI, Bird GS, Putney JW (2007) Role of the microtubule cytoskeleton in the function of the store-operated Ca2+ channel activator STIM1. J Cell Sci 120:3762–3771.

Soboloff J, Spassova MA, Tang XD, Hewavitharana T, Xu W, Gill DL (2006) Orai1 and STIM Reconstitute Store-operated Calcium Channel Function. Journal of Biological Chemistry 281:20661–20665.

Solovyova N, Veselovsky N, Toescu EC, Verkhratsky A (2002) Ca(2+) dynamics in the lumen of the endoplasmic reticulum in sensory neurons: direct visualization of Ca(2+)-induced Ca(2+) release triggered by physiological Ca(2+) entry. The EMBO Journal 21:622–630.

Somlyo AP (1984) Cell physiology: cellular site of calcium regulation. Nature 309:516–517.

Song H, Ming G, He Z, Lehmann M, McKerracher L, Tessier-Lavigne M, Poo M (1998) Conversion of neuronal growth cone responses from repulsion to attraction by cyclic nucleotides. Science 281:1515–1518.

Song HJ, Ming GL, Poo MM (1997) cAMP-induced switching in turning direction of nerve growth cones. Nature 388:275–279.

Song HJ, Poo MM (1999) Signal transduction underlying growth cone guidance by diffusible factors. Current Opinion in Neurobiology 9:355–363.

Spada F, Haemmer A, Kuch D, Rothbauer U, Schermelleh L, Kremmer E, Carell T, Längst G, Leonhardt H (2007) DNMT1 but not its interaction with the replication machinery is required for maintenance of DNA methylation in human cells. The Journal of Cell Biology 176:565–571.

Sperry RW (1963) Chemoaffinity in the orderly growth of nerve fiber patterns and connections. Proc Natl Acad Sci USA 50:703–710.

Steinbeck JA, Henke N, Opatz J, Gruszczynska-Biegala J, Schneider L, Theiss S, Hamacher N, Steinfarz B, Golz S, Brüstle O, Kuznicki J, Methner A (2011) Experimental Neurology. Experimental Neurology 232:185–194.

Stepanova T, Slemmer J, Hoogenraad CC, Lansbergen G, Dortland B, De Zeeuw CI, Grosveld F, van Cappellen G, Akhmanova A, Galjart N (2003) Visualization of microtubule growth in cultured neurons via the use of EB3-GFP (end-binding protein 3-green fluorescent protein). J Neurosci 23:2655–2664.

Stephens RE, Edds KT (1976) Microtubules: structure, chemistry, and function. Physiol Rev 56:709–777.

Su LK, Burrell M, Hill DE, Gyuris J, Brent R, Wiltshire R, Trent J, Vogelstein B, Kinzler KW (1995) APC binds to the novel protein EB1. Cancer Res 55:2972–2977.

Sun S, Zhang H, Liu J, Popugaeva E, Xu N-J, Feske S, White CL III, Bezprozvanny I (2014) Reduced Synaptic STIM2 Expression and Impaired Store-Operated Calcium Entry Cause Destabilization of Mature Spines in Mutant Presenilin Mice. Neuron 82:79–93.

Suter DM, Errante LD, Belotserkovsky V, Forscher P (1998) The Ig superfamily cell adhesion molecule, apCAM, mediates growth cone steering by substrate-cytoskeletal coupling. The Journal of Cell Biology 141:227–240.

Suter DM, Forscher P (2000) Substrate-cytoskeletal coupling as a mechanism for the regulation of growth cone motility and guidance. J Neurobiol 44:97–113.

Takahashi T, Momiyama A (1993) Different types of calcium channels mediate central synaptic transmission. Nature 366:156–158.

Takei K, Shin RM, Inoue T, Kato K, Mikoshiba K (1998) Regulation of nerve growth mediated by inositol 1,4,5-trisphosphate receptors in growth cones. Science 282:1705–1708.

Tanaka E, Ho T, Kirschner MW (1995) The role of microtubule dynamics in growth cone motility and axonal growth. The Journal of Cell Biology 128:139–155.

Tang F, Dent EW, Kalil K (2003a) Spontaneous calcium transients in developing cortical neurons regulate axon outgrowth. J Neurosci 23:927–936.

Tang F, Dent EW, Kalil K (2003b) Spontaneous calcium transients in developing cortical neurons regulate axon outgrowth. J Neurosci 23:927–936.

Terasaki M, Chen LB, Fujiwara K (1986) Microtubules and the endoplasmic reticulum are highly interdependent structures. The Journal of Cell Biology 103:1557–1568.

Terasaki M, Slater NT, Fein A (1994) Continuous network of endoplasmic reticulum in cerebellar Purkinje neurons.

Terman JR, Mao T, Pasterkamp RJ, Yu H-H, Kolodkin AL (2002) MICALs, a family of conserved flavoprotein oxidoreductases, function in plexin-mediated axonal repulsion. Cell 109:887–900.

Tessier-Lavigne M, Goodman CS (1996a) The molecular biology of axon guidance. Science 274:1123–1133.

Tessier-Lavigne M, Goodman CS (1996b) The molecular biology of axon guidance. Science 274:1123–1133.

Togashi K, Schimmelmann von MJ, Nishiyama M, Lim C-S, Yoshida N, Yun B, Molday RS, Goshima Y, Hong K (2008) Cyclic GMP-Gated CNG Channels Function in Sema3A-Induced Growth Cone Repulsion. Neuron 58:694–707.

Tojima T, Akiyama H, Itofusa R, Li Y, Katayama H, Miyawaki A, Kamiguchi H (2007) Attractive axon guidance involves asymmetric membrane transport and exocytosis in the growth cone. Nat Neurosci 10:58–66.

Tojima T, Hines JH, Henley JR, Kamiguchi H (2011) Second messengers and membrane trafficking direct and organize growth cone steering. Nat Rev Neurosci 12:191–203.

Tojima T, Itofusa R, Kamiguchi H (2009) The Nitric Oxide-cGMP Pathway Controls the Directional Polarity of Growth Cone Guidance via Modulating Cytosolic Ca2+ Signals. J Neurosci 29:7886–7897.

Tojima T, Itofusa R, Kamiguchi H (2010) Asymmetric Clathrin-Mediated Endocytosis Drives Repulsive Growth Cone Guidance. Neuron 66:370–377.

Tsien RW, Lipscombe D, Madison DV, Bley KR, Fox AP (1988) Multiple types of neuronal calcium channels and their selective modulation. Trends Neurosci 11:431–438.

Vale RD, Hotani H (1988) Formation of membrane networks in vitro by kinesin-driven microtubule movement. The Journal of Cell Biology 107:2233–2241.

Vale RD, Reese TS, Sheetz MP (1985) Identification of a novel force-generating protein, kinesin, involved in microtubule-based motility. Cell 42:39–50.

van Haren J, Boudeau J, Schmidt S, Basu S, Liu Z, Lammers D, Demmers J, Benhari J, Grosveld F, Debant A, Galjart N (2014) Dynamic microtubules catalyze formation of navigator-TRIO complexes to regulate neurite extension. Curr Biol 24:1778–1785.

van Haren J, Draegestein K, Keijzer N, Abrahams JP, Grosveld F, Peeters PJ, Moechars D, Galjart N (2009) Mammalian Navigators are microtubule plus-end tracking proteins that can reorganize the cytoskeleton to induce neurite-like extensions. Cell Motil Cytoskeleton 66:824–838.

Vasiliev JM, Gelfand IM, Domnina LV, Ivanova OY, Komm SG, Olshevskaja LV (1970) Effect of colcemid on the locomotory behaviour of fibroblasts. J Embryol Exp Morphol 24:625–640.

Vigers AJ, Pfenninger KH (1991) N-type and L-type calcium channels are present in nerve growth cones. Numbers increase on synaptogenesis. Brain Res Dev Brain Res 60:197–203.

Vitriol EA, Zheng JQ (2012) Growth Cone Travel in Space and Time: the Cellular Ensemble of Cytoskeleton, Adhesion, and Membrane. Neuron 73:1068–1081.

Wada F, Nakata A, Tatsu Y, Ooashi N, Fukuda T, Nabetani T, Kamiguchi H (2016) Myosin Va and Endoplasmic Reticulum Calcium Channel Complex Regulates Membrane Export during Axon Guidance. CellReports 15:1329–1344.

Wang Y, Deng X, Mancarella S, Hendron E, Eguchi S, Soboloff J, Tang XD, Gill DL (2010) The calcium store sensor, STIM1, reciprocally controls Orai and CaV1.2 channels. Science 330:105–109.

Wang YL (1985) Exchange of actin subunits at the leading edge of living fibroblasts: possible role of treadmilling. The Journal of Cell Biology 101:597–602.

Watanabe T, Wang S, Noritake J, Sato K, Fukata M, Takefuji M, Nakagawa M, Izumi N, Akiyama T, Kaibuchi K (2004) Interaction with IQGAP1 links APC to Rac1, Cdc42, and actin filaments during cell polarization and migration. Dev Cell 7:871–883.

Waterman-Storer CM, Gregory J, Parsons SF, Salmon ED (1995) Membrane/microtubule tip attachment complexes (TACs) allow the assembly dynamics of plus ends to push and pull membranes into tubulovesicular networks in interphase Xenopus egg extracts. The Journal of Cell Biology 130:1161–1169.

Waterman-Storer CM, Salmon ED (1998) Endoplasmic reticulum membrane tubules are distributed by microtubules in living cells using three distinct mechanisms. Current Biology 8:798–806.

Waterman-Storer CM, Worthylake RA, Liu BP, Burridge K, Salmon ED (1999) Microtubule growth activates Rac1 to promote lamellipodial protrusion in fibroblasts. Nat Cell Biol 1:45–50.

Wei C, Wang X, Chen M, Ouyang K, Song L-S, Cheng H (2009) Calcium flickers steer cell migration. Nature 457:901–905.

Wen Y, Eng CH, Schmoranzer J, Cabrera-Poch N, Morris EJS, Chen M, Wallar BJ, Alberts AS, Gundersen GG (2004a) EB1 and APC bind to mDia to stabilize microtubules downstream of Rho and promote cell migration. Nature Publishing Group 6:820–830.

Wen Z, Guirland C, Ming G-L, Zheng JQ (2004b) A CaMKII/Calcineurin Switch Controls the Direction of Ca2+-Dependent Growth Cone Guidance. Neuron 43:835–846.

Wen Z, Han L, Bamburg JR, Shim S, Ming G-L, Zheng JQ (2007) BMP gradients steer nerve growth cones by a balancing act of LIM kinase and Slingshot phosphatase on ADF/cofilin. The Journal of Cell Biology 178:107–119.

Wheeler DB, Randall A, Tsien RW (1994) Roles of N-type and Q-type Ca2+ channels in supporting hippocampal synaptic transmission. Science 264:107–111.

Williams RT, Manji SS, Parker NJ, Hancock MS, Van Stekelenburg L, Eid JP, Senior PV, Kazenwadel JS, Shandala T, Saint R, Smith PJ, Dziadek MA (2001) Identification and characterization of the STIM (stromal interaction molecule) gene family: coding for a novel class of transmembrane proteins. Biochem J 357:673–685.

Williams RT, Senior PV, Van Stekelenburg L, Layton JE, Smith PJ, Dziadek MA (2002) Stromal interaction molecule 1 (STIM1), a transmembrane protein with growth suppressor activity, contains an extracellular SAM domain modified by N-linked glycosylation. Biochim Biophys Acta 1596:131–137.

Wittmann T, Bokoch GM, Waterman-Storer CM (2003) Regulation of leading edge microtubule and actin dynamics downstream of Rac1. The Journal of Cell Biology 161:845–851.

Wozniak MJ, Bola B, Brownhill K, Yang YC, Levakova V, Allan VJ (2009) Role of kinesin-1 and cytoplasmic dynein in endoplasmic reticulum movement in VERO cells. J Cell Sci 122:1979–1989.

Wu MM, Buchanan J, Luik RM, Lewis RS (2006) Ca2+ store depletion causes STIM1 to accumulate in ER regions closely associated with the plasma membrane. The Journal of Cell Biology 174:803–813.

Yalçın B, Zhao L, Stofanko M, O'Sullivan NC, Kang ZH, Roost A, Thomas MR, Zaessinger S, Blard O, Patto AL, Sohail A, Baena V, Terasaki M, O'Kane CJ (2017) Modeling of axonal endoplasmic reticulum network by spastic paraplegia proteins. Elife 6:101.

Yamamoto H, Fukunaga K, Goto S, Tanaka E, Miyamoto E (1985) Ca2+, calmodulin-dependent regulation of microtubule formation via phosphorylation of microtubule-associated protein 2, tau factor, and tubulin, and comparison with the cyclic AMP-dependent phosphorylation. J Neurochem 44:759–768.

Yang S, Zhang JJ, Huang X-Y (2009) Orai1 and STIM1 Are Criticalfor Breast Tumor Cell Migration and Metastasis. Cancer Cell 15:124–134.

Yuan JP, Zeng W, Huang GN, Worley PF, Muallem S (2007) STIM1 heteromultimerizes TRPC channels to determine their function as store-operated channels. Nature Publishing Group 9:636–645.

Zalk R, Lehnart SE, Marks AR (2007) Modulation of the ryanodine receptor and intracellular calcium. Annu Rev Biochem 76:367–385.

Zhang SL, Yu Y, Roos J, Kozak JA, Deerinck TJ, Ellisman MH, Stauderman KA, Cahalan MD (2005) STIM1 is a Ca2+ sensor that activates CRAC channels and migrates from the Ca2+ store to the plasma membrane. Nature 437:902–905.

Zhang X, Li F, Bulloj A, Zhang Y-W, Tong G, Zhang Z, Liao F-F, Xu H (2006) Tumor-suppressor PTEN affects tau phosphorylation, aggregation, and binding to microtubules. FASEB J 20:1272–1274.

Zhang X-F, Forscher P (2009) Rac1 Modulates Stimulus-evoked Ca2+ Release in Neuronal Growth Cones via Parallel Effects on Microtubule/Endoplasmic Reticulum Dynamics and Reactive Oxygen Species Production. Mol Biol Cell 20:3700–3712.

Zheng JQ (2000) Turning of nerve growth cones induced by localized increases in intracellular calcium ions. Nature 403:89–93.

Zheng JQ, Felder M, Connor JA, Poo MM (1994) Turning of nerve growth cones induced by neurotransmitters. Nature 368:140–144.

Zheng JQ, Wan JJ, Poo MM (1996) Essential role of filopodia in chemotropic turning of nerve growth cone induced by a glutamate gradient. J Neurosci 16:1140–1149.

Zhou F-Q, Waterman-Storer CM, Cohan CS (2002) Focal loss of actin bundles causes microtubule redistribution and growth cone turning. The Journal of Cell Biology 157:839–849.

Zhou F-Q, Zhou J, Dedhar S, Wu Y-H, Snider WD (2004) NGF-induced axon growth is mediated by localized inactivation of GSK-3beta and functions of the microtubule plus end binding protein APC. Neuron 42:897–912.

Zucker RS (1999) Calcium- and activity-dependent synaptic plasticity. Current Opinion in Neurobiology 9:305–313.

Zurek N, Sparks L, Voeltz G (2011) Reticulon short hairpin transmembrane domains are used to shape ER tubules. Traffic 12:28–41.